Mapping a Th17 network: microRNA and Polycomb in cell fate specification

by

Thelma Minnelli Escobar

A dissertation submitted to Johns Hopkins University in conformity with the requirements for the degree of Doctor of Philosophy

Baltimore, Maryland

April 2014

Abstract

Host detection of foreign pathogens can trigger both innate and adaptive immune responses; CD4$^+$ T helper (Th) cells play a critical role in the latter. Upon encountering its cognate antigen and receiving appropriate co-stimulatory signals, a naïve CD4$^+$ Th cell can differentiate into a variety of effector subsets that include, but are not limited to, CD4$^+$ Th1, Th2, Th17, Tfh, and iTregs. This dissertation focuses on the regulatory circuitry that enables the differentiation of distinct CD4$^+$ Th cell lineages; concentrating on the role of microRNA (miRNA) in this T cell fate decision. Experimentally, *in vitro* polarization of primary murine CD4$^+$ Th cells by addition of exogenous cytokines is used to decipher the molecular and signaling events that control the differentiation process of each subset. Examination of Th1, Th2, and Th17 cells deficient in Signal Transducers and Activators of Transcription (STAT) signaling, reveals the critical function of these transcription factors in inducing expression of non-coding RNA.

Focusing on the CD4$^+$ Th17 cell subset, a key role for STAT3 is identified in regulating the expression of miR-29 and miR-155. We find that miR-29 expression in Th17 cells prevents aberrant cytokine expression, and this miRNA has a further role in the *in vivo* generation of pathogenic Th17 cells during autoimmune disease. Moreover, we show that miR-155 promotes Th17 cytokine expression by altering the chromatin state through the inhibition of Jarid2 expression. In the context of embryonic stem cells, Jarid2 recruits the Polycomb Repressive Complex 2 (PRC2) to epigenetically silence key developmental genes by catalyzing the trimethylation of H3K27. We find that high expression of miR-155 in Th17 cells alleviates Jarid2-PRC2 inhibition of genes encoding

Th17 signature cytokines. Thus, miR-155 targeting of Jarid2 favors a more open chromatin state at both cytokine loci and genes promoting Th17 cell development.

Through collaboration with the National Center for Advancing Translational Sciences (NCATS), the translational aspects of these research questions were investigated. MiR-155 and Th17 cells are highly expressed in many autoimmune diseases and Th17 cells have a detrimental role in such diseases. By examining the molecular networks involving miRNAs in CD4$^+$ Th cell development, our goal is to find new drugs that can target mir-155 for therapeutic purposes and potentially alleviate disease progression.

Thesis Committee

Dr. Stefan Muljo   Advisor, Laboratory of Immunology, NIAID/NIH

Dr. Susan Gottesman   Laboratory of Molecular Biology, NCI/NIH

Dr. Alan Sher   Laboratory of Parasitic Diseases, NIAID/NIH

Dr. Karen Beemon   Department of Biology, JHU

Dr. Xin Chen   Department of Biology, JHU

Readers

Drs. Stefan Muljo and Karen Beemon

Preface and Acknowledgements

I have been extremely fortunate to be part of the Laboratory of Immunology (LI) at NIAID for my graduate research. LI is filled with talented and dedicated individuals and it has been a pleasure to work with them. I would like to thank current and past members of the Integrative Immunobiology Unit, including Hunter Oliver-Allen, Joan Yuan, Steven Witte, and Idalia Yabe and special thanks to Rami Zahr, Cuong (KC) Nguyen, Yves-Olivier Guettard, Brenna Brady, Gokhul Kilaru, Xiuhuai Liu, and Patrick Burr. I would also like to extend my gratitude to the entire LI and a special thanks to Kimberly Shaffer-Weaver, Sadiye Rieder, Tim Gilpatrick, Suvenna Sharma, and Ryoji Yagi.

I would like to thank all my many collaborators. From the Laboratory of Parasitic Diseases (Sher Lab), thank you to Dragana Jankovic and David Kugler for all your support. From Ethan Shevach's group, I would like to thank Michael Holt, Sadiye Rider, Ravikiran Bhairavabhotla, George Punkosdy, and Amal Ephren for training me with *in vivo* animal models. I am very thankful for Jinfang Zhu's mentorship, especially at the beginning of my graduate research. In addition, I would like to thank Daniel Northrup, Brian Abraham and Keji Zhao's laboratory in the Systems Biology Center at NHLBI for teaching me and sharing their expertise in ChIP-seq. I thank my collaborators Cheng-Rong Yu and Charles Egwuagu in the Molecular Immunology Section at NEI for their hard work and enabling me to have my first, first author publication. I also thank Anju Singh and Marc Ferrer at the National Center for Advancing Translational Sciences (NCATS) for an outstanding collaboration.

Table of Contents

3. Regulation of non-coding RNA by Signal Transducer and Activator of

Transcription (STAT)s in CD4^{+} Th differentiation

4. The intricate network of transcription factors, microRNA and epigenetics shape Th17 cell differentiation

List of Figures

Introduction

Regulation of non-coding RNA by Signal Transducer and Activator of

Transcription (STAT)s in CD4$^+$ Th differentiation

The intricate network of transcription factors, microRNA and epigenetics shape Th17 cell differentiation

Small molecule inhibitor screen to identify targets that alter miR-155 expression

in CD4$^+$ Th17 cells

Discussions and Conclusions

1. Introduction

1.1   CD4^{+} T helper cell differentiation and function

The immune system is made of various cell types whose function is to protect the host from infection by foreign pathogens while sparing self-tissues. This protection involves a dynamic and highly coordinated process that includes 1) recognition of an infectious agent, 2) initiation and progression of an appropriate response to eliminate the foreign agent, 3) the ability to self regulate, and 4) acquisition of immunological memory to combat pathogen re-exposure (Murphy et al., 2008). To accomplish this process, the immune system is comprised of a vast array of cell types and molecules that constitute two branches, each with unique properties and function. The innate immune system represents a "first line of defense" against foreign pathogens and is made up of macrophages, neutrophils, basophils, eosinophils, mast cells, natural killer cells, and dendritic cells. Although innate immunity provides an early and broad inflammatory response to bacteria, viruses, and fungi, these responses to a foreign pathogen are not tailored and are recognized through a series of common receptors. A key feature of innate immunity is the ability to activate the second branch of the immune response in order to specialize a response and retain immunological memory (Murphy et al., 2008).

The adaptive immune system is composed of B and T lymphocytes that enable a highly specialized and specific response to pathogens. This type of tailored response is due to unique receptors, B cell receptors (BCR) and T cell receptors (TCR) on the surface of B and T cells, respectively, that are able to recognize a potentially unlimited array of agents. Activation of B cells via their BCR results in a humoral immune response: the release of a variety of soluble antibodies that are able to bind to and neutralize infectious

pathogens. Although B cells are critical for immunity, this thesis focuses on T cell development.

T cells represent a functionally diverse population of immune cells that include both CD8^{+} and CD4^{+} T cells. After development within the thymus, CD8^{+} and CD4^{+} T cells emigrate throughout the body as antigen-inexperienced, naïve T cells. Such naïve T cells continuously circulate from the bloodstream through secondary lymphoid tissues, sampling antigens being presented by antigen-presenting cells. During an immune response, a naïve T cell expressing a particular TCR may encounter a foreign pathogen in the context of peptide/MHC (signal 1). CD8^{+} T cells recognize peptides presented in the context of major histocompatibility complex (MHC) class I and are typically classified as cytotoxic T lymphocytes due to their ability to recognize and eliminate virally infected cells and cancerous cells via the release of a variety of soluble mediators, including cytokines and lytic granules. Focusing on the content of this thesis research, CD4^{+} T cells recognize peptides presented in the context of MHC class II on the surface of antigen presenting cells and are activated to differentiate into multiple "T helper" (Th) cell subsets that, in turn, help activate other cells of the immune system.

In addition to signal 1, a second stimulus (signal 2) is required to enable the T cell to proliferate and proceed with its functional role. Without appropriate co-stimulation, the T cell is rendered functionally inactivated and anergic. This secondary signal is also an important check for preventing inappropriate activation that may lead to autoimmunity. A unique feature of adaptive immunity is the ability to generate immunological memory. Following an immune response, a portion of B and T cells are retained as long-lived

memory cells that are able to rapidly respond upon pathogen re-exposure (Murphy et al., 2008).

The differentiation of CD4$^+$ T cells into various Th cell subsets is highly dependent on the cytokine milieu during an inflammatory response. Contingent on the environment, activated CD4$^+$ T cells can develop into Th lineages that are defined primarily by the expression of specific master transcription factors, which initiate distinct differentiation programs affecting cell function and cytokine production. The various CD4$^+$ Th cell subsets include Th1, which express the transcription factor T-bet and the signature cytokine interferon (IFN)γ; Th2, which are characterized by Gata3 expression and interleukin (IL)-4 production; Th17, which express RAR-related orphan receptor (ROR)γt and produce IL-17; T follicular helper cells (Tfh), which are defined by Bcl6 expression and IL-21 production; and regulatory T cells (Treg), which express the transcription factor Foxp3 and produce IL-10 (Zhu et al., 2010). Each CD4$^+$ Th cell subset and their respective cytokines provide a highly specialized immunological defense that protects the host from various foreign pathogens. For example, a Th1-biased immune response with prominent IFNγ production is tailored to fight and eliminate intracellular infection resulting from viruses or parasites (Awasthi and Kuchroo, 2009). Infection with extracellular pathogens, such as fungal infection, results in a response dominated by Th-17 cells (Awasthi and Kuchroo, 2009).

The central role of CD4$^+$ Th cells in the context of an immune response is highlighted in HIV-induced acquired immunodeficiency syndrome (AIDS), where there is a severe reduction of CD4$^+$ T cells and concomitant predisposition to opportunistic infections (Douek et al., 2003). Although protective in nature, improper or chronic

activation of CD4^{+} Th cells can cause autoimmunity. Furthermore, defective differentiation of CD4^{+} T cells also contributes to severe disease states, such as the immunodysregulation, polyendocrinopathy, enteropathy, X-linked (IPEX) syndrome that is evident as a result of mutations in the *FOXP*3 gene (Bennett et al., 2001; Brunkow et al., 2001; Wildin et al., 2001). Thus, understanding the molecular basis of CD4^{+} Th cell differentiation will provide key information into subset specification and facilitate the design of more effective strategies for targeting autoimmunity or opportunistic infections.

The molecular development of distinct CD4^{+} Th cell lineages is orchestrated by a regulatory network that integrates signals from the TCR-MHC interaction, co-stimulatory ligands, and the extracellular cytokine milieu in order to achieve a series of programmed gene expression changes (Figure 1). For example, during the differentiation program of Th1 cells, engagement of IL-12 and IFNγ with their corresponding receptors on the surface of naïve CD4^{+} T cells is required for the initial commitment and corresponding phosphorylation of signal transducer and activator of transcription (STAT)4 and STAT1. Following phosphorylation, STAT4 and STAT1 homodimerize and translocate to the nucleus where they induce the transcription of key Th1-associated genes, including T-bet and IFNγ. The Th2 differentiation program involves binding of IL-4 to the IL-4 receptor (IL-4R), which triggers STAT6 activation and subsequent activation of GATA3 and IL-4. The presence of IL-6 and transforming growth factor (TGFβ) initiates STAT3 activation and translocation to the nucleus to induce the expression of RORγt and IL-17. Lastly, TGFβ is able to stimulate the up-regulation of Foxp3 and the Treg differentiation program (Figure 1) (Egwuagu, 2009).
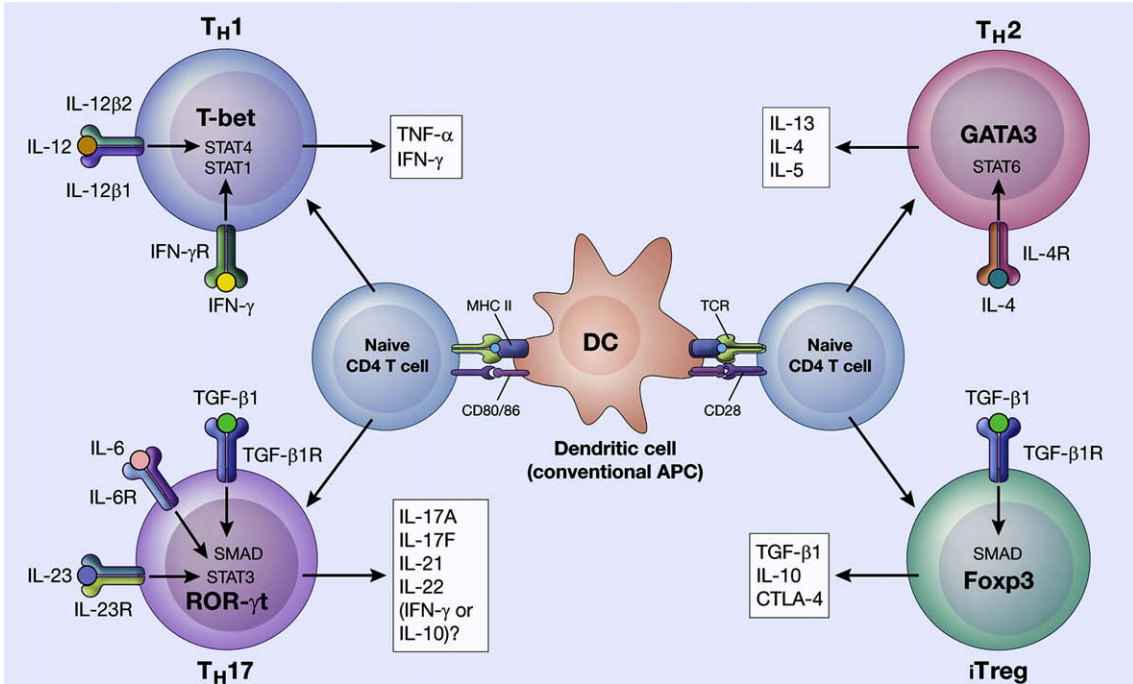
Figure 1. Outline of CD4^{+} T helper cell differentiation. During the initial activation of CD4^{+} lymphocytes, antigen-presenting dendritic cells secrete a variety of cytokines that instruct the naïve T cell to initiate one of several Th cell developmental pathways leading to the Th1, Th2, Th17, or Treg cell lineages. Each CD4^{+} Th cell subset produces a range of signature cytokines that mediates its distinct immunoregulatory functions (Reprinted from Cytokine, 47(3), Charles Egwuagu, STAT3 in CD4^{+} T helper Cell differentiation and Inflammatory Diseases, 148-156, Copyright 2009, with permission from Elsevier.)

1.2 The transcription factor network that regulates Th17 cell development

The well-defined function and characterization of different CD4$^+$ Th cell lineages provides the ideal opportunity to study the effect of transcription factors whose gene expression changes confer unique cellular functions (Zhu et al., 2010). Recently, the transcription factor network necessary for Th17 cell development was identified (Fujita-Sato et al., 2011; Li et al., 2012; Yosef et al., 2013b). This network includes STAT3, interferon regulatory factor (IRF)4 and basic leucine zipper transcription factor, ATF-like (BATF) that are expressed early in the Th17 cell differentiation program and drive the induction of the *Rorc* gene (encoding the transcription factor RORγt) (Ciofani et al., 2012; Yosef et al., 2013b). The induction of RORγt expression, in concert with other transcription factors such as RORα, c-Maf and the aryl hydrocarbon receptor (AHR), promotes the expression of the signature Th17 cytokines that include IL-17a, IL-17f, IL-22, IL-9, and IL-10 (Figure 2) (Yosef et al., 2013b).
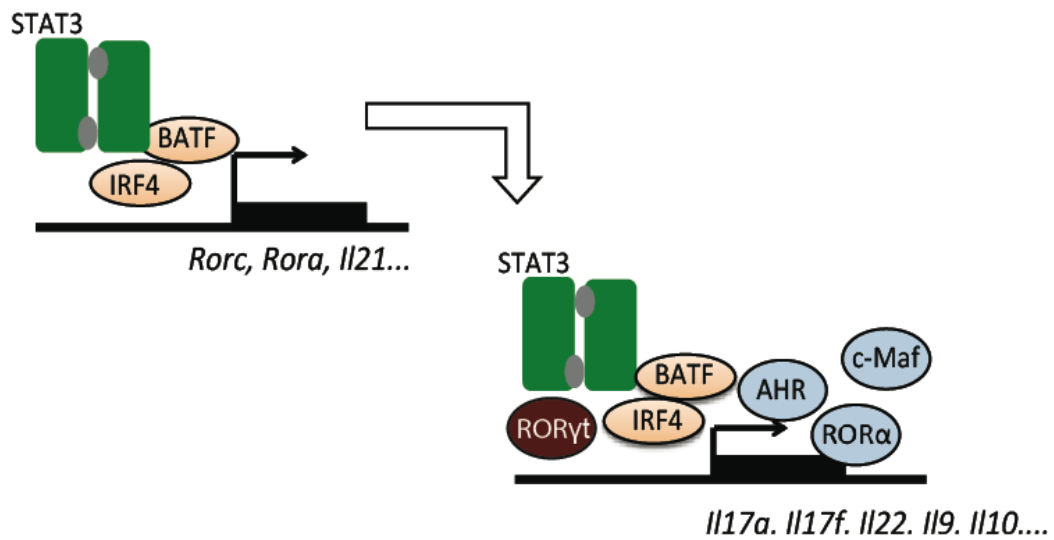
Figure 2. A transcription factor network promotes Th17 cell development and function. Upon the initial activation of naïve CD4^{+} T cells, STAT3, BATF and IRF4 induce the expression of key transcription factors and genes that promote the differentiation of CD4^{+} T cells towards a Th17 lineage. Following the induction of RORγt expression, Th17 cell specification leads to the production of Th17 signature cytokines.

1.3   Therapeutic potential of targeting Th17 cells in chronic inflammatory diseases

Amongst the critical roles of CD4$^+$ T cells in host defense and protection, Th17 cells constitute a key lineage involved in mucosal defense. In response to pathogens Th17 cells mount an inflammatory response through the secretion of pro-inflammatory cytokines. When this pro-inflammatory function becomes unregulated, it can also be a major contributor to autoimmune inflammatory diseases. For example, Th17 associated molecules, such as IL-17a and IL-22, are protective against an array of pathogenic organisms, such as the Gram-negative bacteria *Escherichia coli* (Shibata et al., 2007) and *Salmonella enterica enteritidis* (Schulz et al., 2008), as well as the fungus *Candida albicans* (Huang et al., 2004; O'Connor et al., 2010). The protective potential of Th17 cells is due in large part to their induction of antimicrobial peptides and the direct regulation of neutrophils via IL-17 and IL-22 (O'Connor et al., 2010). In addition to their ability to provide host defense, IL-17 and IL-22 also have secondary roles in the control of inflammatory damage. IL-22 plays a prominent role during tissue regeneration, particularly at mucosal surfaces found in the lungs and intestine. The activation of IL-22 increases epithelial proliferation, enhances mucus-associated proteins important in forming the mucus layer, and induces expression of matrix metalloproteinases (MMPs) to allow epithelial cell migration and apoptosis (Witte et al., 2010).

Yet, the same inflammatory and tissue regenerative properties of Th17 cells that are necessary for host defense can lead to undesirable and adverse conditions, including autoimmune disease and cancer. For example, in autoimmune conditions such as psoriasis, IL-22 promotes keratinocyte migration leading to hyperplasia and thickening of

the epidermis (Boniface et al., 2005; Kebir et al., 2007; Zheng et al., 2007). In rheumatoid arthritis, Th17 cells lead to bone erosion and cartilage proteoglycan loss (Sato et al., 2006; van den Berg and Miossec, 2009). Likewise, in multiple sclerosis, Th17 lymphocytes have the capacity to pass the blood brain barrier and promote central nervous system inflammation, through the production of both IL-17 and IL-22, which results in neuronal loss (Kebir et al., 2007). In addition to the damaging effects of Th17 cells in inflammatory diseases, it was found that through an IL-22 axis, chronic mucosal inflammation and tissue damage predisposes patients to the development of colorectal cancer (Huber et al., 2012).

Although CD4^{+} Th17 cells are protective in host defense, this same lineage is highly pathogenic during autoimmune disease. As such, the ability to find therapeutic treatments that limit inflammatory pathology without inducing generalized immunosuppression is key to improving Th17 autoimmune therapy. Thus far, small molecule screens to find Th17 inhibitors have identified Halofuginone (Sundrud et al., 2009), SR1001 (Solt et al., 2011), and Digoxin (Huh et al., 2011) as potential Th17 therapeutic candidates in mice. SR1001 and Digoxin were found to compete with natural agonists of the master transcription factor for Th17 development, RORγt, thus reducing its transcriptional activity and suppressing autoimmunity (Figure 3) (Fujita-Sato et al., 2011; Jetten, 2011). These therapeutics work, but are not ideal because they prevent Th17 development and therefore loss of a major component of the immune system. For this reason, finding small molecule inhibitors that do not affect Th17 differentiation but do affect cytokine production are of great interest.
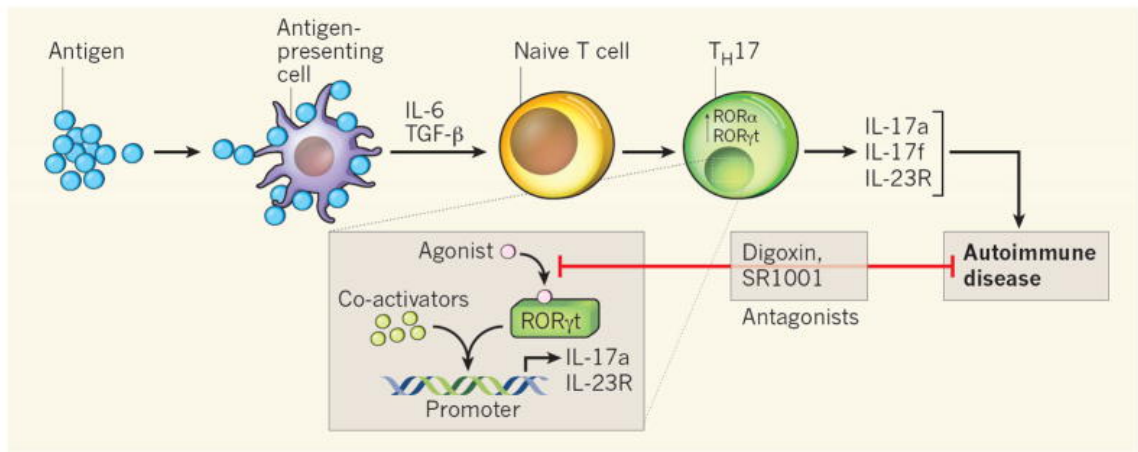
Figure 3. Th17 cell differentiation and therapeutic candidates for autoimmune disorders. In response to antigen encounter on the surface of antigen-presenting cells (and in the presence of IL-6 and TGF-β), naïve CD4$^+$ T cells differentiate into Th17 cells. This event is associated with expression of the nuclear receptors RORγt and RORα. These receptors, particularly RORγt, are required for Th17 cell differentiation and for the expression of IL-23R and IL-17a. Two studies have shown that digoxin (Huh et al., 2011) and SR1001 (Solt et al., 2011) bind to RORγt, possibly by competing with the natural agonists of is receptor. By inhibiting the recruitment of co-activators and promoting the recruitment of co-repressors, these antagonists reduce RORγt transcriptional activity, Th17 cell differentiation and IL-17 production, and delay the onset and reduce the severity of autoimmune disease in mice (Reprinted by permission from Macmillan Publishers Ltd: Nature, Jetten, 2011). http://www.nature.com/nature/index.html

1.4   Non-coding RNA regulation of gene expression

Although a large amount of research has been dedicated to the transcriptional factor network necessary for proper Th17 cell development, the roles of chromatin regulators and microRNA (miRNA) in this process have remained less well understood. To identify chromatin signatures in CD4$^+$ Th cell development, global mapping of 'active' H3K4me3 and 'inactive' H3K27me3 in T cells was conducted (Wei et al., 2009). This work revealed epigenetic patterns that govern Th cell lineage specificity and suggests mechanisms other than transcription factors may command Th cell specificity (Wei et al., 2009). However, the exact mechanism by which transcription factors and the epigenetic programs work together remains unclear. One example of the interdependence between these two regulatory systems is seen with the requirement of STATs for proper P300 and H3K4me3 deposition in the Th1 and Th2 cell lineages (Vahedi et al., 2012). Furthermore, we now know that ablation of Dicer, an RNAse III enzyme required for the generation of mature miRNA, results in impaired T cell development (Muljo et al., 2005) and suggests an important role for the Dicer-dependent miRNA pathway in controlling T cell development. These findings support the idea that the roles of miRNA and chromatin regulators should be analyzed in conjunction with transcriptional networks in T cells.

MiRNA are evolutionarily-conserved, small, non-coding RNA (ncRNA) of approximately 21-24nt that control gene expression at the post-transcriptional level. A miRNA gene is first transcribed by RNA polymerase II into primary RNA transcripts (primary miRNA) that are recognized and processed by the ribonuclease III enzyme, Drosha in the nucleus (Figure 4A) (Baumjohann and Ansel, 2013). The processed

12

miRNA (precursor miRNA) is then exported to the cytoplasm where Dicer further processes it to the mature form (Figure 4A) (Baumjohann and Ansel, 2013). By guiding the Argonaute (Ago) protein complex (miRISC) to the complementary Watson-Crick base pairing of a target mRNA, a single stranded miRNA alters expression of the target mRNA by translational repression and/or destabilization (Figure 4A) (Baumjohann and Ansel, 2013). The importance of miRNA in CD4^{+} Th cells is highlighted by genetic ablation of key molecules of the miRNA biogenesis resulting in impaired T cell proliferation, apoptosis, and aberrant cytokine expression (Figure 4B) (Baumjohann and Ansel, 2013; Chong et al., 2008; Muljo et al., 2005; Steiner et al., 2011).

A number of miRNA have been implicated in the regulation of T cell differentiation and function (Baumjohann and Ansel, 2013; Jeker and Bluestone, 2013). Among these, miR-155 was the first miRNA linked to CD4^{+} T cell differentiation based on its impact on Th2, Th17 and Treg cell development (Lu et al., 2009; O'Connell et al., 2010; Rodriguez et al., 2007; Thai et al., 2007). The transcription factor c-Maf, a miR-155 target, was up-regulated in mir-155 deficient CD4^{+} T cells resulting in enhanced Th2 differentiation (Rodriguez et al., 2007). In addition, miR-155 in Treg cells promotes cell fitness by targeting suppressor of cytokine signaling (SOCS)1 (Lu et al., 2009). In terms of Th17 cell responses, miR-155 is necessary for the production of IL-17 and IFNγ during *Helicobacter pylori* infection (Oertli et al., 2011), as well as mouse models of inflammatory diseases such as experimental autoimmune encephalomyelitis (EAE) (Murugaiyan et al., 2011; O'Connell et al., 2010) and collagen induced arthritis (CIA) (Bluml et al., 2011).

Other miRNA have also been implicated in T cell regulatory pathways. The miR-29a/b and miR-17~92 clusters have also been shown to have a role in CD4^{+} Th cell development and function (Baumjohann and Ansel, 2013). The miR-29 family was shown to limit Th1 cell differentiation and IFNγ production by targeting mRNAs encoding T-bet, eomesodermin (Eomes), and IFNγ (Ma et al., 2011; Steiner et al., 2011). As such, miR-29 can suppress immune responses to intracellular pathogens by limiting pro-inflammatory IFNγ production (Ma et al., 2011). Moreover, it was demonstrated that the miR-17~92 cluster promotes T cell survival and proliferation by targeting Pten and Bim messages. Over expression of the miR-17~92 cluster in T cells results in lymphoproliferation and autoimmunity (Baumjohann and Ansel, 2013; Xiao et al., 2008).

In addition to miRNA, other ncRNA such as long non-coding RNA (lncRNA) are emerging as important players in controlling gene expression programs that are critical for lineage commitment and pluripotency (Guttman et al., 2009; Guttman et al., 2011). During T cell differentiation, a lncRNA NeST was found to enhance IFNγ expression by regulating the epigenetics of the IFNγ locus (Gomez et al., 2013). The enhanced production of IFNγ by NeST led to increased viral and bacterial susceptibility among transgenic animals (Gomez et al., 2013). Assessing the function of ncRNA during CD4^{+} Th cell differentiation is therefore necessary for a comprehensive understanding of T cell specification and gene regulation. For this reason, annotation and function of lncRNAs are emerging for CD4^{+} Th cell subsets (Hu et al., 2013).
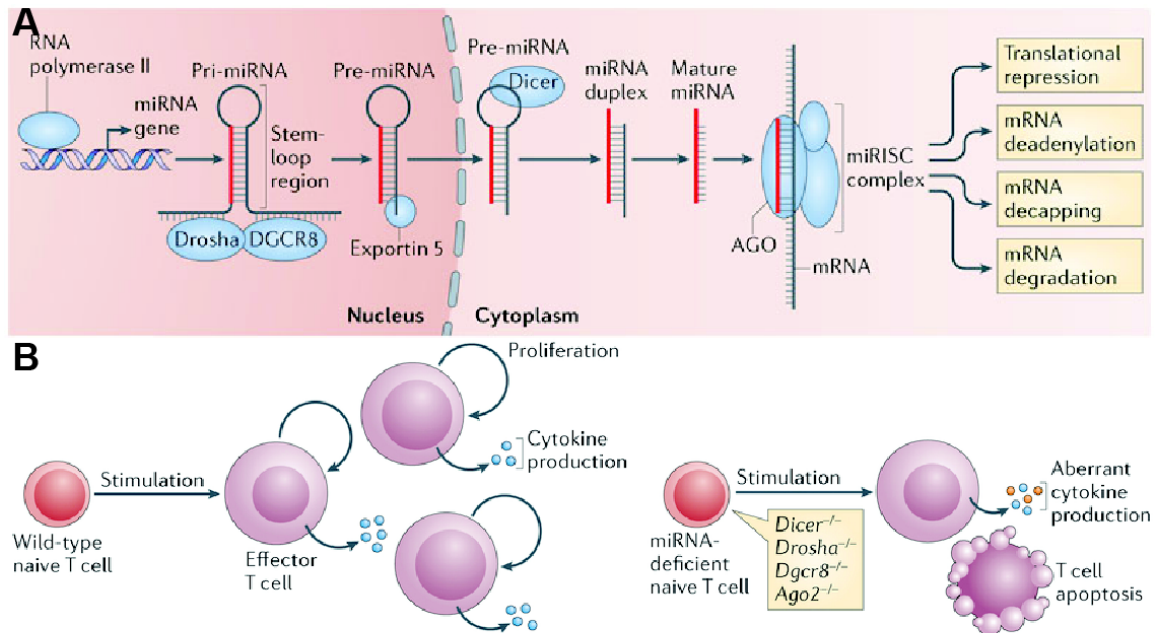
Figure 4. miRNA biogenesis and role of small RNAs in T cell differentiation. (A) The miRNA gene is transcribed by RNA Polymerase II and processed by Drosha and DGCR8 in the nucleus. This pri-miRNA is exported to the cytoplasm by Exportin 5, and then further processed by Dicer to a mature duplex. The guide strand of mature miRNA is incorporated into the miRISC complex where it is directed to its complementary targets, resulting in changes in gene expression. (B) Depiction of aberrant cell proliferation and differentiation upon stimulation of T cells lacking key molecules of the miRNA biogenesis pathway (Reprinted by permission from Macmillan Publishers Ltd: Nature Reviews Immunology, adapted from Baumjohann and Ansel, 2013).

http://www.nature.com/nri/index.html

1.5   Objectives for thesis research and summary of findings

Due to the well-characterized nature of murine CD4$^+$ Th cell differentiation, I chose to focus on the Th17 cell program for my graduate research to examine gene regulatory networks that incorporate miRNA. My research has identified both miR-29 and miR-155 as important factors in regulating Th17 cell development and suppressing alternative Th cell fates. This research has also revealed the importance of chromatin regulators, specifically the Polycomb repressive complex 2 (PRC2) and Jarid2, in altering the chromatin state of Th17 cells and inhibiting lineage commitment. I further highlight the mechanism by which miR-155 promotes Th17 cytokine expression and identify small molecule inhibitors of miR-155 that have the ability to inhibit the production of Th17 cytokines without affecting Th17 cell development.

2. Methods

2.1 Experimental animals

Male and female BALB/c, STAT4 KO (Kaplan et al., 1996b), STAT6 KO
(Kaplan et al., 1996a), and 2D2 (Bettelli et al., 2003) mice were purchased from The
Jackson Laboratory. STAT4 KO and STAT6 KO mice were backcrossed onto the
BALB/c background. miR-155 KO mice (Thai et al., 2007) were purchased from The
Jackson Laboratory and backcrossed up to 12 generations onto the C57BL/6 background
(Taconic). B6.SJL (CD45.1) and Rag2$^{-/-}$ mice were purchased from Taconic. STAT3$^{fl/fl}$;
CD4-cre on a C57BL/6 background and littermate controls were provided by Charles
Egwuagu's laboratory (National Eye Institute, NIH, USA). The the knock-out first
conditional strategy was utilized to create a Jarid 2 floxed allele. Briefly the
Jarid2$^{tm1a(KOMP)Wtsi}$ allele on a C57BL/6 background obtained from the International
Knockout Mouse Consortium was bred to Flp transgenic mice from The Jackson
Laboratory to genetrate a conditional allele (*Jarid2*$^{fl/+}$) (Rodriguez et al., 2000). In this
conditional allele, exon 3 is flanked by loxP sites in a strategy that is essentially identical
to a previously published conditional allele of Jarid2 (Mysliwiec et al., 2006). The
Jarid2$^{fl/+}$ mice were bred to CD4-cre transgenic mice purchased from Taconic (Lee et al.,
2001) to generate CD4^{+} Jarid2 ff mice which delete Jarid2 in T cells at the double
positive stage; all mature T cells in these mice are Jarid 2 deficient.

Primers for CD4-cre genotyping were Forward 5' CCCAACCAACAAGAGCTC
3' and Reverse 5' CCCAGAAATGCCAGATTACG. Jarid2 genotyping primers for the
floxed allele were Forward 5' TAGTCAGGGCAAGGTGGAAG 3' and Reverse 5'
TCCCAACCTTCCTAATGCT 3'.

For bone marrow reconstitution, B6.SJL (CD45.1) recipient mice were conditioned with 900 Rads via a Cs137 source prior to injection of 3 million donor bone marrow cells. Mice were administered Trimethoprim/Sulfamethoxazole (TMS) antibiotics via drinking water for 5 weeks. All animal experiments were done in compliance with the guidelines of the NIH/NIAID Institutional Animal Care and Use Committee.

2.2 Parasites and infection

T. gondii cysts from the Type II avirulent strain ME-49 were prepared from the brains of infected C57BL/6 mice. For experimental infections, mice were inoculated by oral gavage with 0.5 mL of PBS for an average of 50 *T. gondii* cysts per animal (Wilson et al., 2010).

2.3 Isolation of small intestine lamina propia

Single-cell suspensions were prepared from spleen, pooled peripheral lymph node, and mesenteric lymph node by mechanical disruption and passage through 40 μm cell strainers (BD Biosciences). For isolation of lamina propria lymphocytes, the small intestine was collected in ice-cold HBSS buffered in 25 mM HEPES with 5% FBS. After careful removal of fatty tissue and fecal contents, the intestine was opened longitudinally and cut into small pieces. The intestinal fragments were washed once with HBSS containing 2 mM EDTA and 25 mM HEPES followed by an incubation step at 37°C with shaking in HBSS containing 10% FBS, 5 mM EDTA, 15 mM HEPES, and 0.015% DTT. The intestinal fragments were washed 5 times with HBSS containing 25 mM HEPES and 5% FBS and digested with Liberase TL (0.17 mg/ml) and DNAse (30 μg/ml) in pre-

warmed Iscove's Complete Media containing 5% FBS and then incubated for 30-60

minutes at 37°C with shaking. Digested intestinal fragments were washed with HBSS

containing 25 mM HEPES and 5% FBS followed by passing tissue through a 70 μm and

40 μm strainer (BD Biosciences) to obtain single cell suspensions for downstream

analysis.

2.4 Polarization and activation of mouse T cells

Splenic and lymph node T cells were obtained by disrupting organs of 6-9 week-

old mice. Single-cell suspensions were prepared from spleen, pooled peripheral lymph

node and mesenteric lymph node by mechanical disruption and passage through 40 μm

cell strainers (BD Biosciences). Naïve T cells were obtained either by sorting using a BD

FACS Aria cell sorter to identify CD4$^+$CD44$^-$CD62L^{high}CD25^{low} cells or were positively

selected for CD4$^+$ cells using a Miltenyi Biotec AutoMACS. Cells were cultured on

plate-bound anti-CD3 (1 μg/mL) (clone 145-2C11) and anti-CD28 (1μg/ml) (clone

37.51) for 4 days with various combinations of antibodies and cytokines: for Th1

conditions, 10 ng/mL of IL-12 and 10 μg/mL of anti-IL-4 (clone 11B11); for Th2

conditions, 10 ng/mL of IL-4, 10 ng/mL of IL-2, 10 μg/mL anti-IL-12 (clone C17.8) and

anti-IFNγ (clone XMG1.2); for Th17 conditions, 10 ng/mL of IL-6 and 0.5 ng/mL of

TGFβ, with 10 μg/mL of anti-IL-4, anti- IL-12 and anti-IFNγ and when indicated 10

ng/mL of IL-1β was also added; for iTregs, 50 U/mL of IL-2, 10 μg/mL of TGFβ with 10

μg/ml of anti-IL-4, anti- IL-12 and anti-IFNγ; for Th0 conditions, 50 U/mL of IL-2 with

10 μg/ml of anti-IL-4, anti- IL-12 and anti-IFNγ. Cells were cultured in 24 well plates for

3 days and then expanded in the presence of 50 U/mL IL-2 in 12 well plates for 1 or 2

days, except for Th17 cells that were expanded in the presence of all cytokines and antibodies. For murine studies, all recombinant cytokines were purchased from R&D and blocking antibodies and crosslinking antibodies were custom made from hybridomas (Harlan).

2.5 Polarization and activation of human T cells

Human peripheral blood mononuclear cells (PBMCs) were prepared from 20-60 year-old healthy donors by the Department of Transfusion Medicine at NIH. The acquisition of blood products was approved according to the Institutional Review Board and in accordance with the Declaration of Helsinki. Naïve $CD4^+$ T cells were sorted using the markers of $CD4^+CD25^-CD45RA^+$. For Th cell subset skewing, 24-well plates were coated overnight at 4°C or 4 hours at 37°C with 2 μg/mL in PBS containing anti-CD3 (clone UCHT1) and anti-CD28 (clone CD28.2). The cells were cultured with 10% FBS IMDM (GIBCO) for 5-6 days along with the respective cytokine cocktail. If necessary, cells were split after 3 days with a similar cocktail of antibodies. For Th1 conditions, 1 ng/mL of IL-12, 50 U/mL of IL-2 with 1 μg/mL of anti-IL-4; for Th2 conditions, 20 ng/mL of IL-4, 50 U/ml of IL-2 with 1 μg/mL of anti-IL-12 and anti-IFNγ; for iTreg conditions, 50 U/mL of IL-2, 10 μg/mL of TGFβ with 1 μg/mL of anti-IL-4 and anti-IFNγ; for Th17 conditions, 50 U/mL of IL-2, 10 ng/mL of each IL-1β, IL-6, and IL-23 and 10 ng/mL of TGFβ with 1μg/mL of anti-IL-4 and anti-IFNγ. For human cultures, all recombinant cytokines were purchased from Peprotech and blocking antibodies for IL-12, IL-4, and IFNγ were affinity-purified polyclonal goat IgG from R&D Systems.

2.6 Retroviral cloning and T cell transduction

Mouse *Atf3* was PCR amplified from cDNA clones obtained from Origene (MC201919) and subcloned into the MSCV-IRES-GFP vector provided by Ken Murphy (Washington University). Mouse miR-29a was first amplified from the mouse genome and then cloned into a MDH1-PGK-GFP based vector. Plasmid insertion was verified by sequencing and retroviral supernatants were generated. Transductions of CD4$^+$ T cells was achieved by first polarizing mouse T cells towards Th17 cell differentiation (described above) for one day. The following day, Th17 cell cultures were transduced by spin-infection at 700 x g at 32°C for 90 minutes in the presence of retroviral supernatant and 5 μg/mL polybrene (Sigma-Aldrich). Cells were returned to the incubator for another 6 hours and then viral media was replaced with fresh media. Th17 polarization was continued for 3 days followed by re-stimulation with PMA and Ionomycin in the presence of Golgi block for 4 hours. Transduced Th17 cell cultures were then fixed with 1% paraformaldehyde (Electron Microscopy Sciences) followed by intracellular cytokine staining in 1x PBS with 0.1% TritonX100 (Sigma-Aldrich).

2.7 Flow cytometry of intracellular cytokines

Mouse or human polarized T cells were stimulated with 20 ng/mL of phorbol 12-myristate 13-acetate (PMA) and 1 μg/mL of ionomycin in the presence of BD Golgi Plug (BD Bioscience) containing brefeldin A for 4 h at 37°C. Cells were subsequently stained with fixable viability dye (eBioscience) and then permeabilized in 500 μL of eBioscience Perm-Fix solution overnight at 4°C. Cells were washed with PBS and stained with anti-CD4, CD44, TCRβ, CD45.2, CD45.1, Vβ11, IL-17A, IL-22, IFNγ, IL-4, Foxp3, RORγt,

BATF, and IRF4 antibodies (eBioscience) for 1 h at 4°C. After washing, stained cells were assayed with a BD LSRII flow cytometer and the results analyzed using FlowJo software.

2.8 Passive Experimental Autoimmune Encephalomyelitis (EAE) and mean clinical score

Sorted naïve $CD4^+V\beta11^+CD44^-$ T cells from TCR(2D2) mice were activated with plate-bound anti-CD3 and anti-CD28 (10 μg/mL) in serum-free media under Th17(TGFβ) or Th17(23) conditions. After one day of polarization, T cells were transduced with miR-29a GFP-rv or vector control GFP-rv. Following transduction and 5 days of Th17 polarization, activated T cells were sorted based on GFP and 0.5 million cells were adoptively transferred into female Rag2-/- mice. Mice were scored according to the following criteria: 0, no disease; 1, decreased tail tone; 2, hind-limb paralysis; 3, complete hind-limb paralysis; 4, both hind- and front-limb paralysis; 5, moribund state.

2.9 Induction of Experimental Autoimmune Uveitis (EAU) by active immunization

Mice were immunized with 150 μg interphotoreceptor retinoid-binding protein (IRBP) and 300 μg of human IRBP peptide (1–20) in a 0.2 mL emulsion 1:1 vol/vol with Complete Freund's adjuvant (CFA) containing Mycobacterium tuberculosis strain H37RA (2.5 mg/mL). The mice also received *Bordetella pertussis* toxin (0.2 μg/mouse) concurrent with immunization, and clinical disease was established by funduscopy. Eyes were harvested for histologic or funduscopic evaluation at 0, 7, 10, 14, or 21 days after immunization. For histology, eyes were harvested, fixed in 4% glutaraldehyde for 30 minutes, and then transferred to 10% buffered formalin. After adequate fixation,

specimens were dehydrated through graded alcohols and embedded in methacrylate. Serial vertical sections through the papillary–optic nerve plane were cut and stained with hematoxylin and eosin. Photographs of representative sections were taken on a photomicroscope (Carl Zeiss AG, Oberkochen, Germany). Clinical disease was established and scored by funduscopy (Oh et al., 2011; Yu et al., 2011). Briefly, following intraperitoneal (IP) injection of ketamine (1.4 mg/mouse) and xylazine (0.12 mg/mouse), pupils were dilated by topical administration of 1% tropicamide ophthalmic solution (Alcon, Inc., Fort Worth, TX). To avoid a subjective bias, evaluation of the fundus photographs was conducted without knowledge of the mouse identity by a masked observer. At least six images (2 posterior central retinal views, 4 peripheral retinal views) were taken from each eye by positioning the endoscope and viewing from superior, inferior, lateral, and medial fields. Each individual lesion was identified, mapped, and recorded. The clinical grading system for retinal inflammation was used as established previously (Xu et al., 2008).

2.10 RNA Purification and quantitative PCR

Total RNA was isolated using a mirVana (Applied Biosystems) isolation kit. cDNA was prepared using TaqMan Reverse Transcription Reagents (Applied Biosystems) with random hexamers for primer/probe sets IL-22, IL-17A, IL-17F, IL-10, IL-9, ATF3, JARID2, IFNγ, Eomes, Tbet, IRF4, RORC, and BATF. For microRNA expression, cDNA was prepared using TaqMan microRNA reverse transcription kit (Applied Biosystems) with primer/probe sets for miR-155, miR-29a, miR-29b, and U6. Quantitative PCR was performed on a 7900HT Fast Real Time PCR Systems (Applied

Biosystems). C_T values from triplicate samples were averaged and relative expression

was calculated using the 2-$\Delta\Delta C_T$ method.

2.11 miRNA expression profiling

Total RNA was extracted from cell cultures on day 4. RNA concentration was

determined using the Qubit RNA broad range assay in the Qubit Fluorometer

(Invitrogen). A Eukaryote Total RNA Nano Series II chip on a 2100 Bioanalyzer

(Agilent) was used to confirm the concentration and determine the integrity of the RNA.

One hundred ng of total RNA was used as the starting material for miRNA profiling

using the nCounter Mouse miRNA Expression Assay Platform (NanoString

Technologies). Sample preparation and flow-cell hybridization was performed per

manufacturer's instructions at the DNA Sequencing and Digital Expression Core Facility

(National Cancer Institute). Per manufacturer's instructions, data were normalized to the

sum of positive control count values provided in assay to account for lane to lane

variation. Background determination was set by the mean +2x standard deviation of the 8

negative control detectors. Expression counts were normalized to the mean signal level of

a number of housekeeping genes (*Actb, B2m, Gapdh, Rpl19, Rplp0*).

2.12 Protein quantitation

Cell lysates were prepared by lysis in 420 mM NETN buffer containing protease

inhibitor and western blot analysis was performed using standard methods. Image J

(http://imagej.nih.gov/ij/) was used to quantify protein expression levels from digital

images of western blots and each assay was normalized to α-tubulin loading controls. The

concentration of IL-22, IL-9, and IL-10 in the supernatant of Th17 cell cultures was

measured using the corresponding Mouse ELISA Ready-Set-Go! Kit (eBioscience) following the manufacturer's instructions.

2.13 Chromatin Immunoprecipitation (ChIP), ChIP-seq and ChIP-exo

Polarized Th17 cells on day 4 were cross-linked with 2% paraformaldehyde at room temperature for 5 minutes followed by quenching with 125 mM glycine. The cells were then harvested and washed with cold phosphate-buffered saline. After obtaining a cell pellet for 10 million cells, these cells were lysed in RIPA buffer containing proteinase inhibitors. Chromatin was sheared into fragments of 200 base pairs in length by sonication of the cell lysate with a Diagenode Bioruptor (ten pulses of 30s, followed by eight pulses of 15s). After spinning down the cell debris, the sheared chromatin was added to the respective antibody immobilized on Protein A magnetic beads (Invitrogen), followed by overnight incubation at 4°C with rotation. Protein-DNA complexes were washed in low-salt, high-salt RIPA buffer, LiCl and Tris-EDTA buffers. Protein-DNA complexes were treated with 0.3% SDS, 1 mg/mL proteinase K (Invitrogen) and incubated overnight at 65°C to reverse crosslinking. The eluted DNA was purified by phenol-chloroform extraction and ethanol precipitation and suspended in 40 μL of Tris-EDTA. Real-time PCR was performed to quantify the ChIP assay and the amount of the immunoprecipitated DNA samples was normalized against input DNA samples. Antibodies include H3K4me3 (ab8580, Abcam), H3K27me3 (07-449, Millipore), Jarid2 (ab48137, Abcam), Suz12 (D39F6, Cell Signaling), c-Maf (M-153, Santa Cruz), Pol II (4H8, Abcam), and STAT3 and IgG control from Cell Signaling. For STAT3 ChIPs, Th17 polarized cells were stimulated for 60 min with recombinant IL-6 (25 ng/mL) to allow STAT3 translocation to the nucleus. For ChIP-exo, chromatin was sheared to 200

base pairs and frozen chromatin was provided to Peconic LLC (State College, PA) along with antibodies.

2.14 High throughput RNA sequencing procedure

Total RNA was extracted from activated miR-155 KO, STAT3KO, STAT4KO, STAT6KO and WT CD4^{+} T cells cultured under Th1, Th2 or Th17 polarizing conditions for 4-5 days. RNA concentration was determined using the Qubit RNA broad range assay in the Qubit Fluorometer (Invitrogen) and RNA integrity was determined using Eukaryote Total RNA Nano Series II ChIP on a 2100 Bioanalyzer (Agilent). Three independent biological replicates were pooled for RNA-seq. RNA-seq libraries were prepared from 1 μg of total RNA using the TruSeq RNA sample prep kit following manufacturer's instructions (Illumina). Briefly, oligo-dT purified mRNA was fragmented and subjected to first and second strand cDNA synthesis. cDNA fragments were blunt-ended, ligated to Illumina adaptors, and PCR amplified to enrich for the fragments ligated to adaptors. The resulting cDNA libraries were verified and quantified on Agilent Bioanalyzer, and single-end 96 cycle RNA-seq was conducted using the GAIIx Genome Analyzer (Illumina) for miR-155 KO and WT Th17 cells and 50 cycle paired-end RNA-seq was conducted for STAT4 KO and STAT6 KO Th1 and Th2 cells, respectively.

2.15 RNA-seq analysis

For RNA-seq analysis, reads from single or paired-end RNA-seq were mapped to the mouse genome (NCBI 37, mm9) using the splice-aware aligner TopHat (version-1.3.1) (Trapnell et al., 2009) with option --mate-inner-dist 160 --coverage-search --microexon-search --max-multihits 20. In short, using a two-step mapping processes,

TopHat first calls Bowtie (version-0.12.7) (Langmead et al., 2009) to align reads that are directly mapped to the reference genome (with no gaps). Bowtie then determines the possible location of gaps in the alignment based on canonical and non-canonical splice sites flanking the aligned reads. Finally, Bowtie uses gapped alignments to align the reads that were not aligned in the first step. Aligned reads were then visualized on a local mirror of the UCSC Genome Browser (Kent et al., 2002).

For differentially expressed gene and miRNA signature analyses, gene expression quantification was performed by counting aligned reads on each gene for each condition using in-house codes. DEGseq (Wang et al., 2010) was then applied to identify differentially expressed genes between two conditions with addition options *p value* threshold 1e-5 and fold change threshold 1.4. To identify putative target genes, a ranked gene list from up-regulated to down-regulated based on the $\log_2$ of the ratio of the expression level of each gene in the two conditions was supplied to Sylamer (van Dongen et al., 2008) to statistically calculate the enrichment of seed sequences of all known miRNAs (version 15 from miRbase.org). A list of 220 putative target genes was identified by choosing up-regulated genes containing miR-155 seed sequences (AGCATTA and GCATTAA) that pass the E-value threshold (Bonferroni-corrected) of *p value* < 0.01. Comparison of this putative target gene list against 134 and 256 putative miR-155 target mRNAs phylogenetically predicted by PicTar (http://pictar.mdc-berlin.de/) (Krek et al., 2005) and TargetScan (http://www.targetscan.org/)(Lewis et al., 2003) gave 15 putative miR-155 target mRNAs in common among the three methods. The False Discovery Rate (FDR) of the overlapped genes was then estimated by shuffling the RefSeq gene list 1000 times, randomly picking up 134 and 256 genes and getting the

average number of genes that overlap with the Sylamer miR-155 target gene list, which are 1.4 and 2.5, respectively. The FDR for the overlapped genes (1.4 out of 25 and 2.5 out of 42 genes) is about 6% for both comparisons.

2.16 ChIP-seq and ChIP-exo analysis

Reads from ChIP-seq were mapped to the mouse genome (NCBI 37, mm9) using the short read, memory efficient aligner Bowtie (version-0.12.7) (Langmead et al., 2009) with option -p 8 --chunkmbs 256 -a --best --strata -m 20. Unique reads were considered by instructing Bowtie to refrain from reporting any alignments for reads that have more than 20 reportable alignments. Reads from ChIP-exo were mapped by Peconic (State College, PA) to the mouse genome (NCBI 37, mm9) using BWA (version 0.5.9) with default options allowing one gap open and a maximum number of three alignments for any read that aligned across the genome. Sub-module of SICER (version-1.1) (Zang et al., 2009) was used on BED files containing the unique reads to determine window size (Abraham et al., 2013) for Jarid2, Suz12 and H3K27me3. The window sizes for each ChIP-seq were as follows: 2102 bp for Jarid2, 397 bp for Suz12 and 2852 bp for H3K27me3. SICER-df.sh was used for Suz12, Jarid2 and H3K27me3 analysis with a gap size of 0 for Jarid2, Suz12 and H3K27me3. All SICER-df.sh analysis had an FDR cutoff of 0.01. For ChIP-exo analysis, SICER-rb.sh was used to find enriched Jarid2 and Suz12 islands with an E value cut-off of 0.1, a window size of 50 and a gap size of 100. For c-Maf analysis, MACS (Version 1.4.2) was used for c-Maf binding enrichment using the following parameters "–f BED –g mm –p 1E-5 –w –S" using the duplicates processed BED files of c-Maf-miR-155-WT against c-Maf-miR155-WT-Input and c-Maf-miR-155-KO against c-Maf-miR155-KO-Input. For comparison of c-Maf miR-155 KO vs WT,

MACS2 (Version-2.0.9) was used with the following parameters "–f BED –g mm –p 1E-5 –B" against the duplicates processed BED files. The output from MACS2.0 was used with a sub-module of MACS2 "bdgdiff" tool that identifies differential binding regions, with a minimum peak length of 200, differential peak consideration cutoff of 5 and a gap size between any two peaks to be 30.

For visualization of RNA-seq and ChIP-seq tracks, wiggle files were generated from BAM files using custom Python scripts and then provided to D-Peaks (Brohee and Bontempi, 2012) to plot the coverage tracks (tags per million) at specified locations on the genome.

The Th17 cell specification regulatory network (KCRI) (Ciofani et al., 2012) was downloaded from http://th17.bio.nyu.edu/pages/cytoscape.html. Targets of miR-155 and Jarid2-PRC2 were integrated into the KCRI network to generate an updated Th17 cell regulatory network. Associations between transcription factors and miR-155 were added based on available ChIP-seq evidence. Network data integration, visualization and analysis were performed using the Cytoscape platform (Smoot et al., 2011).

2.17 Statistics

GraphPad Prism 5.0 was used for statistical analysis (unpaired, two-tailed, *t* test with a confidence interval of 95%). A *p* value ≤ 0.05 was considered a statistically significant difference.

3. Regulation of non-coding RNA by Signal Transducer and Activator of Transcription (STAT)s in CD4$^+$ Th differentiation

3.1 STATs regulate Th1, Th2 and Th17 cell differentiation

Naïve CD4$^+$ T cells differentiate into distinct Th cell populations and subsequently produce signature cytokines based on the variety of pathogens they encounter. The identification of distinct factors and *in vitro* culture conditions that can polarize CD4$^+$ T cells into the unique lineages has enabled mechanistic insight into the various signaling pathways and gene expression profiles that are associated with each of the subsets. It became apparent that activation of the STAT family of transcription factors is critical for proper CD4$^+$ Th cell differentiation (O'Shea and Paul, 2010). The phosphorylation of STATs by Janus kinases (JAK-STAT signaling pathway) results in STAT dimerization and translocation to the nucleus. In the nucleus, STATs bind to a recognition sequence (TTCCC) where they can either promote or suppress transcription of neighboring genes (Stark and Darnell, 2012).

The activation of STATs and expression of key transcriptional regulators form a complex network involving positive regulation of a lineage differentiation while suppressing alternative fates. Among the seven STAT family members, STAT4 in conjunction with STAT1 plays a pivotal role in Th1 cell differentiation by enhancing Th1 master regulator Tbet expression leading to the production of IFNγ (Mullen et al., 2001). In Th2 cells, IL-4 activates STAT6 resulting in the transcription of Gata3 and in turn augmenting IL-4 production (Takeda et al., 1996). STAT3 and STAT5 are key players in Th17 and Treg cell differentiation, respectively. In Th17 cells, IL-6 signaling activates STAT3 to induce RORγt expression (Yang et al., 2011), whereas IL-2 allows STAT5 to induce Foxp3 expression in Treg cells (Burchill et al., 2007). Although the role of STATs in CD4$^+$ Th cell differentiation has been extensively studied, STAT regulation of ncRNAs in the context of the immune system is less well understood. We explored the

role of STATs in modulating the expression profile of regulatory non-coding RNAs in the CD4$^+$ Th cell subsets.

As an overview, we initially performed miRNA expression profiling on CD4$^+$ T cells from mice with specific STAT-deficiencies and littermate controls during *in vitro* polarization to different Th cell subsets (Th1, Th2, and Th17). From this profile, we discovered numerous differentially expressed miRNA that are putatively regulated by different STAT family members (STAT4, STAT6 and STAT3). As a result, we hypothesized that the expression of certain miRNAs among the different CD4$^+$ Th cell subsets are induced by STAT4 in Th1, STAT6 in Th2 and STAT3 in Th17 cells. To address whether STATs directly upregulate miRNA, we took advantage of publicly available genome-wide binding profiles for STAT3 (Durant et al., 2010). We found that STAT3 binds to miRNA genes that are highly expressed in Th17 cells. Herein we describe our analyses of the miRNA profiling and published ChIP-seq datasets. We further reveal a STAT3-miR-155 and STAT3-miR-29a axis and investigate the putative role of STAT3 in inducing miRNA-29 expression in Th17 cells.

3.2 Altered CD4$^+$ T helper cell miRNA expression in the absence of STAT4, STAT6 and STAT3

To assess whether STATs regulate miRNA expression in CD4$^+$ T cells, we differentiated CD4$^+$ T cells from STAT4 KO, STAT6 KO and STAT3fl/fl; CD4-cre mice along with littermate controls into Th1, Th2, and Th17 cells, respectively. We performed miRNA expression profiling on these cells using the NanoString platform. Following normalization, we plotted the miRNA counts in a scatter plot and highlighted miRNA

with at least a 1.5 fold difference between STAT-deficient and littermate control mice (Figure 5A-C). Based on this profile, we observed unique STAT-dependent miRNA signatures among the different CD4$^+$ Th cell lineages. For example, miR-21, miR-155 and the miR-29a/b cluster were highly expressed in the Th17 cells, and these miRNAs required STAT3 expression (Figure 5C-D). Using RT-qPCR, we were able to further validate the differential expression of miR-132 in Th1 cells; miR-132, miR-101 and miR-21 in Th2 cells; miR-155, miR-21, miR-29 cluster, and miR-182 cluster in Th17 cells (Figure 5E-G). These validations revealed statistically significant miRNA differential expression between the relevant STATs in each of the CD4$^+$ Th cell subsets.
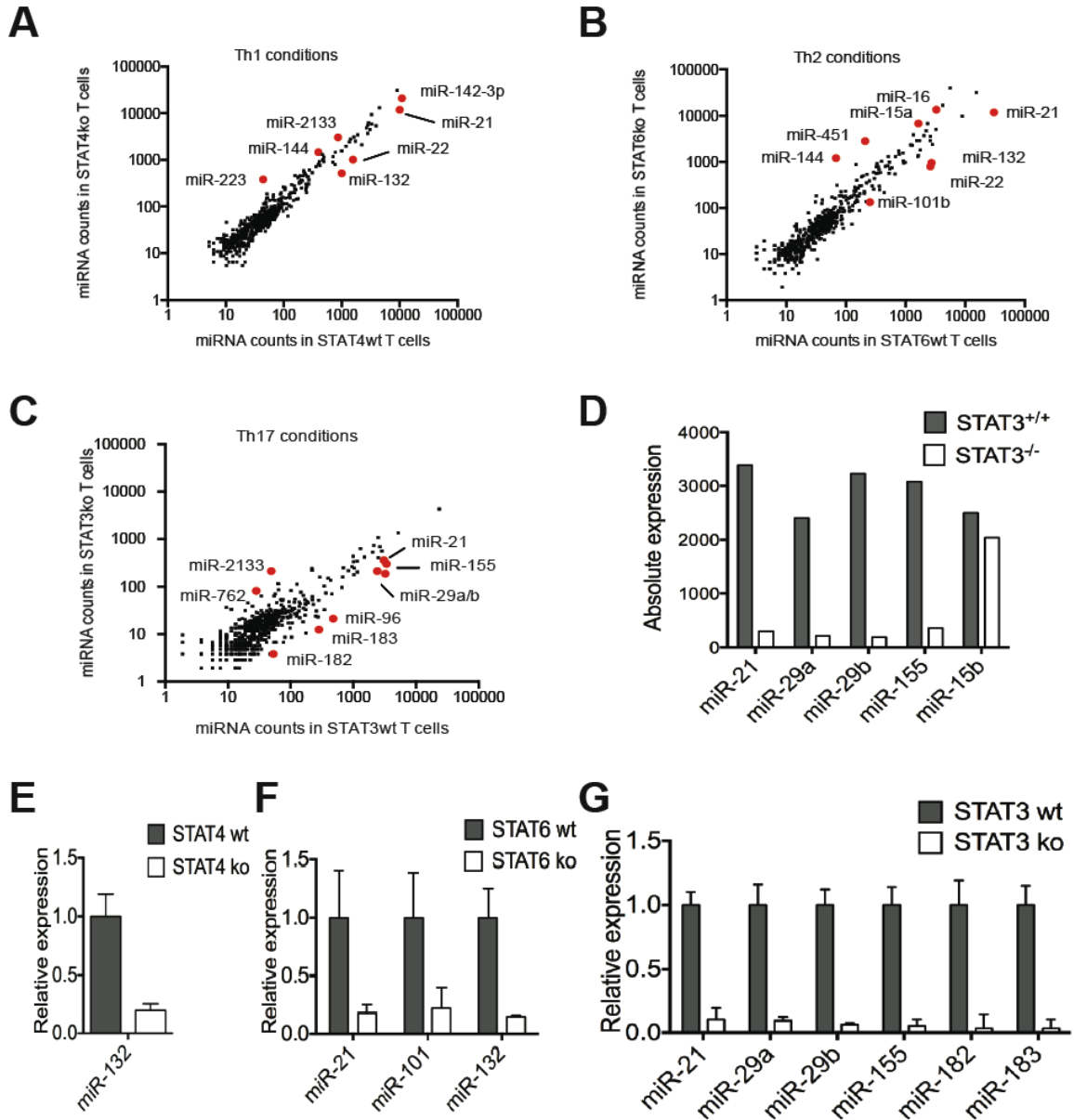
Figure 5. STATs are required for miRNA expression in CD4⁺ Th cell subsets.

Analysis of absolute miRNA read counts obtained from Th1 cells (A), Th2 cells (B) and

Th17 cells (C) in the presence and absence of their relevant STATs. miRNA with >1.5

fold change are highlighted in red and raw digital reads were first normalized to the sum

of positive control count values per manufacturer's recommendation and to

housekeeping genes. (D) Depiction of absolute expression for representative miRNA

from Th17 cells that require STAT3 for expression and miR-15b as a control. (E-F) Taqman validations from differentially expressed miRNA found in (A), (B) and (C) and normalized to U6 and to their littermate controls. CD4$^+$ T cells were obtained from lymph nodes of STAT4 KO, STAT6 KO and STAT3 KO and littermate controls (wild type) and were polarized under Th1 cell, Th2 cell and Th17 cell conditions for 4 days prior to miRNA profiling experiments.

3.3 The Th17 cell transcriptional program targets miRNA and STAT3 promotes the *in vivo* expression of miR-155

Since miR-155 and miR-29a/b are highly expressed in Th17 cells and require STAT3 for their expression, we investigated whether the Th17 cell transcriptional components (Figure 3) directly bind to these miRNA genes. Analysis of the *Mir29* and *Mir155* loci revealed highly enriched H3K4me3 and P300 sites, which suggests an active transcriptional region in Th17 cells (Figure 6A-B). Furthermore, through ChIP-seq analysis we established that STAT3, IRF4 and BATF, but not RORγt bind to *Mir29* and *Mir155* (Figure 6A-B). Of note, a similarly active transcriptional pattern was found for *Rorc*, the gene encoding the Th17 cell "master" regulator RORγt (Figure 6C). To validate the enrichment of STAT3 binding in the vicinity of these miRNA, we performed STAT3 ChIP on *Mir29ab* and *Mir155* loci (Figure 6D). We found increased occupation of STAT3 at the highly expressed miRNA loci compared to a 5kb distant region from the miR-155 promoter as a negative control (Figure 6D).

To determine whether CD4$^+$ T cell expression of STAT3 is necessary for the upregulation of miR-155 *in vivo*, we set up a collaboration with the laboratory of Dr. Charles Egwuagu in the National Eye Institute (NIH). We chose Experimental Autoimmune Uveitis (EAU) as an experimental model, as this eye disorder involves T cell specific expression of STAT3 for disease development (Figure 7A), as well as results in a Th17 cell-rich environment that requires STAT3 (Figure 7B). In comparison to littermate controls (wild type), CD4-STAT3 KO mice did not induce miR-155 expression during EAU (Figure 7C), which can implicate miR-155 in disease progression (Escobar et al., 2013).

37
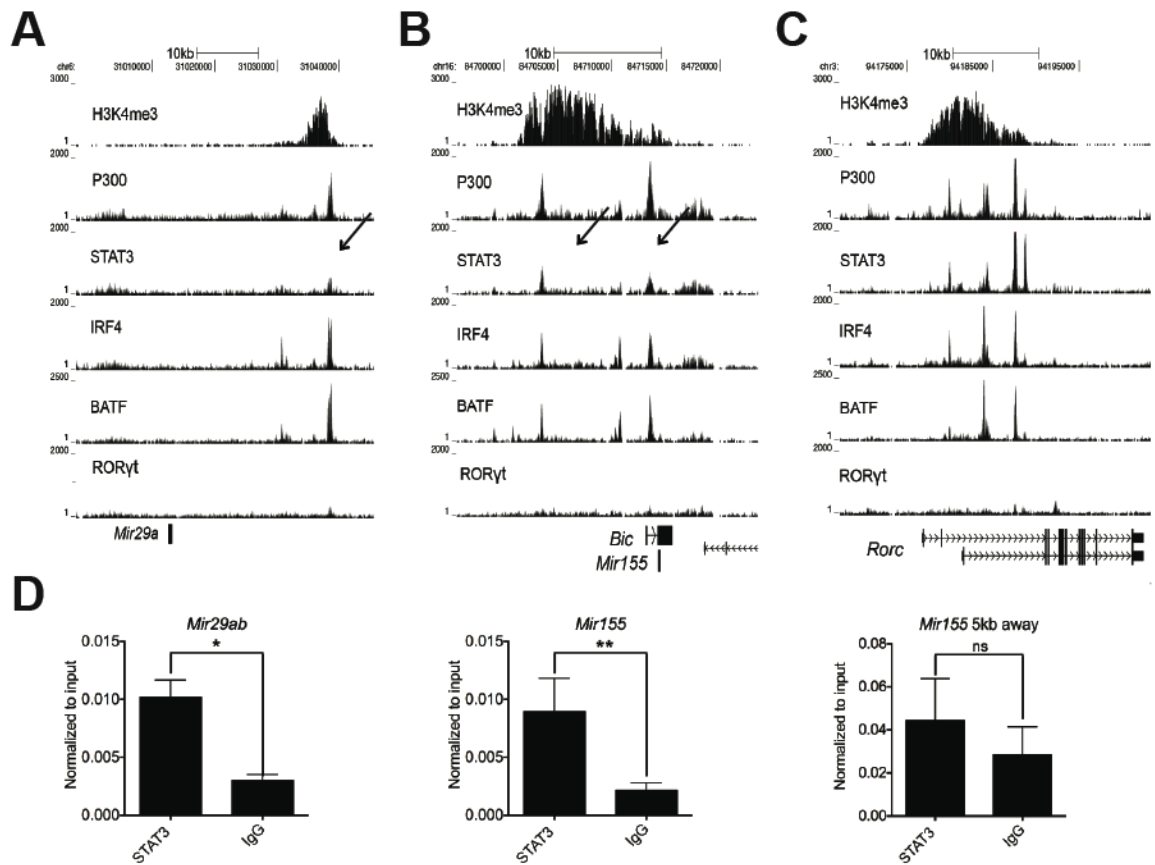
Figure 6. The Th17 cell transcriptional network targets miRNA genes. (A-C)

Genome browser screen-shot of mouse *Mir29ab* (A), *Bic/Mir155* (B) and *Rorc* (C) loci

depicting H3K4me3, P300, STAT3, IRF4, BATF, and RORγt ChIP-seq of Th17 cell

cultures. Data were downloaded from GSE40918 (Ciofani et al., 2012). Arrows depict

regions used for validation. (B) STAT3 or IgG ChIP-qPCR for *Mir29ab*, *Mir155* and a

negative control (5kb distant region from the miR-155 promoter). ChIPs were normalized

to input and statistical significance was determined using Student's t test ($*p < 0.05$, $**p$

< 0.01, ns = not significant).
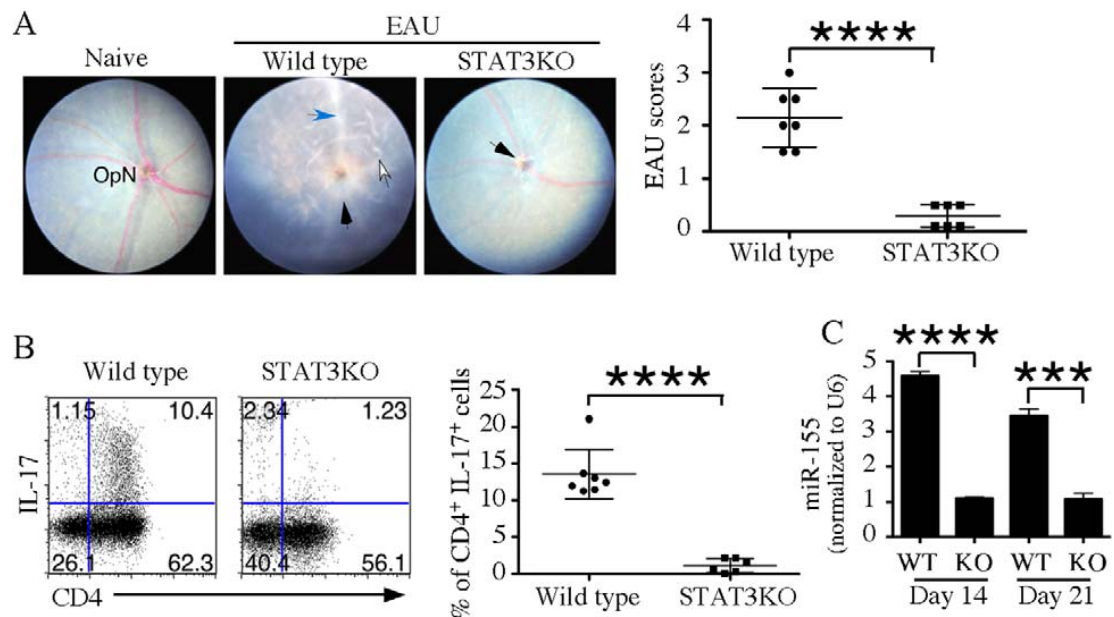
Figure 7. Resistance of CD4-STAT3 KO mice to EAU correlates with defective expression of miR-155. (A) Wild type or CD4-STAT3 KO mice were immunized with IRBP in CFA, and 21 days after immunization the eyes were examined by funduscopy. (B) Freshly isolated lymph node cells from wild type or CD4-STAT3 KO mice (day 21 after immunization) were analyzed for intracellular cytokine staining. CD4$^+$ T cells were gated on and the numbers in each quadrant indicate the percentage of CD4 or IL-17A expression. (C) Lymph node cells were isolated at Day 14 and Day21 time points after immunization from mice described, and RNA was analyzed for the expression of miR-155 by RT-qPCR. Data are representative of at least 2 independent batches of experiments (n = 4 or 5 mice per experiment). Statistical significance was determined using Student's t-test (***$p < 0.001$ and ****$p < 0.0001$) (Reprinted by permission from Association for Research in Vision and Ophthalmology, Escobar et al., 2013).

3.4 A role for STAT3 and miR-29a/b expression in CD4^{+} Th cell differentiation

MiR-29 was recently identified to regulate IFNγ and its Th1 associated genes, Tbet and Eomes (Ma et al., 2011; Steiner et al., 2011). In our miRNA profiling experiments, we found high miR-29a/b expression in Th17 cells (Figure 5C), which required STAT3 for expression (Figure 5C-D and 5G). Since the miR-29a/b cluster is also a direct STAT3 target (Figure 6A and D), we investigated the role of miR-29 in Th17 cells. Analysis of Th17 cells from STAT3 KO mice revealed a lack of IL-17a expression and high IFNγ expression (Figure 8A). Based on these findings, we hypothesized that this increased production of IFNγ in absence of STAT3 is due to the inability to upregulate miR-29a/b expression, which prevents IFNγ production by downregulating Tbet and Eomes. We validated the increased expression of miR-29 targets Tbet and Eomes along with IFNγ transcript levels in STAT3 KO Th17 cells when compared to WT littermates (Figure 8B).

We next investigated the expression profile of miR-29a/b among the different polarized CD4^{+} Th cell lineages (Th1 cells, Th2 cells, Th17 cells, and Treg cells). We found highest miR-29a expression in Th17 cells and iTreg cells (Figure 8C). Since STAT3 was necessary for the expression of miR-29 in Th17 cells, we examined whether STAT3 similarly drives miR-29a/b expression in iTreg cells. When CD4^{+} T cells were differentiated into iTreg cells in the presence or absence of STAT3, we observed a decrease in miR-29a/b expression in absence of STAT3 as compared to littermate controls (Figure 8D). The STAT3 KO iTreg cells also had a 5% increase in IFNγ (Figure 8E) as well as an increase in Tbet and Eomes expression in comparison to littermate controls (wild type) (Figure 8F).
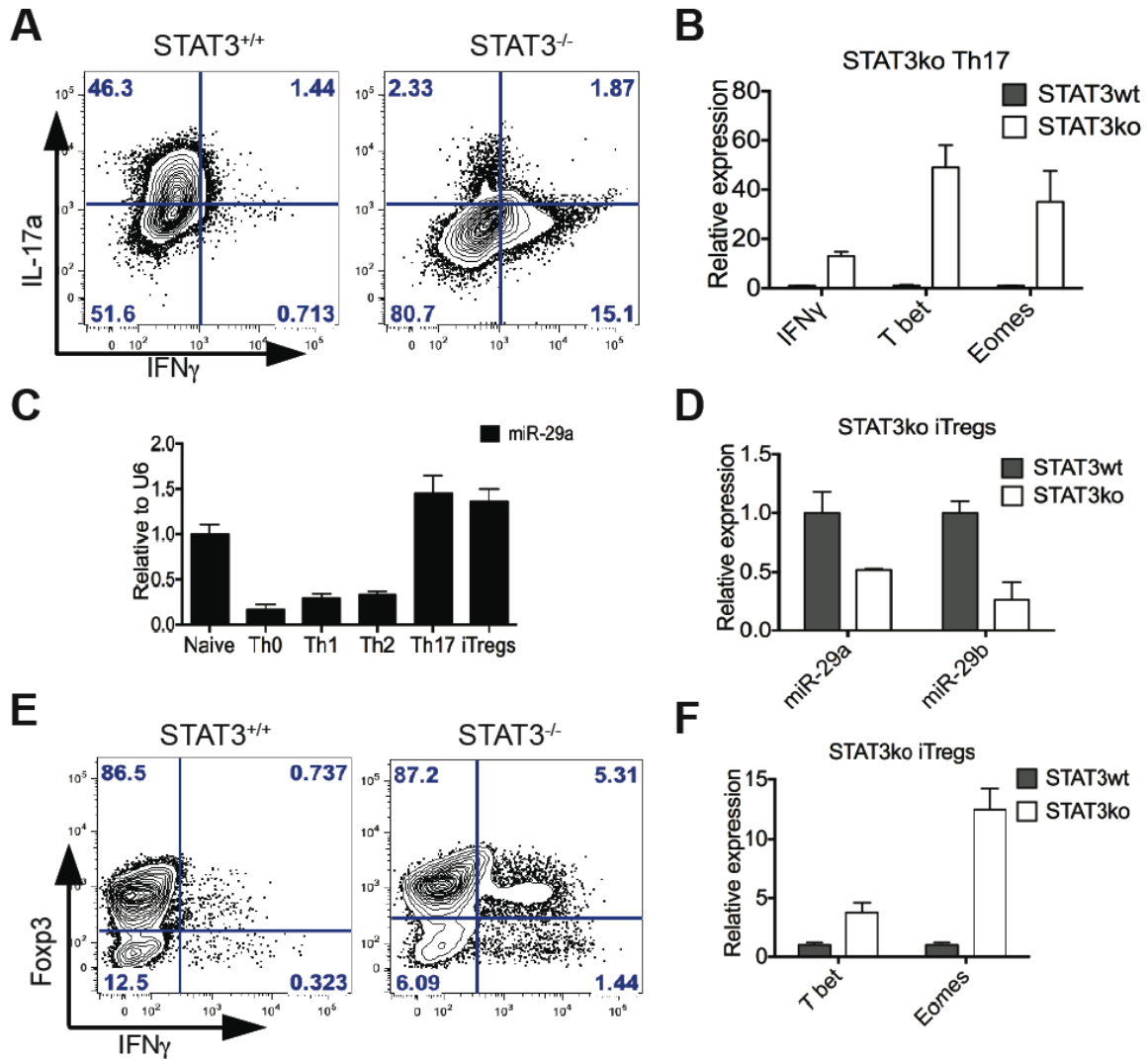
Figure 8. miR-29 downregulation correlates with increased IFNγ expression in STAT3 KO CD4^{+} Th cells. (A) Phenotypic analysis of Th17 cells from STAT3 KO and littermate control mice depicting IL-17a and IFNγ expression by flow cytometry. (B) Relative mRNA expression of IFNγ, Tbet and Eomes determined by RT-qPCR in Th17 cells from STAT3 KO and littermate control mice. (C) RT-qPCR of miR-29a expression in CD4^{+} T cells cultured under Th0, Th1, Th2, Th17, and iTreg cell conditions for 4 days. (D) miR-29a/b expression in iTreg cells from STAT3 KO and littermate control (wild type) mice. (E) Phenotypic analysis of iTreg cells from STAT3 KO and littermate control

mice depicting Foxp3 and IFNγ expression by flow cytometry. (F) Expression of Tbet

and Eomes in iTreg cells from STAT3 KO and littermate control mice. Relative gene

expression was determined by normalizing to Gapdh and relative miRNA expression was

found by normalizing to U6 and to naïve miR-29a expression. For all panels, the data are

representative of two independent experiments using two mice per experiment. Error bars

represent standard error of two experimental replicates.

3.5 A STAT3-miR-29 axis in Th17 (TGFβ) and Th17 (IL-23) cells

IFNγ production by Th17 and iTreg cells has been described in multiple systems, mostly *in vivo,* as IL-17a⁺IFNγ⁺ and iTreg⁺IFNγ⁺ are associated with increased autoimmunity (Hirota et al., 2011). The adoptive transfer of *in vitro* derived Th17 cells has recently been shown to lead to the induction of Experimental Autoimmune Encephalitis (EAE) in mice. Following adoptive transfer, these pathogenic Th17 cells begin to produce high levels of IFNγ and express Tbet and Eomes (Ghoreschi et al., 2010). Interestingly, the differentiation requirements for these pathogenic Th17 cells do not involve TGFβ signals that are conventionally associated with Th17 cell polarization, but rather require IL-23 signaling. These cells were subsequently named Th17 (23) cells since they require IL-23 to delineate from the conventional *in vitro* polarization of Th17 cells that need TGFβ, Th17 (TGFβ) (Ghoreschi et al., 2010).

To determine whether miR-29a/b expression was altered in the pathogenic Th17 (23) cells, accounting for the upregulation of IFNγ, Tbet and Eomes, we polarized naïve CD4⁺ T cells in presence of TGFβ to generate Th17 (TGFβ) cells or IL-23 to generate Th17 (23) cells. We observed a significant decrease in miR-29a/b expression under Th17 (23) cell polarization compared to Th17 (TGFβ) cells (Figure 9A). Moreover, Tbet and Eomes were overexpressed in Th17 (23) cells (Figure 9B). Using flow cytometry to assess the production of IL-17a and IFNγ in Th17 (TGFβ) and Th17 (23) cells, we found high levels of IL-17a expression under both polarizing conditions. Surprisingly, we did not observe increased production of IFNγ in polarized Th17 (23) cells even when Tbet and Eomes expression is high (Figure 9C). Therefore, miR-29 expression is differentially regulated between Th17 (TGFβ) and Th17 (23) cells.

We next assayed whether STAT3 influences the differential expression of the miR-29a/b cluster under Th17 (TGFβ) and Th17 (23) cell polarizing conditions. Following analysis of the publically available dataset (Durant et al., 2010; Ghoreschi et al., 2010), we found that although a STAT3 peak is present at the *Mir29ab* locus under Th17 (TGFβ) cell polarizing conditions, no such binding of STAT3 is present for Th17 (23) cells (Figure 9D, top panel). The ability of STAT3 to bind to the *Il21* promoter under both conditions (Figure 9D, lower panel) suggests that the STAT3-miR-29 axis is impaired in Th17 (23) cells. This impaired STAT3-miR-29 axis may account for the increased Tbet and Eomes expression in Th17 (23) cells.

Due to the enhanced Tbet and Eomes expression of Th17 (23) cells compared to Th17 (TGFβ) cells, we decided to overexpress miR-29a in Th17 (23) cells to examine whether miR-29 alone can decrease these transcription factors' expression. The introduction of a miR-29a GFP-retrovirus (rv) during Th17 (23) conditions corrected the aberrant Tbet expression and partially reduced Eomes expression when compared to Th17 (23) cells transduced with GFP-rv (Figure 9E). Furthermore, the level of Tbet expression in Th17 (23) cells transduced with miR-29a GFP-rv was comparable to Th17 (TGFβ) differentiated cells. As such, the forced expression of miR-29a in Th17 (23) cells is sufficient to reduce Tbet and Eomes expression.
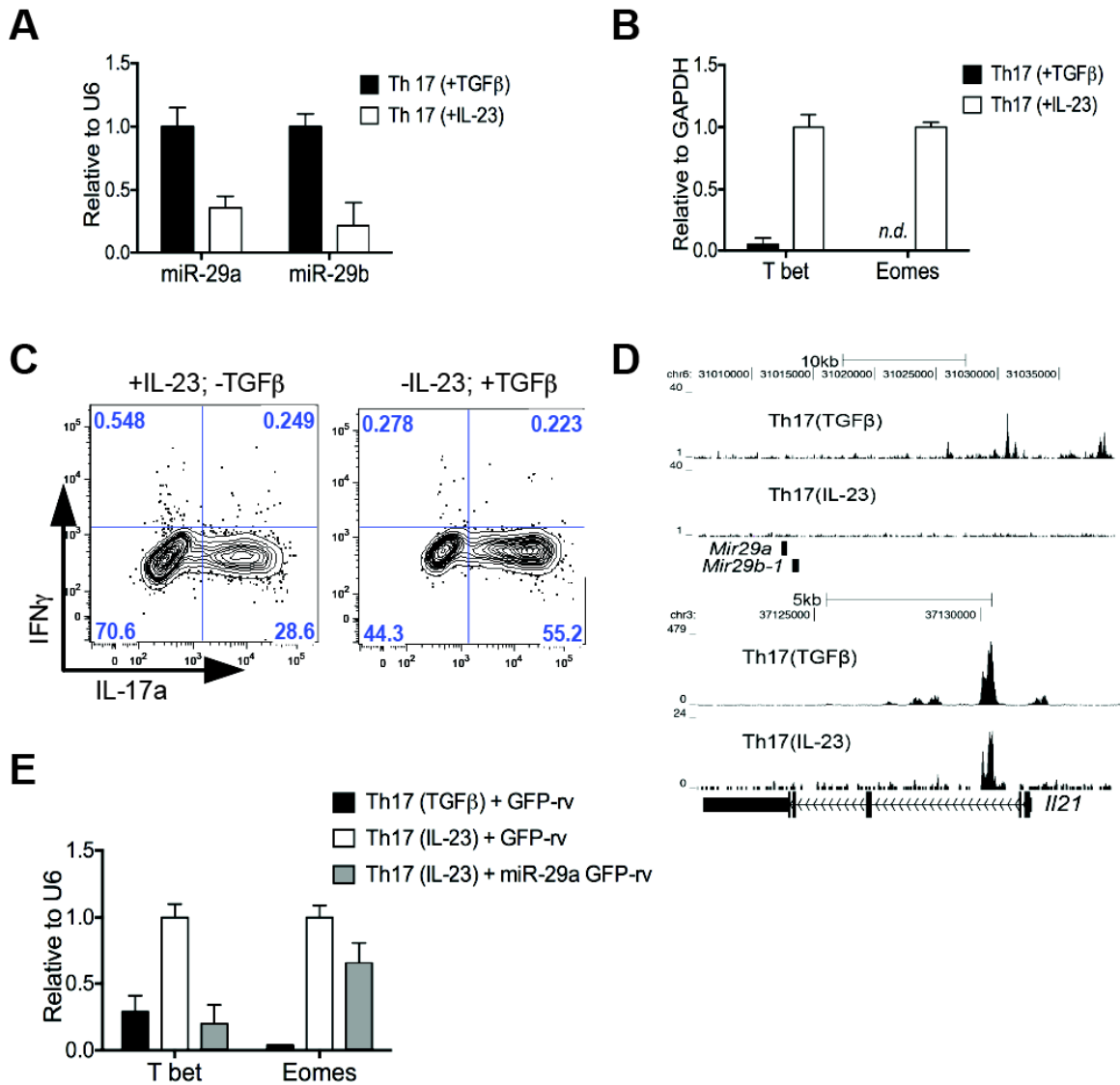
Figure 9. A STAT3-miR-29 axis in polarized Th17 cells in the presence of IL-23 and absence of TGFβ. RT-qPCR analysis of (A) miR-29a and miR-29b expression and (B) T-bet and Eomes expression from Th17 (TGFβ) and Th17 (23) polarized cells. (C) Phenotypic analysis of CD4+CD44+ Th17 (23) cells (left panel) and Th17 (TGFβ) cells (right panel) depicting IFNγ and IL-17a expression by flow cytometry. (D) Genome Browser screen shots from ChIP-seq experiments showing STAT3 binding sites on

45

Mir29ab and *Il21* loci in Th17 (TGFβ) and Th17 (23) cells. (E) Differential expression of

Tbet and Eomes in Th17 (TGFβ) and Th17 (23) cells when transduced with miR29a

GFP-rv or GFP-rv. The relative miRNA expression was normalized to U6 and the

relative mRNA expression was normalized to Gapdh. For this experiment, cells were

cultured in serum-free media. N.d. (not detected).

3.6 Overexpression of miR-29a GFP-rv in Th17 (23) cells reduces Th17 pathogenicity

Given that the transduction of Th17 (23) cells with miR-29a GFP-rv reduced the altered Tbet expression and partially decreased Eomes expression, we tested the pathogenicity of these miR-29a GFP-rv transduced Th17 (23) cells in an adoptive transfer model of EAE. For this purpose, we transduced TCR transgenic (2D2) T cells that are specific for myelin oligodendrocyte glycoprotein with either miR-29a GFP-rv or GFP-rv under Th17 (23) polarizing conditions. GFP$^+$ cells were then isolated via FACS and adoptively transferred to Rag2 deficient mice (Figure 10A). After the onset of disease, we found that mice given miR-29a GFP-rv transduced Th17 (23) cells had less disease progression when compared to mice given GFP-rv Th17 (23) cells (Figure 10B). These findings suggest that overexpression of miR-29a halts disease pathogenicity of Th17 (23) cells, maybe through the reduction of Tbet, Eomes and IFNγ expression.
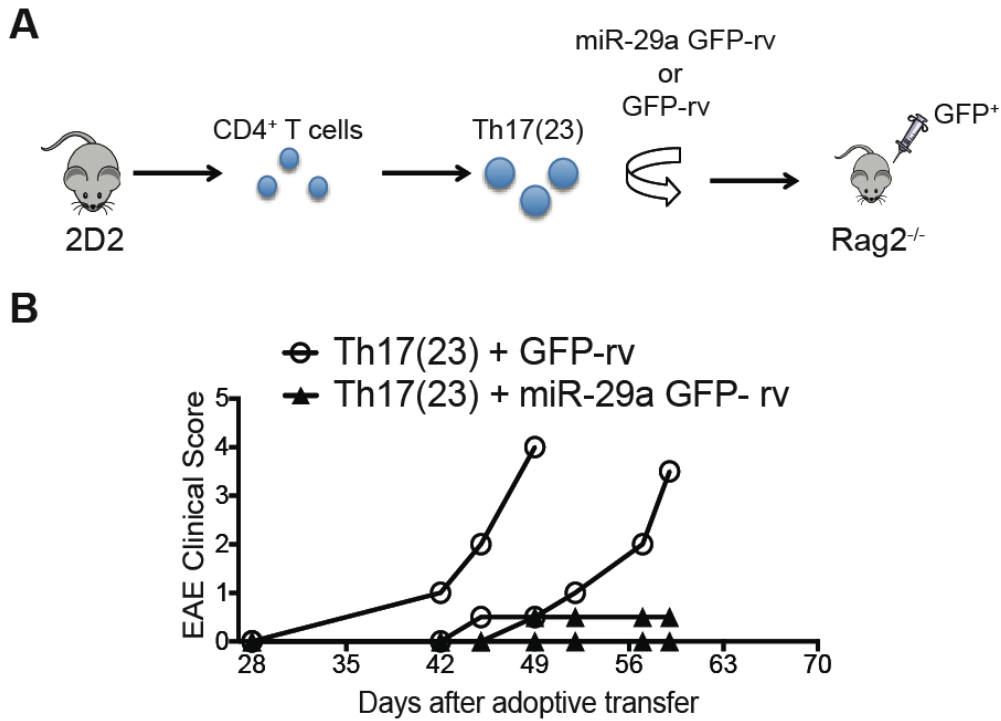
Figure 10. miR-29 overexpression reduces the pathogenicity of Th17 (23) cells. (A) Schematic of a passive model of EAE using T cells from 2D2 TCR transgenic mice to initiate the onset of disease. (B) EAE clinical score denoting disease progression from Rag2 KO mice that were given either miR-29 GFP-rv or GFP-rv transduced Th17 (23) cells.

3.7 Summary of Findings

Although several studies have shown critical roles of miRNA in the differentiation and function of CD4$^+$ Th cells (Baumjohann and Ansel, 2013), the mechanism(s) controlling miRNA expression in these cells remains unknown. We aim to understand the transcriptional networks involved in regulating miRNA in CD4$^+$ Th cells and find that STATs have a critical role in this process (Figure 5A-C). Furthermore, our analysis of STAT3 in Th17 cell differentiation uncovers the necessary role for STAT3 in upregulating miR-21, miR-155 and miR-29a/b expression in Th17 cells (Figure 5C, D and G). We also find that the Th17 transcriptional network binds to the miRNA genes, *Mir155* and *Mir29ab* (Figure 6A-B) to promote Th17 development.

Based on our observation of a direct STAT3-driven regulation of miR-29/b expression in Th17 cells, we further explore the role of miR-29 in repressing Th1 cell associated genes in Th17 and iTreg cells. We find that Th17 and iTreg cells deficient in STAT3 have a dramatic decrease in miR-29a and miR-29b expression (Figure 5D and 8D), suggesting that failure to induce miR-29a/b expression is accompanied by an increased expression of Tbet, Eomes and IFNγ. Our data indicates that STAT3 enhances miR-29a/b expression in order to repress Th1 cell associated genes, thereby eliminating a Th1 cell fate in Th17 and iTreg cells. To this extent, we are interested in generating a miR29a/b KO mouse to determine if the absence of miR-29 results in increased expression of IFNγ in Th17 and iTreg cells. This line of experimentation may have implications for the role of miR-29 in the development of autoimmune disease.

Furthermore, we find that the pathogenicity of Th17 (23) cells can be alleviated *in vivo* by the over-expression of a single miRNA (Figure 10B). We need to next examine

whether the decrease in disease severity by the introduction of miR-29a is the result of decreased Tbet and Eomes expression leading to the attenuation of IFNγ producing Th17 cells. In a model of autoimmune colitis, a higher proportion of IFNγ$^+$ CD4$^+$ T cells were recovered from spleens of mice after adoptive transfer of STAT3 KO T cells (Durant et al., 2010). It would be of interest to determine whether miR-29 also governs abberant IFNγ production in this model. Genome-wide association studies have identified polymorphisms in the IL23R, JAK2 and STAT3 genes associated with increased susceptibility to Inflammatory Bowel Disease (IBD) (Barrett et al., 2008; Duerr et al., 2006). As such, it would again be of interest to examine if polymorphisms in the *Mir29ab* gene are also associated with IBD and potentially other autoimmune diseases.

In summary, our strategy examining a requirement for STAT4, STAT6 and STAT3 in miRNA expression led us to find critical roles for STATs in regulating the expression of miRNAs. These data contribute to the understanding of STATs in regulating miRNA expression and the function of miRNAs in the differentiaiton of CD4$^+$ Th cell lineages.

Chapter 4: The intricate network of transcription factors, microRNA

and epigenetics shape Th17 cell differentiation

4.1 Determining the mechanism behind the regulation of Th17 cells by miR-155

Transcriptional and epigenetic programs initiated within CD4^{+} T cells must work together to promote changes in gene expression, ultimately resulting in production of Th subset signature cytokines (Ciofani et al., 2012; Kanno et al., 2011; Yosef et al., 2013a). miRNA provide a layer of post-transcriptional gene expression in addition to the more classical transcriptional networks. Recently, the transcription factor network necessary for Th17 cell differentiation was determined (Ciofani et al., 2012). However, the role of miRNAs and chromatin regulators in association with this intricate transcriptional network is still lacking.

In this project, we performed unbiased transcriptomic analyses comparing wildtype (WT) and miR-155 knock-out (KO) Th17 cells and found Jarid2 to be upregulated in the absence of miR-155. Jarid2 was discovered to be essential for the recruitment of PRC2 to genomic sites in embryonic stem (ES) cells (Herz and Shilatifard, 2010; Li et al., 2010; Peng et al., 2009; Shen et al., 2009). However, the function of Jarid2 in adult somatic cells such as lymphocytes is not known. Analysis of Jarid2-deficient CD4^{+} T cells allowed us to identify direct targets of PRC2 in Th17 cells. Furthermore, deletion of Jarid2 in the miR-155 KO CD4^{+} T cells results in rescue of Th17 cytokine expression and partial rescue of Treg cells. Thus, we demonstrate that miR-155 and Jarid2 form a regulatory circuit that can control lineage specific gene expression in Th17 and Treg cells through its effect on Polycomb recruitment. Finally, we propose an integrated model for miR-155 and Jarid2 in the regulatory network for Th17 cell fate specification.

4.2 miR-155 is required for the proper expression of Th17 cytokines

To determine whether miR-155 plays a cell autonomous role in CD4$^+$ T cells *in vivo*, we generated mixed bone marrow (BM) chimeras and examined miR-155 KO and WT CD4$^+$ T cells within the same host (Figures 11A-B).
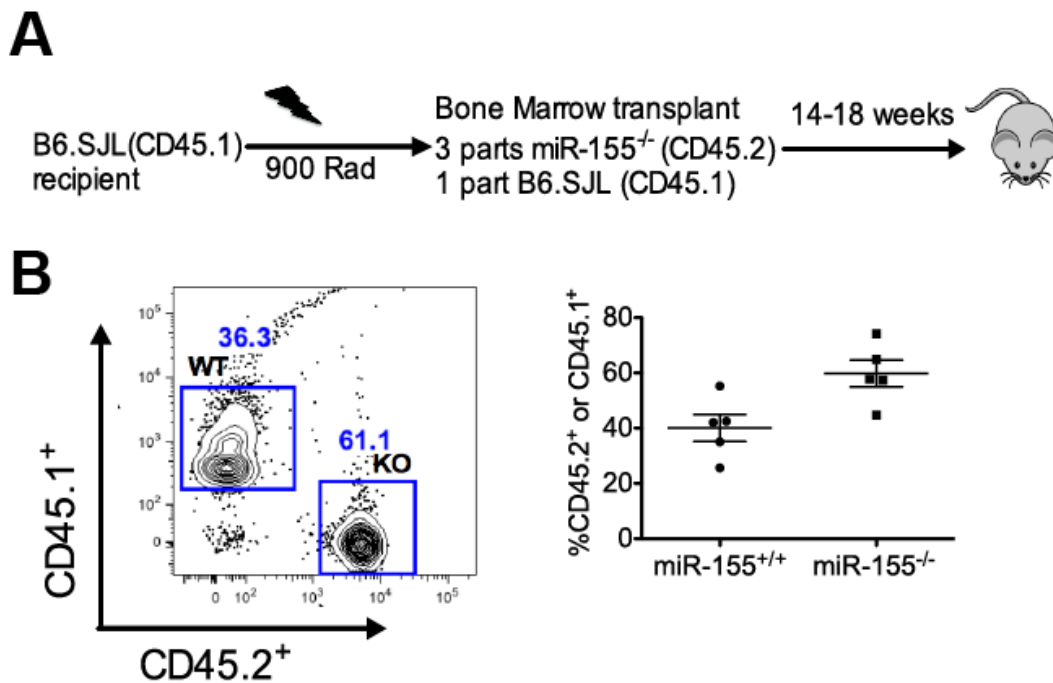
Figure 11. miR-155 KO and WT mixed bone marrow (BM) chimeras. (A) Schematic of mixed BM chimera experiment. (B) FACS analysis of miR-155$^{-/-}$ (CD45.2$^+$) and miR-155$^{+/+}$ (CD45.1$^+$) cells from the mesenteric lymph node (MLN) of mixed BM chimera and the corresponding percentages of total lymphocytes that are either CD45.2$^+$ or CD45.1$^+$ after reconstitution.

We studied a population of Th17 cells present in the mesenteric lymph nodes (MLN) of these mixed BM chimeras. Flow cytometry on restimulated $CD4^+TCR\beta^+CD44^+$ T cells from the MLN revealed a deficit of cytokine-producing $ROR\gamma t^+IL\text{-}17a^+$ Th17 cells among the miR-155 KO population compared to WT (Figures 12A-B). No significant change in $ROR\gamma t^+IL\text{-}17a^-$ Th cells that have undergone lineage specification was observed. We also found a cell autonomous defect in the production of both IL-17a and IL-22 by miR-155 KO $CD4^+$ T cells upon restimulation *ex vivo* (Figures 12C-D). Therefore, $CD4^+$ T cells deficient in miR-155 display cell intrinsic defects in Th17 cytokine expression.

Previously, miR-155 KO $CD4^+$ T cells were reported to have a defect in IFNγ and IL17A expression following *H. pylori* infection (Oertli et al., 2011). To address the role of miR-155 in Th1 and Th17 development, we employed the murine model of peroral *Toxoplasma gondii* infection, which is known to induce a highly polarized Th1 effector population as well as a localized Th17 response in the small intestine (Liesenfeld, 2002). Analysis of $CD4^+TCR\beta^+CD44^+$ T cells in the lamina propria of the small intestine (siLP) revealed a cell intrinsic defect in IL-17a and IL-22 production among the miR-155 KO population upon restimulation (Figures 12E-F). However, we found comparable IFNγ production by both WT and miR-155 KO cells (Figures 12G-H). These data demonstrate that miR-155 is specifically required for Th17 cytokine expression, but dispensable for the antigen-specific Th1 cytokine response upon peroral infection of *T. gondii*.
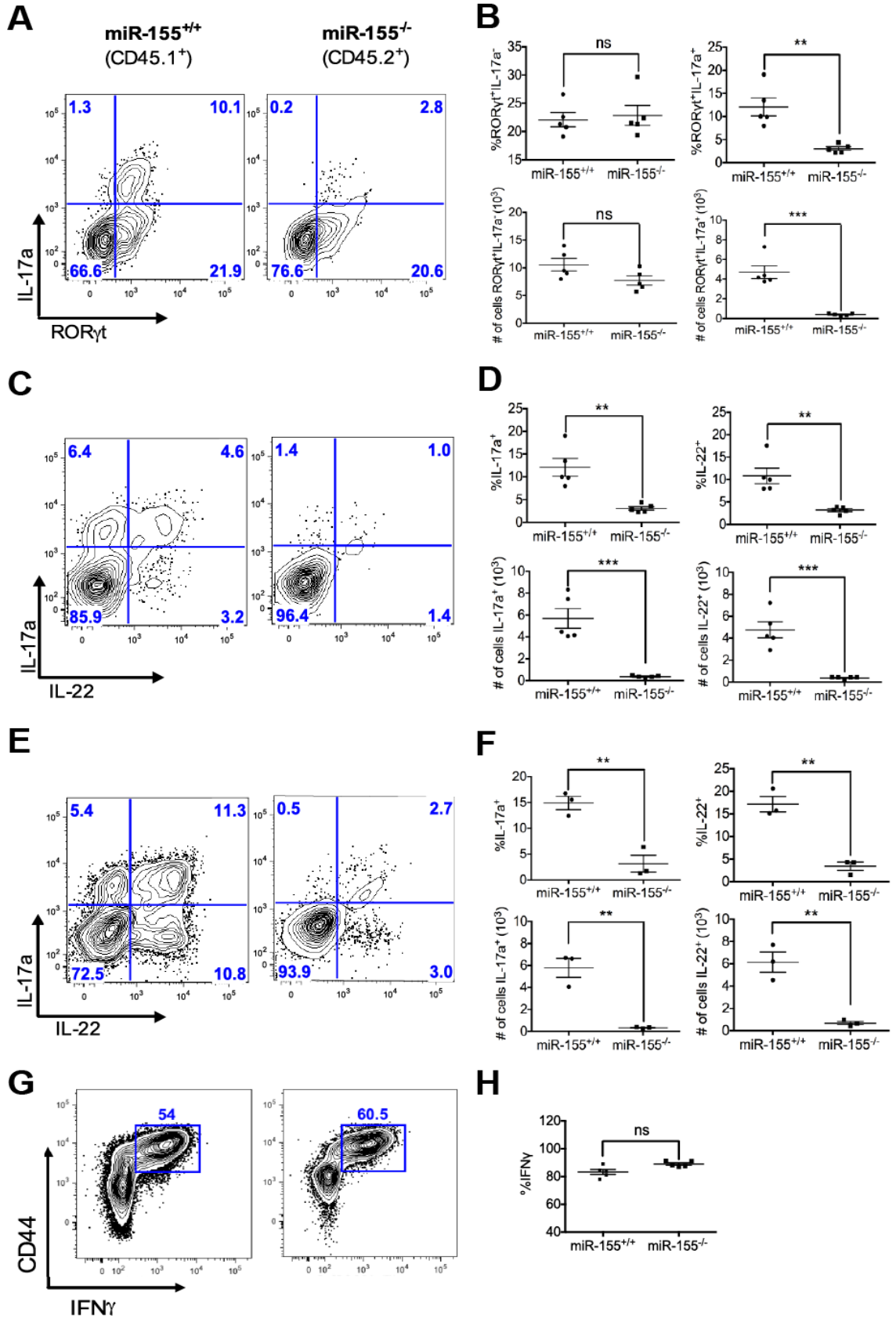
Figure 12. Th17 requirement of miR-155. (A) FACS analysis, (B) percentages and

absolute cell numbers of miR-155$^{+/+}$ (CD45.1^{+}) or miR-155$^{-/-}$ (CD45.2^{+})

CD4^{+}TCRβ^{+}CD44^{+} cells in the MLN of mixed BM chimeras to enumerate IL-17a and/or

RORγt expressing cells (n=5). (C) FACS analysis, (D) percentages and absolute cell

numbers of CD4^{+}TCRβ^{+}CD44^{+} cells that express IL-17a and/or IL-22 among WT and

miR-155 KO cells in the MLN of mixed BM chimeras (n=5). (E,F) FACS analysis (E)

and absolute cell numbers (F) of CD4^{+}TCRβ^{+}CD44^{+} cells that express IL-17a and/or IL-

22 in the siLP of mixed BM chimeras from *Toxoplama* infected mice. (G,H) FACS

analysis (G) and absolute cell numbers (H) of CD4^{+}TCRβ^{+}CD44^{+} cells that express CD44

and IFNγ in the MLN of mixed BM chimeras from *Toxoplama* infected mice. Statistical

significance was determined using unpaired Student's *t* test (* $p<0.05$ and ** $p<0.01$).

4.3 miR-155 is preferentially expressed in mouse and human Th17 cells

Due to the defect in Th17 cells, we hypothesized that miR-155 may be differentially expressed among CD4$^+$ T cell subsets. We found high expression of miR-155 in both the mouse and human Th17 cultures relative to Th1, Th2, Th17 or TGFβ-induced Treg (iTreg) cells (Figures 13A-B). The expression of miR-155 increased over time during polarization of both primary mouse and human Th17 cultures (Figures 13C-D), possibly having a more prominent role in the latter part of Th17 development.
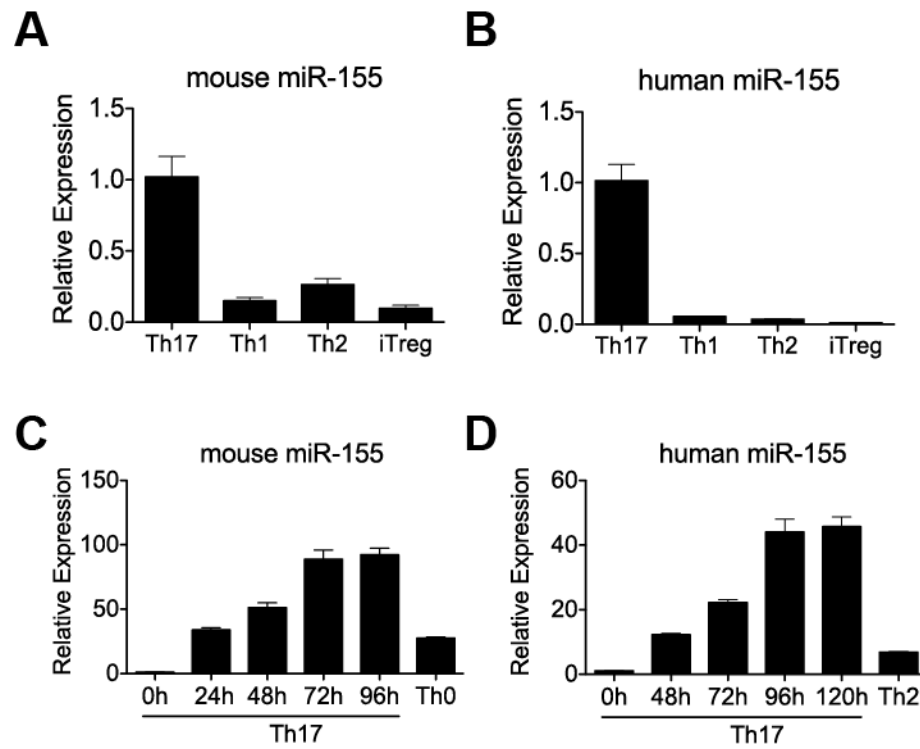
Figure 13. Th17-specific expression of miR-155. (A-D) RT-qPCR analysis of mature miR-155 expression normalized to U6 snRNA levels from the indicated mouse (A) or human (B) CD4$^+$ T cell subsets *in vitro* polarized or during mouse (D) and human (D) Th17 differentiation over a time course of 4 and 5 days, respectively.

4.4 IL-1β can rescue IL-17a defect in miR-155 deficient Th17 cells

To investigate the mechanism of action for miR-155, we polarized CD4$^+$ T cells from miR-155 KO mice and littermate controls towards the Th17 cell fate as previously described with IL-6 and TGFβ cytokines (Korn et al., 2007; Nurieva et al., 2007; Veldhoen et al., 2006). Since IL-1β promotes the *in vivo* development of Th17 cells (Ben-Sasson et al., 2009; Chung et al., 2009; Shaw et al., 2012), we also tested the effects of adding or withholding exogenous IL-1β to Th17 cultures (±IL-1β). Differentiating miR-155 KO Th17 cultures without exogenous IL-1β resulted in reduced IL-17a production as has previously been reported (O'Connell et al., 2010) (Figure 14A). Importantly, we found that miR-155 KO Th17 cultures (- IL-1β) can generate RORγt$^+$IL-17a$^-$ T cells, but they have a defect in producing IL-17a upon restimulation, similar to our results in our *in vivo* mixed BM chimera study (Figure 14A). This defect can be rescued upon addition of exogenous IL-1β to our differentiation conditions (Figure 14B). However, without exogenous IL-1β, we found decreased expression of *Il17a, Il17f, Il1r1*, and *Il22* transcripts in miR-155 KO Th17 cultures compared to WT (Figure 14C). Except for *Il22*, all of these miR-155 dependent gene expression defects were rescued by adding IL-1β to our cultures (Figure 14D). We hypothesize that IL-1 signaling is bypassing the miR-155 regulation of IL-17 expression by inducting a factor that promotes this cytokine expression.
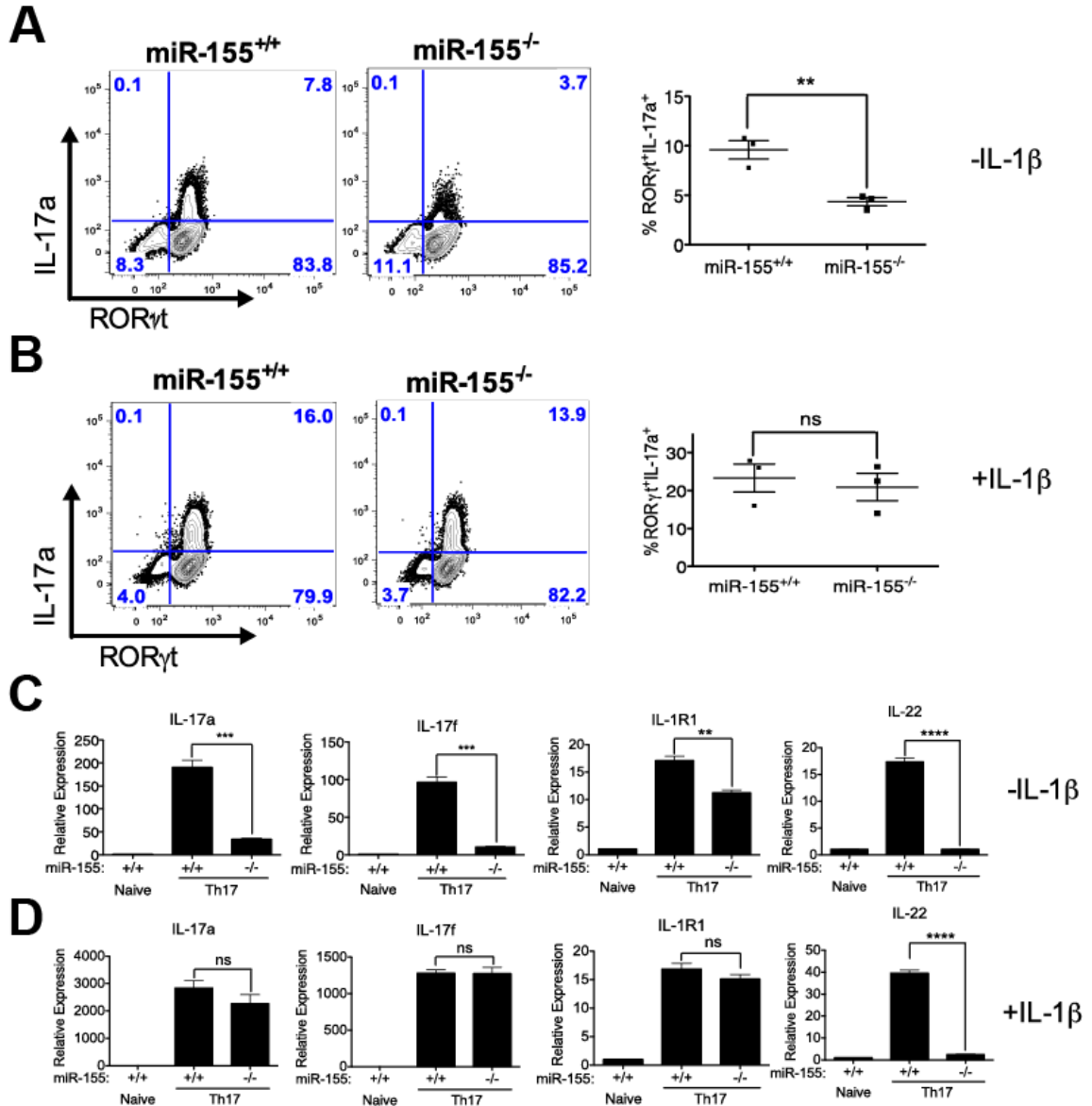
Figure 14. IL-1 signaling can partially rescue gene expression defects in miR-155 KO Th17 cells. (A,B) FACS analysis and percentages of CD4^{+}CD44^{+} T cells expressing IL-17a and RORγt in miR-155 KO or WT Th17 cultures polarized (A) without or (B) with exogenous IL-1β. (C,D) RT-qPCR analyses of *Il17a*, *Il17f, Il1r1*, and *Il22* in miR-155 KO or WT Th17 cultures polarized (C) without or (D) with IL-1β. Relative expression was calculated by normalizing to *Gapdh*. Statistical significance was determined using Student's t test ($*$ p<0.05, $**$ p<0.01 and $****$ p<0.0001).

4.5 Repression of IL-22 expression in miR-155 KO Th17 cultures occurs at the transcriptional level

To systematically determine the consequences of miR-155 deletion on gene expression, we conducted RNA-seq of miR-155 KO and WT Th17 cultures (+ IL-1β). As a result, we found 553 and 551 transcripts that are up- and down-regulated respectively in miR-155 KO Th17 cultures compared to WT controls (Figure 15A). In the absence of miR-155, the known Th17-associated transcription factors and the IL-17 cytokines were unaffected (Figure 15A). However, RNA-seq revealed that expression of *Il22*, *Il10* and *Il9* are reduced in miR-155 KO Th17 cultures (Figures 15A-B).

We first focused on *Il22* gene expression because it was the most differentially expressed transcript between miR-155 KO and WT Th17 cultures. IL-22 production could be regulated at multiple levels, including transcriptional regulation through transcription factors or epigenetic modification and miRNA mediated post-transcriptional regulation. To measure recently transcribed *Il22*, we performed RT-qPCR of unspliced transcripts using primers that amplified an intron of *Il22*, and found that it was significantly decreased in miR-155 KO Th17 cultures compared to WT (Figure 15C). Due to the reduction in transcripts observed, we next performed chromatin immunoprecipitation (ChIP) of RNA polymerase (pol) II at the *Il22* transcriptional start site (TSS) to assess promoter accessibility. There was decreased occupancy of Pol II at the IL-22 TSS in the absence of miR-155 (Figure 15D). Furthermore, we also found a reduction in H3K4me3 at the IL-22 promoter, another indication that the *Il22* promoter is less active in miR-155 KO Th17 cells (Figure 15E). Taken together, our data are consistent with a reduction in *Il22* transcription in miR-155 KO Th17 cultures.

61

Given the above results, we hypothesized that miR-155 is targeting a transcriptional repressor of *Il22*. We considered c-Maf as a reasonable candidate, since it was previously reported as a target of miR-155 as well as a repressor of *Il22* transcription (Rodriguez et al., 2007; Rutz et al., 2011). Indeed, we observed a 2.4 fold up-regulation of c-Maf protein by Western analysis, (Figure 15F). In contrast, SHIP1 and SOCS1, other known miR-155 targets (Lu et al., 2009; O'Connell et al., 2009), were not differentially expressed (Figure 14F). Thus, we considered c-Maf as a viable miR-155 target in Th17 cells.

ChIP-seq was conducted in miR-155 KO and WT Th17 cells to map the locations of c-Maf binding to the genome. In total, we identified about 12,554 and 8,815 c-Maf peaks in WT and miR-155 KO Th17 cells respectively, indicating a loss of c-Maf binding in miR-155 KO cells. Although c-Maf is overexpressed in miR-155 KO Th17 cells, we unexpectedly found fewer peaks of c-Maf binding to chromatin. Importantly, we determined that c-Maf failed to bind to the *Il22* locus in miR-155 KO Th17 cultures (Figure 15G), although it can bind in WT. We did not observe a difference in c-Maf binding to the control *Il17a* locus in miR-155 KO cells under these culture conditions (Figure 15G). All ChIP-seq findings were validated by qPCR (Figure 15H). These findings indicate that another transcriptional repressor is responsible for directly silencing *Il22* in the absence of miR-155, as c-Maf does not bind there.

Since aryl hydrocarbon receptor (AHR) plays a critical role in *Il22* transcription (Veldhoen et al., 2008), we assessed whether stimulating AHR activity could rescue *Il22* expression in miR-155 KO Th17 cells. We found that upon ligation of AHR by an agonist, 6-formylindolo[3,2-b]carbazole (FICZ), the expression of *Il22* is increased, but

still impaired in miR155 KO Th17 cells compared to WT (Figure 15I). In contrast, the

canonical AHR target, *Cyp1a1*, was not differentially regulated in miR-155 KO and WT

Th17 cultures with or without FICZ treatment (Figure 15I). These results suggest that

AHR activity is specifically inhibited at the *Il22* locus and may contribute to the inability

of miR-155 KO Th17 cells to express *Il22*.
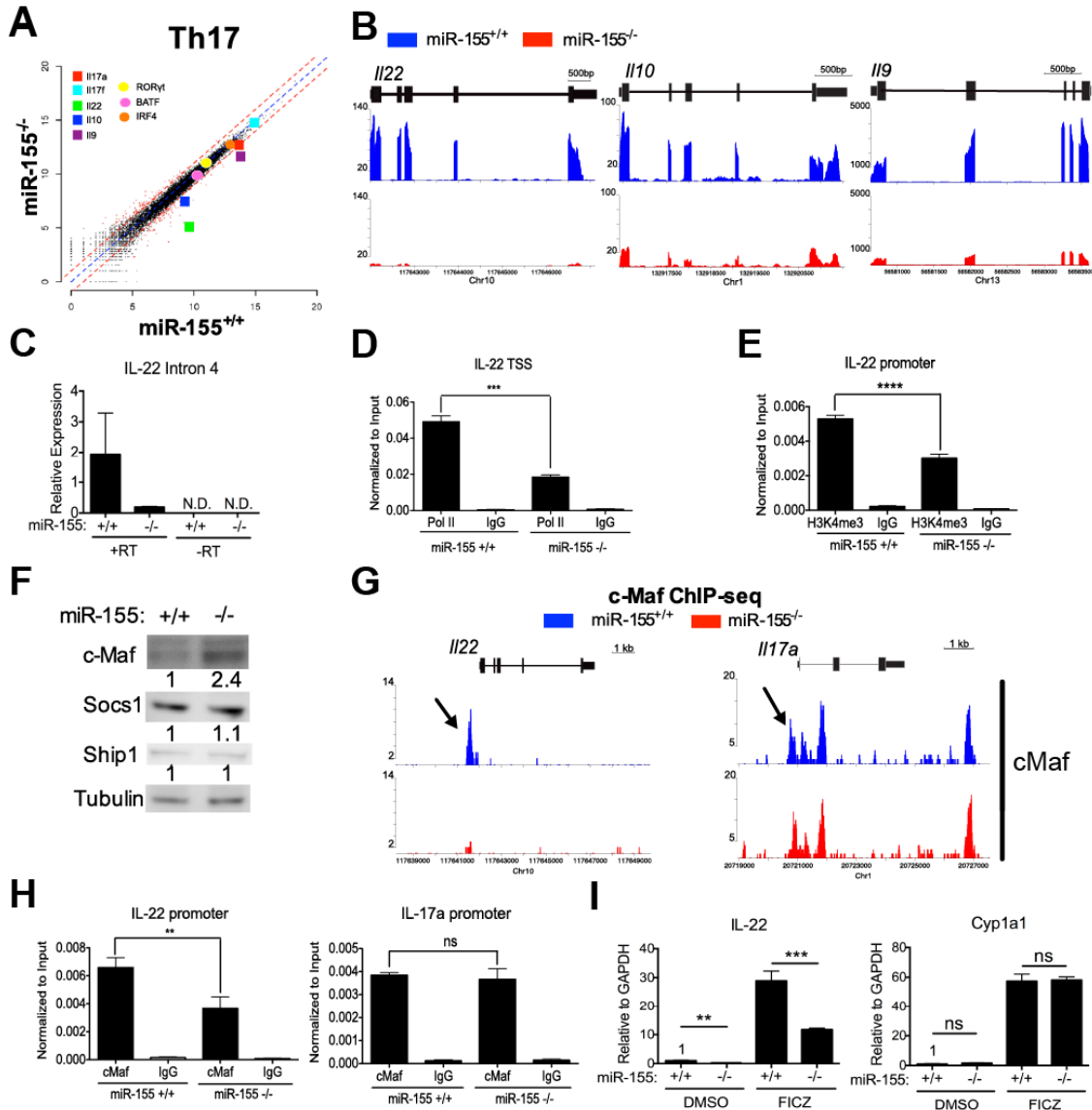
Figure 15. RNA-seq of miR-155 KO and WT Th17 cells identifies altered cytokine expression and putative miR-155 targets. (A) Scatter plot of gene expression for 20,096 RefSeq transcripts in miR-155 KO and WT Th17 cultures measured by RNA-seq. Notable transcription factors and cytokines are highlighted. Dashed red lines indicate a fold change of 2. (B) Genome browser screenshots of *Il22, Il10* and *Il9* loci depict RNA-seq results as normalized coverage tracks in miR-155 KO (red) and WT (blue) Th17 cultures. (C) RT-qPCR of *Il22* intron 4 ± reverse transcriptase (RT) in miR-155 KO and

WT Th17 cultures (+IL-1β). (D) ChIP-qPCR of RNA polymerase II (Pol II) at *Il22* TSS

or (E) H3K4me3 at *Il22* promoter in miR-155 KO and WT Th17 cultures. (F) Western

analysis for c-Maf, Socs1 and Ship1 in miR-155 KO and WT Th17 cultures with protein

expression quantitated using ImageJ and normalized to Tubulin as a control. (G) Genome

browser screenshots of c-Maf peaks in the *Il22* and *Il17a* loci in miR-155 KO (red) and

WT (blue) Th17 cultures. Arrows mark the regions validated by ChIP-qPCR. (H)

Enrichment of *Il22* and *Il17a* promoter was measured by ChIP-qPCR of c-Maf in miR-

155 KO or WT Th17 cultures. (I) Relative expression of *Il22* and *Cyp1a1* mRNA

normalized to *Gapdh* was determined by RT-qPCR in miR-155 KO or WT Th17 cultures

(+ IL-1β) and treated with DMSO or 0.3 μM of FICZ. Statistical significance was

determined using Student's t test (∗∗ p<0.01, ∗∗∗ p<0.001; ns denotes not significant).

4.6 Genome-wide analysis of *in vitro* derived miR-155 KO and WT Th17 cells to identify targets of miR-155 in Th17 cells

To look for additional potential targets of miR-155, we used the computational tool Sylamer, which searches for correlations between gene expression changes in RNA-seq data and the enrichment of sequence motifs in the 3' UTR of the corresponding genes (van Dongen et al., 2008). As a testament to the specificity of this analysis, we found that out of the 970 heptameric seed sequences tested, only the two overlapping motifs that match the miR-155 seed sequence (AGCATTA and GCATTAA) were significantly enriched in genes up-regulated in cells from miR-155 KO compared to WT Th17 cultures (Figure 16A). Sylamer analysis revealed 220 transcripts up-regulated in miR-155 KO Th17 cultures that contain at least one miR-155 seed sequence in their 3' UTR. To further narrow down the putative miR-155 targets, we compared our gene list with two computational miRNA target prediction methods which invoke evolutionary conservation: TargetScan and PicTar (Krek et al., 2005; Lewis et al., 2003) (Figure 16B). In conclusion, we used the signature of miR-155 mediated tuning within the transcriptome of Th17 cultures and identified a list of 15 candidates for further testing.

Our hypothesis that miR-155 is targeting a transcriptional repressor of *Il22* led us to further investigate PRC2 complex member Jarid2 (Figure 16B). Jarid2 was recently shown in mouse ES cells to recruit the histone modifying holoenzyme PRC2 to specific sites in the genome and silence transcription of its target genes through H3K27 trimethylation by Ezh1or Ezh2 (Li et al., 2010; Pasini et al., 2010; Peng et al., 2009; Shen et al., 2009). Jarid2 was previously validated to be a target of miR-155 in chicken and human cells (Bolisetty et al., 2009). Furthermore, it was demonstrated by high-

throughput sequencing of RNA isolated by crosslinking and immunoprecipitation (HITS-CLIP) that Argonaute2 (Ago2), a key protein of the miRNA-induced silencing complex (miRISC), directly binds to the upstream predicted site in the 3' UTR of Jarid2 in activated WT CD4^{+} T cells (Loeb et al., 2012). Notably, we found that Jarid2 transcript and protein levels are both up-regulated in miR-155 KO Th17 cultures by about two-fold (Figures 16C-D). Jarid2 transcripts are also elevated in miR-155 KO Treg cells (Figure 16E).
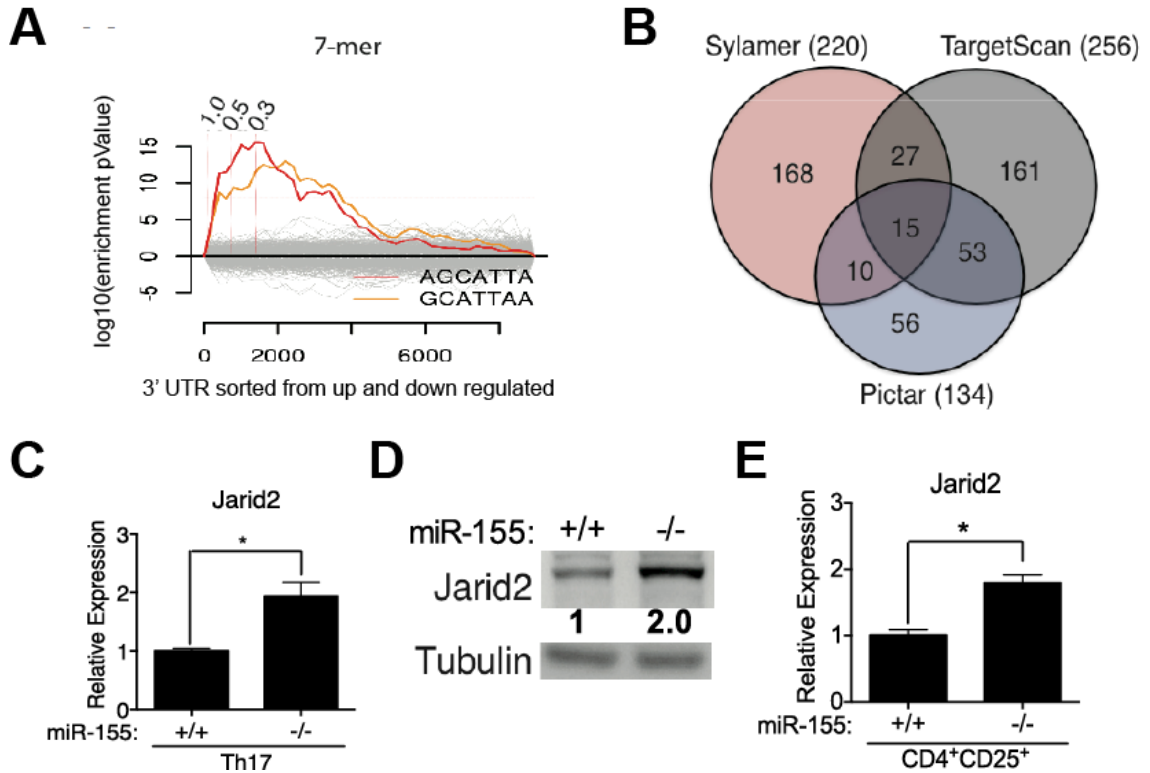
Figure 16. Jarid2 is a miR-155 target in CD4^{+} Th cells. (A) Sylamer analysis of miR-155 KO and WT Th17 RNA-seq is depicted as a landscape plot: hypergeometric significance values for enrichment of heptamers among 3' UTRs of genes (y-axis) and genes sorted from most up-regulated in miR-155 KO to down-regulated (x-axis). Two heptameric motifs are significantly enriched in genes up-regulated in miR-155 KO Th17 cultures (red and orange lines). The horizontal dotted red line represents an E-value threshold of $P < 0.01$ (Bonferroni-corrected for multiple testing). Vertical dotted lines indicate $\log_2$ fold change cutoffs of differentially expressed transcripts. (B) Comparison of our gene list from Sylamer analysis with predictions from TargetScan and Pictar, shows an overlap of 15 genes with putative miR-155 binding sites. (C) Relative expression of *Jarid2* mRNA was determined by RT-qPCR in miR-155 KO or WT Th17 cultures (+ IL-1β). (D) Western blot analysis of Jarid2 protein in miR-155 KO and WT

Th17 lysates quantified using ImageJ and Tubulin as a loading control. (E) Relative expression of *Jarid2* mRNA in Treg cells was determined by RT-qPCR in miR-155 KO or WT CD4$^+$CD25$^+$ T cells sorted from the spleen.

4.7 The epigenome of miR-155 KO Th17 cells is reprogrammed by Jarid2 and PRC2

To determine whether Jarid2 may be directly responsible for silencing *Il22* transcription in miR-155 KO Th17 cultures, we conducted ChIP-seq analyses. We found increased association of Jarid2 with the *Il22* locus in miR-155 KO cells (Figure 17A) and validated enrichment by qPCR at three locations (Figure 17B). As predicted, since we do not observe differential expression of IL-17a under these culture conditions, Jarid2 did not preferentially bind to the *Il17a* promoter in miR-155 KO Th17 cultures, and serves as a negative control (Figure 17B). To determine whether Jarid2 silences *Il22* expression by recruiting PRC2, we conducted ChIP-seq for Suz12, a core component of the PRC2 holoenzyme (Figure 17A). Similar to the analyses with Jarid2, Suz12 ChIP confirmed increased association of Suz12 with the *Il22* locus (Figure 17C), but not at the *Il17a* promoter (Figure 17C), in the absence of miR-155. Next, we examined whether there was increased H3K27 trimethylation at the *Il22* locus; higher occupancy of H3K27me3 was found at the IL-22 locus (Figures 17A and 17D), but not at the *Il17a* promoter (Figure 17D), in miR-155 KO Th17 cultures.
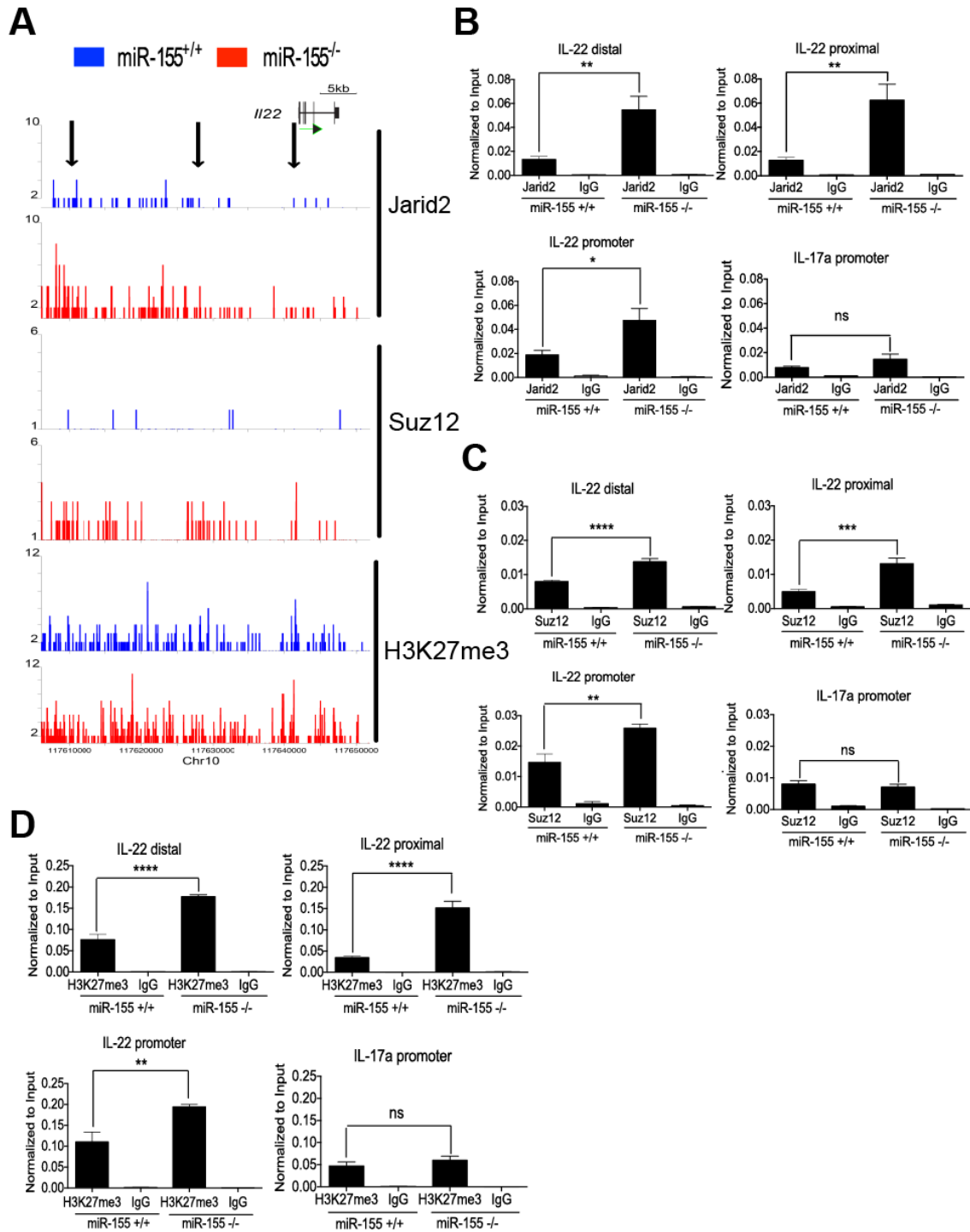
Figure 17. Jarid2 recruits PRC2 to epigenetically silence the *Il22* locus in absence of miR-155. (A) Genome browser screenshots depict Jarid2, Suz12, and H3K27me3 enrichment at the *Il22* locus. Arrows indicate promoter, proximal, and distal regions

71

validated by qPCR. (B) Enrichment of anti-Jarid2, (C) anti-Suz12, and (D) anti-H3K27me3 along with control IgG ChIPs of miR-155 KO and WT Th17 cultures at three indicated locations within *Il22* locus or the *Il17a* promoter was determined by qPCR. Validations were normalized to input controls and results are representative of three independent experiments with statistical significance determined using unpaired Student's *t* test (* $p<0.05$, ** $p<0.01$, *** $p<0.001$, and **** $p<0.0001$; ns denotes not significant).

Since the direct targets of PRC2 in CD4^{+} T cells have not been systematically examined, we performed ChIP-seq analyses for Jarid2, Suz12, and H3K27me3 in miR-155 KO Th17 cultures and WT controls. Our analysis identified 6,786 and 4,070 Jarid2 islands, 13,206 and 14,862 Suz12 islands, and 4,495 and 4,335 H3K27me3 islands in WT and miR-155 KO Th17 cells respectively (Figure 18A). Correlating with the increased Jarid2 expression observed, we found augmented Jarid2 islands as well as Suz12 and H3K27me3 islands when comparing the miR-155 KO to WT Th17 cells (Figure 18A). To find genes that are directly targeted by PRC2, we looked for Jarid2, Suz12, and H3K27me3 islands increased in miR-155 KO Th17 cultures that were co-localized ± 10 kb from a gene body (Figure 18A). This list included canonical PRC2 target genes, such as the *HoxA* gene clusters (Figures 18B). We also found that PRC2 targeted *SCL/Tal1,* a transcription factor gene essential for the specification of hematopoietic stem cells (HSCs) that is silenced upon differentiation (Figure 18C). In summary, we found that Jarid2 up-regulation in miR-155 KO Th17 cells resulted in widespread increased recruitment of the Jarid2-PRC2 holoenzyme at specific sites throughout the genome that coincided with increased deposition of H3K27me3.

In addition to *Il22*, we found that other genes were upregulated; *Il10* and *Il9,* were also directly targeted by the Jarid2-PRC2 holoenzyme (Figures 18D-E). Furthermore, this analysis identified genes not yet described as playing a role in Th17 differentiation such as Activating Transcription Factor 3 (ATF3), a member of the AP-1 superfamily of leucine zipper proteins that includes Fos, Jun and BATF. *Atf3* is differentially targeted by Jarid-PRC2 in miR-155KO and WT Th17 cells (Figure 18F), closely resembling what is

observed for the Th17 cytokines genes. Thus, miR-155 and Jarid2 in Th17 cells may regulate *Atf3*.
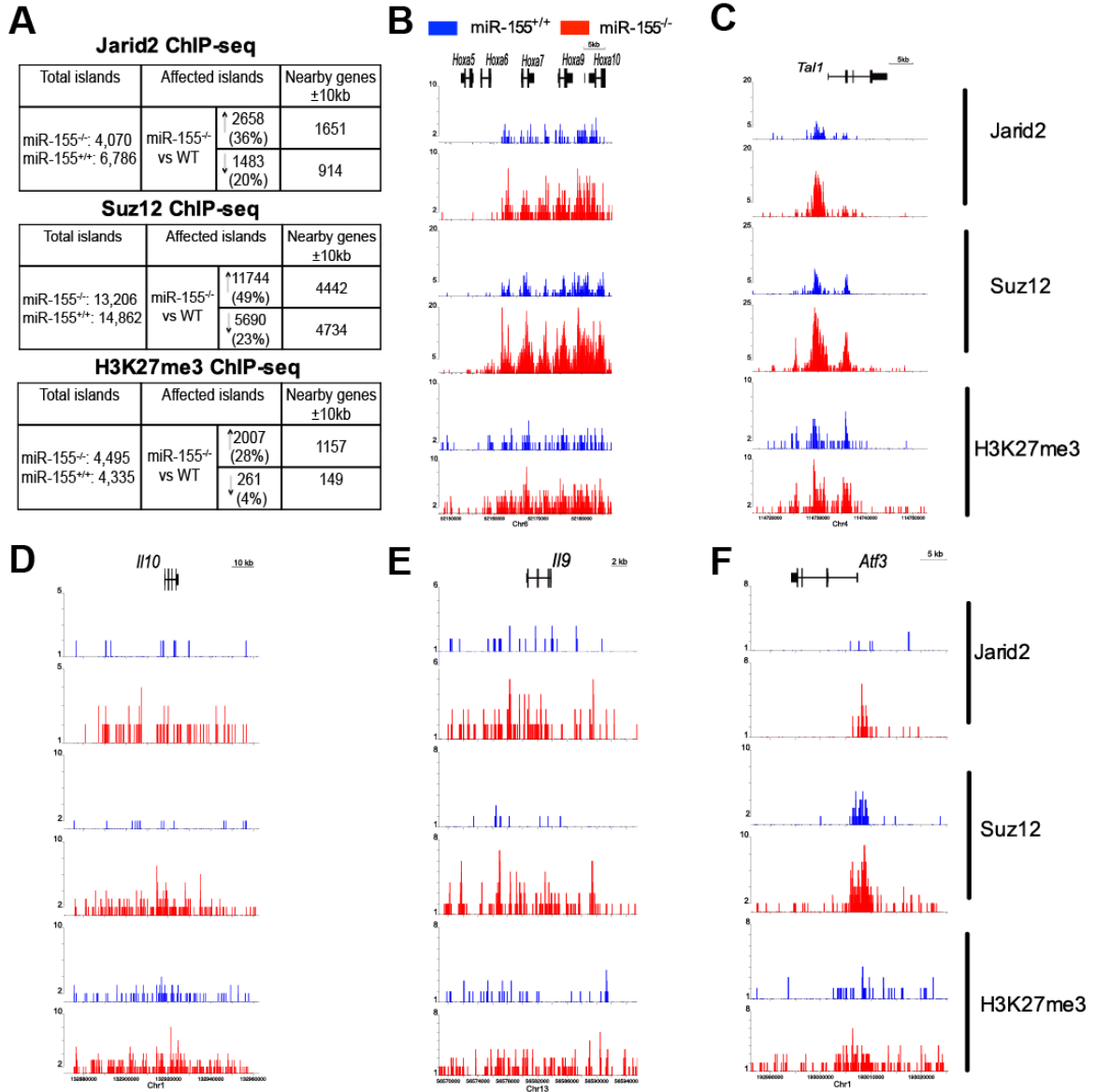
Figure 18. Jarid2 recruits PRC2 to reprogram the epigenome of miR-155 KO Th17 cells. (A) Tables summarize Jarid2, Suz12 and H3K27me3 ChIP-seq experiments in miR-155 KO and WT Th17 cultures. First column is total number of peaks in miR-155 KO and WT identified using SICER 3.1. Second column indicates the number of peaks affected (either ↑ or ↓) in miR-155 KO compared to WT controls using SICER 3.3.1. Third

column indicates the number of RefSeq genes within 10 kb of the peaks in question from SICER 3.3.1. (B-F) Genome browser screenshots depict Jarid2, Suz12, and H3K27me3 enrichment at the *HoxA* cluster (B), *Tal1* (C), *Il10* (D), *Il9* (E) and *Atf3* (F) loci as a result of ChIP-seq experiments in miR-155 KO (red) and WT (blue) Th17 cells.

4.8 IL-17a expression defect in miR-155KO Th17 cells is rescued by ATF3

To determine if *Atf3* is regulated by miR-155 in Th17 cells, we assayed the expression of *Atf3* in miR-155 KO and WT Th17 cells by RT-qPCR. We found increased expression of *Atf3* in absence of miR-155 when compared to controls (Figure 19A). Since the role of *Atf3* in Th17 cells is currently unknown, we used a GFP-rv vector to overexpress *Atf3* (ATF3-rv) during Th17 differentiation. We found that Th17 cultures transduced with ATF3 expressed greater levels of IL-17a compared to empty virus control (GFP-rv) (Figure 19B). To investigate if ectopic expression of ATF3 rescues the IL-17A defect in miR-155 KO Th17 cells, we overexpressed ATF3 in miR-155KO Th17. We found that miR-155KO T cells transduced with ATF3 are able to augment their IL-17a production when compared to untransfected controls (Figure 19C). In summary, *Atf3* has the ability to promote IL-17a expression in Th17 cells.
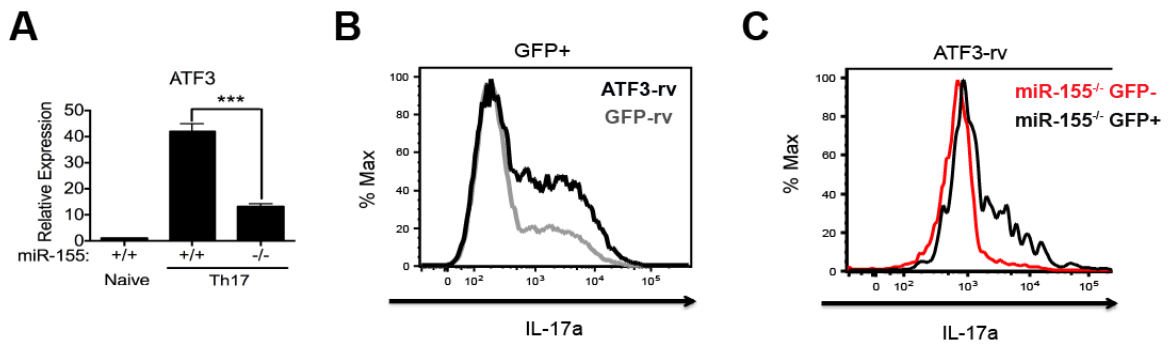
Figure 19. ATF3 promotes IL-17a expression and rescues the IL-17a defect in miR-155KO Th17 cells. (A) Relative expression of *Atf3* mRNA by RT-qPCR of miR-155 KO and WT Th17 cells. (B) Histogram depicts IL-17a expression from FACS analysis of Th17 cultures transduced with ATF3-rv (ATF3 GFP-rv) or empty vector (GFP-rv) and gated on transduced CD4$^+$CD44$^+$GFP$^+$ cells; (C) miR-155 KO Th17 cultures transduced with ATF3-rv and gated on transduced (GFP$^+$) or untransduced (GFP$^-$) CD4$^+$CD44$^+$ cells. Statistical significance was determined using Student's t test (∗∗∗ p<0.001).

4.9 Conditional deletion of Jarid2 in CD4^{+} T cells

The miR-155 KO mouse allowed us to assess Th17 development in the context of Jarid2 increased expression. To determine the direct contribution of Jarid2 during Th17 differentiation, we generated *Jarid2^{fl/fl}*;CD4-cre mice (Figure 20A-C). These mice delete Jarid2 in T cells at the double positive T cell stage. Therefore all periphernal T cells are essentially KO for Jarid2. We performed ChIP-exo, a variant of ChIP-seq that uses lambda 5'-3' exonuclease to reduce background and increase resolution of the assay (Rhee and Pugh, 2012). We found that in the absence of Jarid2, genomic recruitment of Suz12 was diminished. As examples, we show the *Hoxa* and *Hoxd* clusters, *Il22* and *Atf3* (Figures 20D-G).
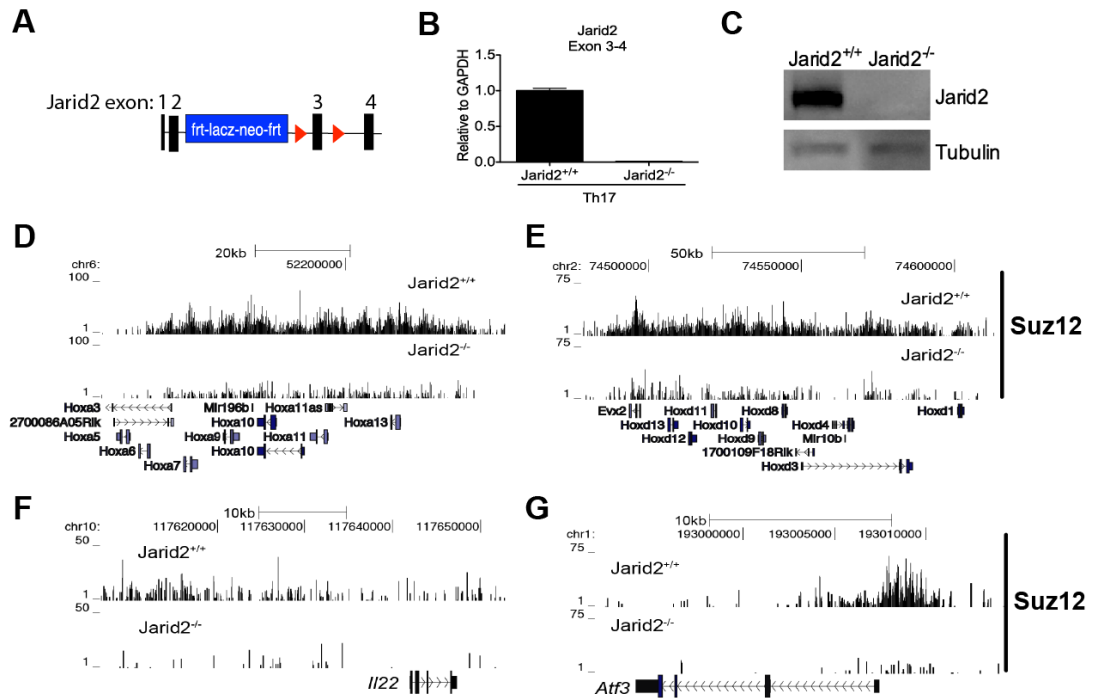
Figure 20. Jarid2 conditional targeting in CD4^{+} T cells. (A) Schematic of Jarid2 conditional targeting. In this conditional allele, exon 3 is flanked by loxP sites in a strategy that is essentially identical to a previously published allele of Jarid2 (Mysliwiec et al., 2006; Shen et al., 2009). (B) RT-qPCR across targeted exon 3 from Jarid2^{-/-} (*Jarid2*^{fl/fl}; CD4-cre) and littermate controls. Relative expression was found by normalizing to *Gapdh* mRNA. (C) Jarid2 western blot of Jarid2 KO (Jarid2^{-/-}) and WT (Jarid2^{+/+}) Th17 cultures. (D-G) Genome browser screenshots of the *HoxA* cluster (D), *HoxD* cluster (E)*, Il22* (F), and *Atf3* (G) from the ChIP-exo of Suz12 in WT and Jarid2 KO (Jarid2^{-/-}) Th17 cultures.

Furthermore, we differentiated CD4$^+$ T cells from *Jarid2*$^{fl/fl}$;CD4-cre mice and littermate controls toward the Th17 cell fate and found a significant increase in IL-17a expression upon Jarid2 ablation (Figures 21A-B). Jarid2-deficient Th17 cells did not aberrantly express IFNγ (Figure 21A). To further assess gene expression changes in the absence of Jarid2, we performed RT-qPCR and found *Il17a*, *Il17f*, *Il22*, *Il10*, *Il9* and *Atf3* transcripts to be increased in Jarid2-deficient Th17 cultures (Figures 21C-D). In contrast, we did not observe changes in expression of RORγt, IRF4 and BATF in Jarid2-deficient Th17 cultures compared to WT (Figures 21C). Furthermore, we measured cytokine concentrations in Th17 cultures and found increased IL-22, IL-10 and IL-9 protein in absence of Jarid2 (Figure 21E). We found that H3K27me3 deposition is decreased at the promoters of *Il22*, *Il10*, and *Il9* upon Jarid2 ablation (Figure 21F). Moreover, we found augmented levels of unspliced message for *Il22* and *Il9* in Jarid2-deficient Th17 cultures suggesting increased transcription of these cytokine genes (Figure 21G). Thus, lack of Jarid2 results in enhanced Th17 development.
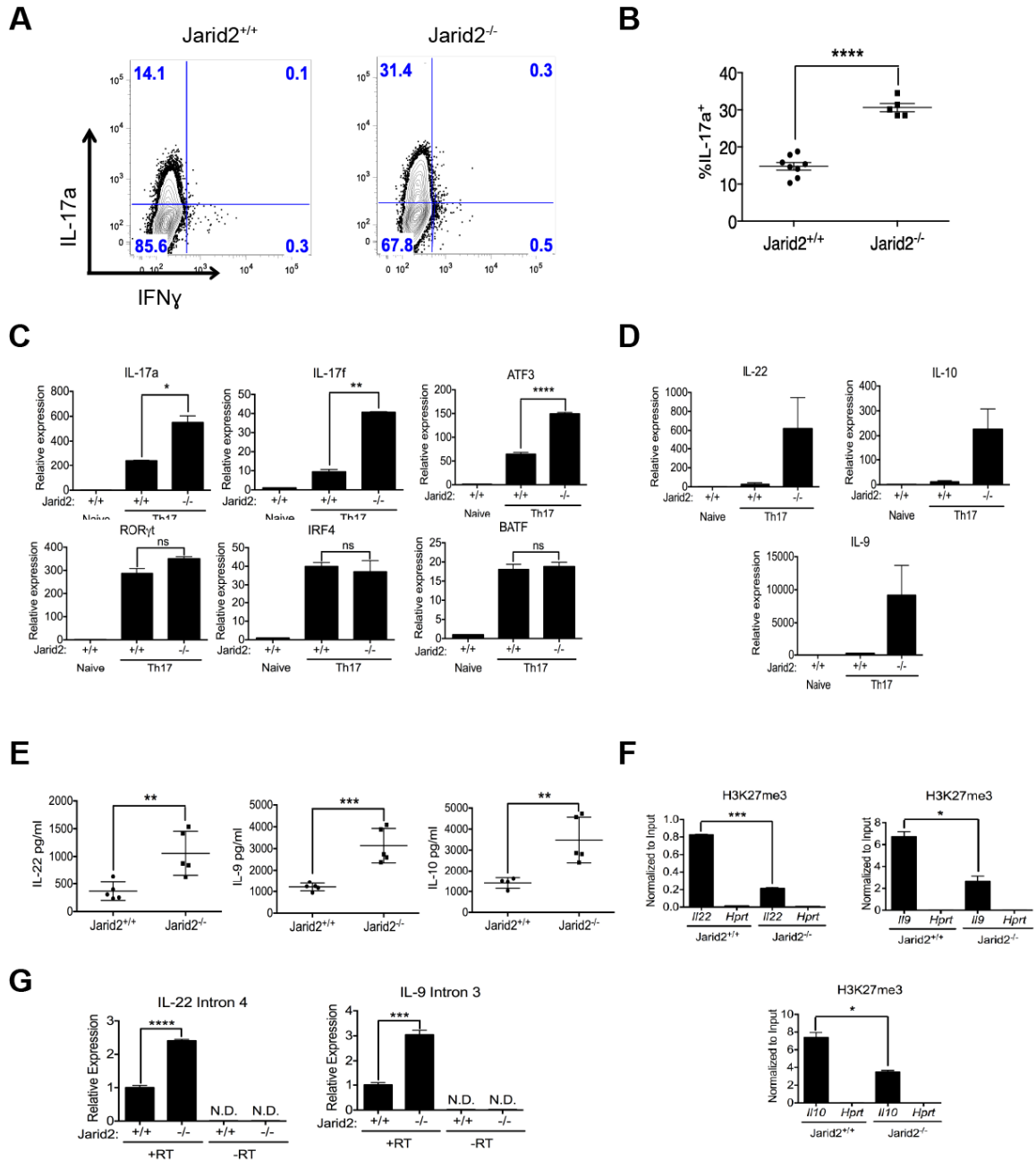
Figure 21. Absence of Jarid2 in CD4$^+$ T cells results in enhanced Th17 development.

(A) FACS analysis of IL-17a and IFNγ expression in CD4$^+$CD44$^+$ cells from *Jarid2*$^{fl/fl}$;

CD4-cre mice and littermate controls cultured under Th17 polarizing conditions without

IL-1β and (B) the corresponding percentages of CD4$^+$CD44$^+$IL-17a$^+$ T cells. (C) Relative

expression of *Il17a, Il17f, Atf3, Rorc, Irf4, Batf* mRNA by RT-qPCR from WT and

Jarid2-deficient Th17 cultures. (D) Relative expression of *Il22*, *Il9* and *Il10* mRNA in Jarid2 KO and WT Th17 cultures was determined by RT-qPCR. (E) Cytokine concentrations in supernatant of Th17 cultures were determined by ELISA. (F) H3K27me3 at promoters of *Il22*, *Il10*, *Il9* and *Hprt* determined by ChIP-qPCR. (G) RT-qPCR of *Il22* intron 4 and *Il9* intron 3 of Jarid2 KO and WT Th17 cultures ± reverse transcriptase (RT).

4.10 Conditional ablation of Jarid2 partially rescues Th17 and Treg cells in miR-155 KO

To determine whether the Th17 and Treg phenotypes observed in miR-155 KO mice are caused by increased expression of Jarid2, we generated double KO (DKO) mice wherein Jarid2 is conditionally deleted at the DP stage in the T cell lineage of miR-155 KO mice. We made mixed BM chimeras of WT (CD45.1$^+$) and DKO (CD45.2$^+$) cells, and infected them with *T. gondii* to assess IL-17a and IL-22 expression as well as Treg homeostasis. Remarkably, DKO Treg cells are competitive with WT Treg cells whereas miR-155 KO Treg cells failed to compete with either DKO or WT Tregs (Figure 22A). In addition, development of CD4$^+$IL-17A$^+$ T cells is restored in the DKO, although IL-22 expression was not rescued (Figure 22B). Thus, we can partially rescue Foxp3$^+$ cells and IL-17a expression *in vivo* upon ablation of Jarid2 in miR-155 KO T cells (Figures 22C-E). We recapitulated the rescue of *Il17a* and *Il17f* expression *in vitro* with DKO Th17 cultures (Figure 22F). Furthermore, through analysis of Jarid2 heterozygous conditional KOs we found that loss of one allele of *Jarid2* in miR-155 KO Th17 cells is sufficient to reduce Jarid2 protein levels to near WT levels (Figure 22G) and to rescue IL-17a expression (Figures 22H-I).

Since deletion of Jarid2 in miR-155 KO CD4$^+$ T cells did not rescue *Il22* expression, we hypothesized that in the absence of Jarid2, the chromatin structure at the *Il22* promoter is now in a permissive state to allow binding of other transcription factors. We focused our investigations on c-Maf, a known repressor. Indeed, in DKO Th17 cultures, we now observe c-Maf binding at the IL-22 promoter by ChIP-seq analysis(Figure 22J). Globally, the Jarid2-PRC2 holoenzyme may have the ability to

dictate where transcription factors such as c-Maf can bind chromatin by reprogramming

the epigenome and affecting the accessibility of different loci.
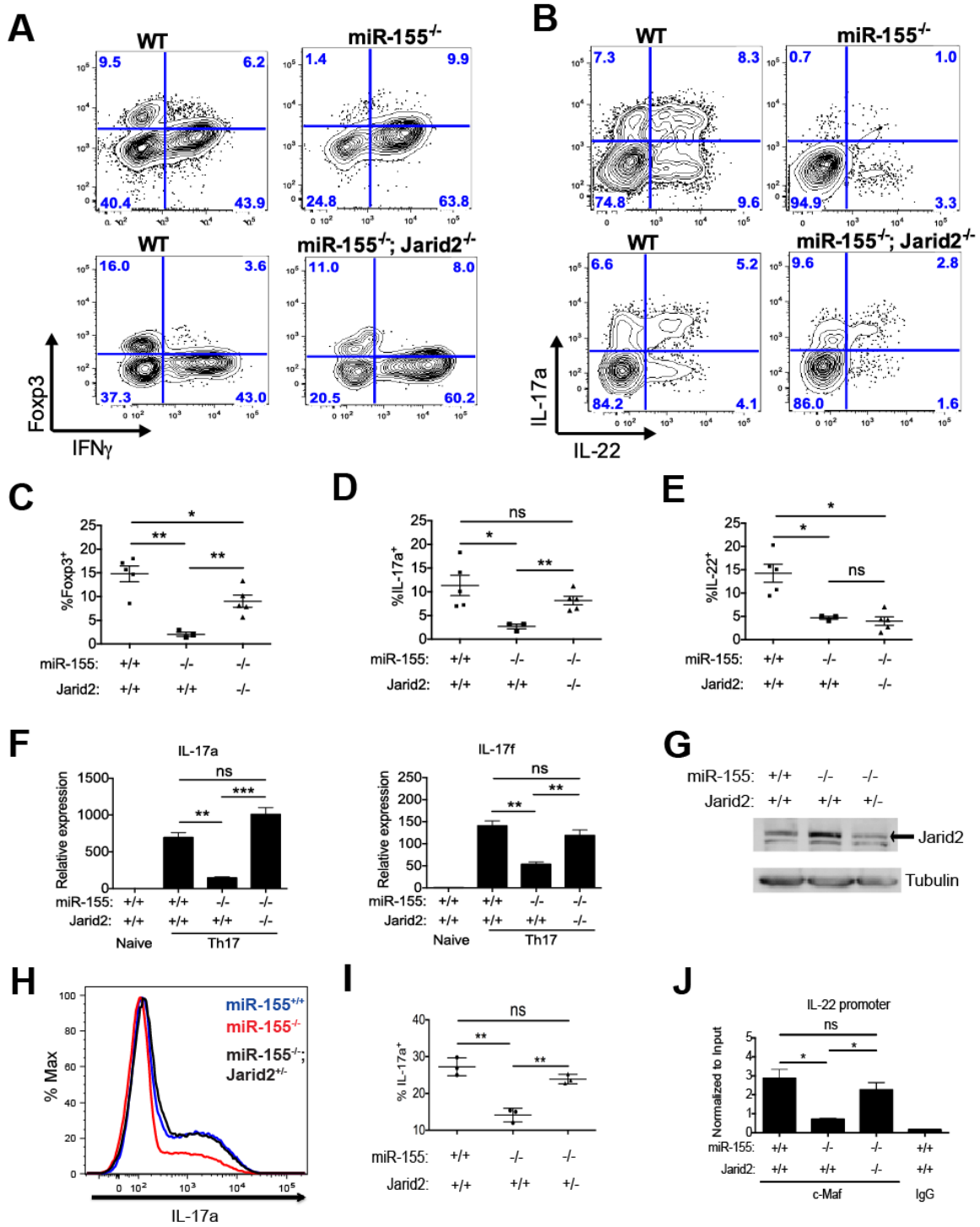
Figure 22. Epistasis between Jarid2 and miR-155 in Treg and Th17 cells. (A,B)

FACS analysis of WT, miR-155 KO or miR-155 KO; *Jarid2*^fl/fl^; CD4-cre (DKO) cells

from siLP of infected mixed BM chimeras to enumerate CD4$^+$TCRβ$^+$CD44$^+$ cells that are

IFNγ or Foxp3 positive (A), or IL-17a and/or IL-22 positive (B), 8 days after *T. gondii* infection. (C-E) Indicated percentages of $CD4^+TCR\beta^+CD44^+$ WT, miR-155 KO or DKO cells from the siLP of infected mixed BM chimeras. (F) Relative expression of *Il17a* and *Il17f* mRNA was determined by RT-qPCR in WT, miR-155 KO or DKO Th17 cultures (-IL-1β). (G) Western blot analysis of Jarid2 and tubulin protein in WT, miR-155-/- and miR-155-/-; Jarid2+/- Th17 cells. (H) Histogram depicts intracellular IL-17a expression in WT, miR-155-/- and miR-155-/-; Jarid2+/- Th17 cultures (- IL-1β). (I) The corresponding percentages of $CD4^+CD44^+IL-17a^+$ T cells. (J) c-Maf and IgG ChIP-qPCR on the *Il22* promoter in WT, miR-155 KO or DKO Th17 cultures normalized to input. Statistical significance determined using unpaired Student's *t* test (∗ $p<0.05$, ∗∗ $p<0.01$, and ∗∗∗ $p<0.001$; ns denotes not significant). ns denotes not significant.

4.11 Summary of findings

We propose a mechanism by which miR-155 regulates the fates of Th17 and Treg cells through PRC2 member Jarid2. By regulating the expression of Jarid2 miR-155 can indirectly promote gene expression through post-translational inhibition of this known repressor. Using high throughput ChIP and RNA-seq approaches, we assessed the genome-wide consequences of Jarid2 up-regulation in miR-155 KO Th17 cultures. We observe increased recruitment of PRC2 to genomic sites accompanied by increased H3K27 trimethylation and silencing of expression of *Il22*, *Il10* and *Il9* cytokines involved in mediating tissue repair and homeostasis in response to inflammation (Goswami and Kaplan, 2011; Ouyang et al., 2011; Zenewicz and Flavell, 2011). Although H3K27me3 is often equated with transcriptional silencing, direct perturbation experiments to address this relationship are lacking in mammalian systems. Here, we have ablated Jarid2 in CD4$^+$ T cells to prevent recruitment of PRC2, the holoenzyme that catalyzes trimethylation of H3K27 at its targets. This allowed us to identify Jarid2-dependent PRC2 targets genome-wide and examine the consequences of the lack of Jarid2 on gene expression in Th17 cells. Jarid2-deficient CD4$^+$ T cells undergo enhanced Th17 differentiation in part manifested by up-regulation of *Il17a* and *Atf3*. Since reduced or excessive H3K27me3 catalysis can affect the efficiency of Th17 differentiation and Treg homeostasis, miR-155 may have evolved to modulate PRC2 recruitment by fine-tuning Jarid2 expression.

Thus, we integrate miR-155 and PRC2 to the Th17 transcriptional network (Ciofani et al., 2012)(Figure 23). We find that in Th17 cells, the Jarid2-PRC2 complex targets genes that can contribute to IL17 expression (*Atf3*), cellular plasticity genes

(*Tbx21* and *Eomes*), and immunoregulatory cytokine expression (*Il22, Il10* and *Il9*). In addition to Jarid2, miR-155 appears to repress c-Maf, an important transcription factor in Th17 cells. Interestingly, we revealed that Jarid2 can prevent c-Maf binding in the *Il22* promoter through regulation of chromatin accessibility. Additionally, we provide an updated view of the complex regulatory network in Th17 cells to exemplify how a miRNA and chromatin regulator might interact to orchestrate gene expression programs.

Taken together, our study reveals novel aspects of the Th17 regulatory network in which miR-155 promotes acquisition of effector functions. By regulating a chromatin modifying complex, miR-155 can mediate global gene expression changes. A two-fold change in Jarid2 expression by a miRNA can reprogram the epigenome of a cell via H3K27 trimethylation. How miRNA, transcription factors and chromatin cooperate to orchestrate a gene expression program has not been systematically analyzed. Using Th17 differentiation as a model system, we demonstrate that miR-155 can have profound effects on the chromatin landscape and links post-transcriptional, epigenetic as well as transcriptional regulation of cellular differentiation.
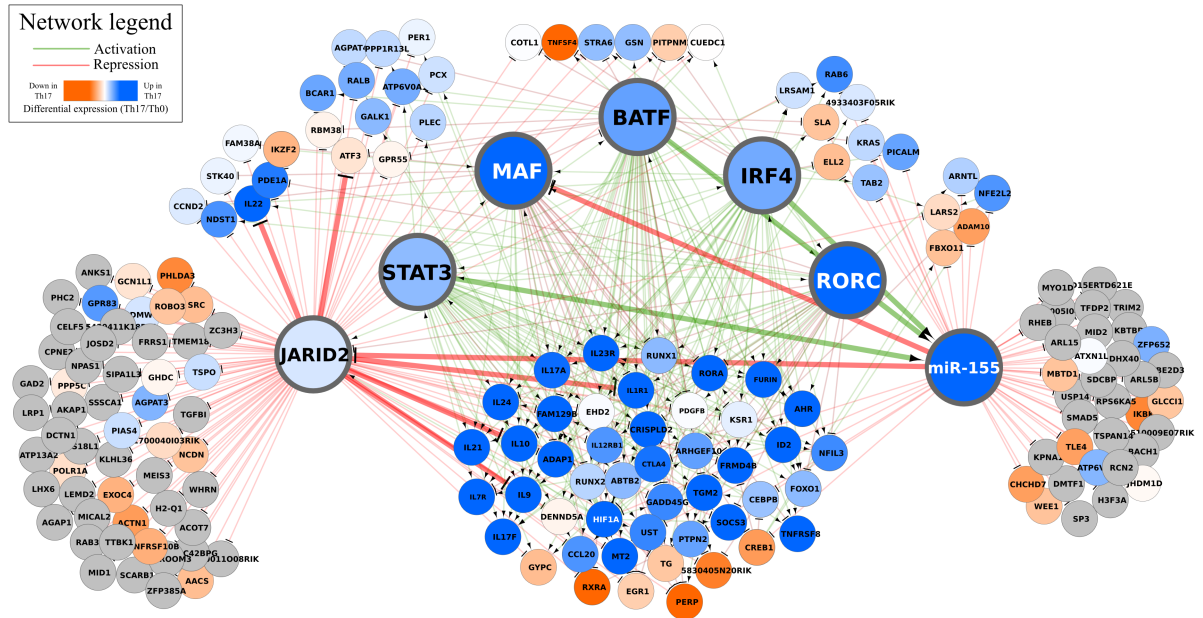
Figure 23. An updated Th17 regulatory network that integrates miR-155 and Jarid2. The KCRI Th17 cell specification regulatory network (Ciofani et al., 2012) was downloaded from http://th17.bio.nyu.edu/pages/cytoscape.html. Targets of miR-155 and Jarid2-PRC2 were integrated in to the KCRI network to generate an updated Th17 regulatory network. Associations between transcription factors and miR-155 were added based on available ChIP-seq evidence. Genes (nodes) are colored based on the level of differential expression (orange to blue correspond to low to high Th17 expression relative to Th0; grey denotes missing expression data). Edges (associations) are colored as either activation (green) or repression (red). Nodes with many associations are denoted by large circles. Nodes with 4 or more connections are grouped in the middle, whereas those with fewer connections are in the periphery.

5. Small molecule inhibitor screen to identify targets that alter miR-155 expression in CD4$^+$ Th17 cells.

5.1 High throughput small molecule screen for inhibitors of miR-155 in Th17 cells

CD4$^+$ Th17 cells are a subset of CD4$^+$ Th cells that have been implicated in a wide variety of autoimmune disorders such as rheumatoid arthritis (Sato et al., 2006), inflammatory bowel disease (Barrett et al., 2008), psoriasis (Zheng et al., 2007), and multiple sclerosis (Kebir et al., 2007). My research has shown that high expression of miR-155 promotes the expression of Th17 cell cytokines. The identification of compounds that inhibit miR-155 expression may therefore offer a new approach to identify drugs in the treatment of autoimmune diseases. As such, we began collaboration with the NIH National Center for Advancing Translational Sciences (NCATS) to identify small molecules that inhibit miR-155 expression.

For this aim, we took advantage of a genetically engineered reporter mouse in which lacZ has been inserted into the endogenous *Mir155* locus (Thai et al., 2007) and began assaying >50,000 small molecules inhibitors that decreased β-galactosidase activity following Th17 polarization. We initially focused on a group of biologically active compounds and tested seven different concentrations of each compound as well as a DMSO control on our miR-155 reporter Th17 cells (Figure 24A-B). The predicted ideal profile of a candidate compound from our assay would have been one that decreased β-galactosidase activity while not affecting cell viability (Figure 24C). Using acurve class classification algorithm developed by our collaborations (Inglese et al., 2006), we selected those compounds that were high quality inhibitors of miR-155 expression in Th17 cells. Upon validation of miR-155 expression levels by RT-qPCR for one compound (NCGC00015205) from our preliminary hit, we observed decreased miR-155 expression upon addition of this compound to *in vitro* differentiating Th17 cells (Figure

91

24D). These results supported the validity of our robust high throughput screen to test

small molecules that alter miR-155 expression in primary Th17 cells.
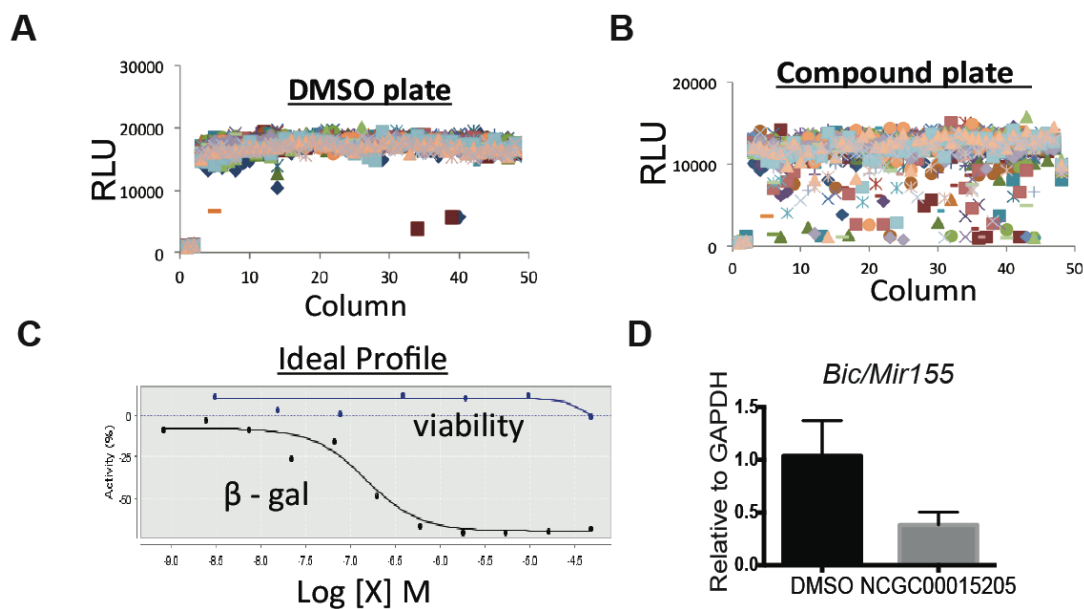
Figure 24. Selection and validation of candidate compounds that inhibit miR-155 expression in Th17 cells. Scatter plot for (A) one control (DMSO) plate and (B) one assay plate from the LOPAC library of biological compounds measuring the Relative light unit (RLU) from miR-155 reporter Th17 cells. (C) Predicted dose response curve for a compound from the LOPAC library with an ideal profile that antagonizes miR-155 expression with minimal effect on cell viability. The black line shows miR-155 expression using the Beta-Glo assay and the blue line shows cell viability measured by CellTiter-Glo. (D) Relative expression of Bic/Mir155 by RT-qPCR assay normalized to GAPDH from an assay using 5 uM of NCGC00015205 during Th17 cell culture conditions.

5.2 NCGC00015205 impairs IL-17a production

Based on our findings in which NCGC00015205 decreased miR-155 expression

in Th17 cells, we were further interested in assessing the effect of this compound on

Th17 cytokine production. For this purpose, we assayed the T cell survival (Figure 25A),

T cell activation (Figure 25B) and IL-17a expression (Figure 25C) on Th17 cultures

treated with NCGC00015205 and DMSO controls. We found that while T cell survival

and activation were not altered in the presence of the miR-155 inhibitor

(NCGC00015205), the production of IL-17a was impaired (Figure 25). These results are

promising for the therapeutic targeting of IL-17a production by a miR-155 inhibitor.
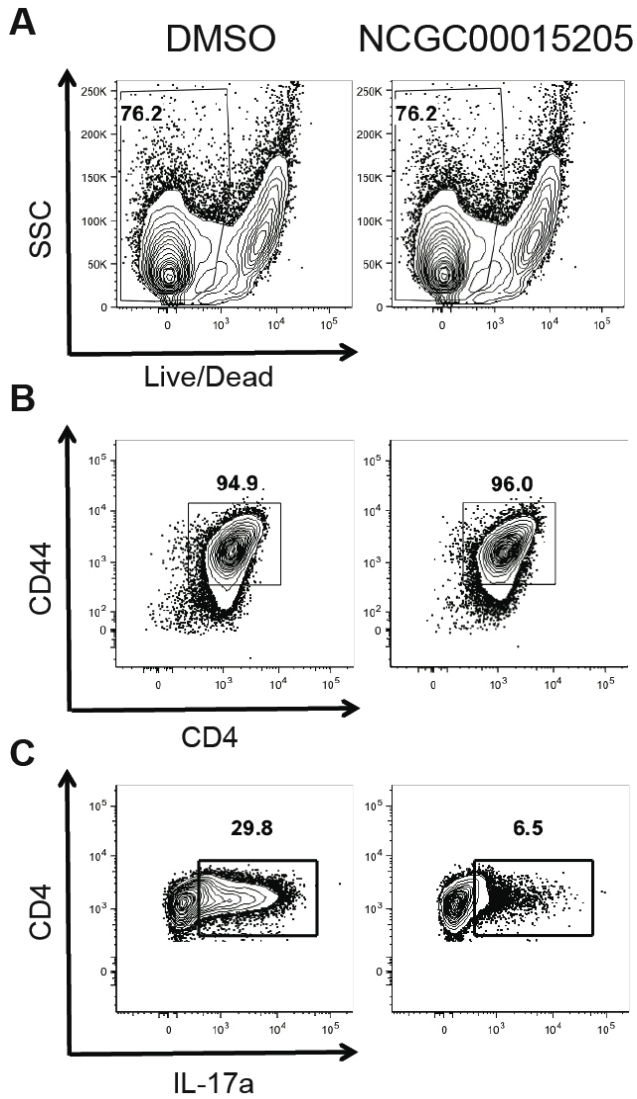
Figure 25. NCGC00015205 decreases IL-17a expression in CD4$^+$ Th17 cells. Flow cytometric analysis of *in vitro* polarized CD4$^+$ Th17 cells treated with either the miR-155 inhibitor (NCGC00015205) or DMSO (as control) showing: (A) the percentage of live cells using a Live/Dead stain; (B) the percentage of activated T cells (CD4$^+$CD44$^+$) gated amongst live cells; and (C) the expression of IL-17a amongst activated cells.

5.3 Summary of Findings

Through collaboration with NIH NCATS, we have identified numerous small molecule inhibitors, including (NCGC00015205), that alter miR-155 expression in a high throughput screen. Further validation of some of these compounds is still required. Validation of NCGC00015205 under Th17 cell culturing conditions resulted in decreased miR-155 expression and impaired Th17 cell differentiation (Figure 24D and 25). In terms of mechanism, NCGC00015205 is highly selective for TSPO, a peripheral benzodiazepine receptor that is localized in the mitochondria. As such, characterization of TSPO in Th17 cell differentiation will be necessary to determine how this receptor affects miR-155 expression. We plan to identify downstream signaling pathways that are altered upon changes in TSPO activity by incorporating different TSPO ligands or TSPO knockdown in Th17 cell cultures. Since our goal for this screen was to identify inhibitors of miR-155 expression for therapeutic potential, we are interested in testing the effectiveness of NCGC00015205 as an inhibitor in the Th17 cell-driven mouse model of EAE.

6. Discussions and Conclusions

6.1 A regulatory network for Th17 development

The differentiation and reprogramming of CD4$^+$ Th cell lineages are mediated by highly orchestrated gene expression programs that require not only activation of specific genes necessary for new cell fate decision, but also repression of alternative and precursor cell fates. miRNA are evolutionarily conserved, small, non-coding RNA of approximately 21-24 nucleotides in length that repress gene expression at a post-transcriptional level via the endogenous RNA interference pathway (Muljo et al., 2010) and have emerged as new regulators of gene expression programs. As such, miRNA can cooperate with transcription factors during cellular differentiation by repressing unwanted gene expression post-transcriptionally. Based on current estimates, mammals have >500 miRNA genes that have the collective potential to target up to 60% of the protein-coding transcriptome and thus regulate a large variety of biological processes (Friedman et al., 2009). In one striking example, enforced expression of the miR-302~367 ES cell-specific cluster is sufficient to reprogram somatic fibroblasts to become induced pluripotent stem (iPS) cells (Anokye-Danso et al., 2011).

By exploiting the well-characterized transcriptional network of CD4$^+$ Th cell differentiation with particular focus on the Th17 cell lineage, my graduate research investigated the function of miRNA in regulation of CD4$^+$ Th17 cell fate. Based on this research, I was able to integrate miR-155, miR-29 and Jarid2 in a regulatory network critical for Th17 cell lineage specification and repression of alternative cell fates (Figure 26). My analysis into the molecular basis of CD4$^+$ Th17 cell differentiation provided the opportunity to devise innovative strategies for the targeting of Th17 cytokine expression. We have begun to assay and validate potential miR-155 inhibitors that can be used for the

treatment of autoimmune diseases and cancer, as both conditions have an over-expression

of miR-155 and Th17 cells, resulting in dire consequences (Tili et al., 2009).
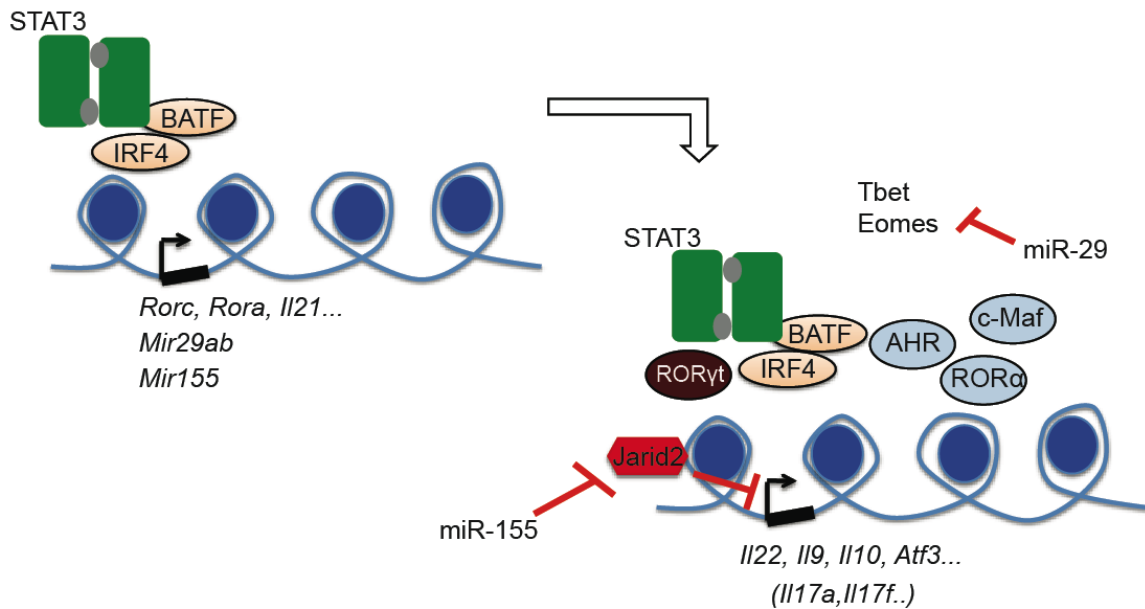
Figure 26. The interplay between transcription factors, chromatin and miRNA that make up a regulatory network to promote CD4^{+} Th 17 cell development and function. After an initial CD4^{+} T cell stimulation, STAT3, BATF and IRF4 induce the expression of key transcription factors and miRNA genes that drive a CD4^{+} Th17 cell differentiation program. Following induction of RORγt, miR-29 and miR-155 expression, further specification towards the Th17 cell lineage continues with the targeting of inhibitory molecules such as Jarid2 by miR-155, the targeting of alternate fates by miR-29 and the initiation of cytokine expression via the Th17 cell transcriptional network.

7. References

7.1 Appendix: Glossary of Abbreviations

Ago	Argonaute
APC	Antigen Presenting Cell
BM	Bone Marrow
ChIP	Chromatin immunoprecipitation
ChIP-seq	Chromatin immunoprecipitation followed by massive-parallel sequencing
CIA	Collagen Induced Arthrits
Cre	Cre recombinase
DKO	Double Knock out
EAE	Experimental Autoimmune Encephalitis
EAU	Experimental Autoimmune Uveitis
ELISA	Enzyme-linked immunosorbent assay
FACS	Fluorescence-Activated Cell Sorting
FC	Fold Change
GEO	Gene Expression Omnibus database
GFP	Green Fluorescent Protein
HIV	Human immunodeficiency virus

IBD	Inflammatory Bowel Disease
IL	Interleukin
IPEX	immunodysregulation, polyendocrinopathy, enteropathy, X-linked syndrome
iTreg	induced regulatory T cell
KO	Knock out
LincRNA	Long intergenic non-coding RNA
MACS	Magnetic Activated Cell Sorting
miRNA	microRNA
MLN	Mesenteric Lymph Node
MMPs	Matrix metalloproteinases
NCATS	National Center for Advancing Translational Sciences
NCBI	National Center for Biotechnology Information
ncRNA	non coding RNA
PBMCs	Human peripheral blood mononuclear cells
PCR	Polymerase Chain Reaction
PFA	Paraformaldheyde
PMA	Phorbol 12-myristate 13-acetate

PolII	Polymerase II
PRC2	Polycomb repressive complex 2
RA	Rheumatoid arthritis
RNA	Ribonucleic acid
RNA-seq	RNA sequencing
RT-qPCR	Real Time quantitative Polymerase Chain Reaction
RV	Retro virus
siLP	Small intestine Lamina Propria
STAT	Signal Transducer and Activator of Transcription
Th	T helper cell
TGFβ	Tumor Growth Factor beta
TCR	T cell receptor
TSS	Transcriptional Start Site

7.2 Bibliography

Abraham, B.J., Cui, K., Tang, Q., and Zhao, K. (2013). Dynamic regulation of epigenomic landscapes during hematopoiesis. BMC Genomics *14*, 193.

Anokye-Danso, F., Trivedi, C.M., Juhr, D., Gupta, M., Cui, Z., Tian, Y., Zhang, Y., Yang, W., Gruber, P.J., Epstein, J.A., and Morrisey, E.E. (2011). Highly efficient miRNA-mediated reprogramming of mouse and human somatic cells to pluripotency. Cell Stem Cell *8*, 376-388.

Awasthi, A., and Kuchroo, V.K. (2009). Th17 cells: from precursors to players in inflammation and infection. Int Immunol *21*, 489-498.

Barrett, J.C., Hansoul, S., Nicolae, D.L., Cho, J.H., Duerr, R.H., Rioux, J.D., Brant, S.R., Silverberg, M.S., Taylor, K.D., Barmada, M.M.*, et al.* (2008). Genome-wide association defines more than 30 distinct susceptibility loci for Crohn's disease. Nat Genet *40*, 955-962.

Baumjohann, D., and Ansel, K.M. (2013). MicroRNA-mediated regulation of T helper cell differentiation and plasticity. Nat Rev Immunol *13*, 666-678.

Ben-Sasson, S.Z., Hu-Li, J., Quiel, J., Cauchetaux, S., Ratner, M., Shapira, I., Dinarello, C.A., and Paul, W.E. (2009). IL-1 acts directly on CD4 T cells to enhance their antigen-driven expansion and differentiation. Proc Natl Acad Sci U S A *106*, 7119-7124.

Bennett, C.L., Christie, J., Ramsdell, F., Brunkow, M.E., Ferguson, P.J., Whitesell, L., Kelly, T.E., Saulsbury, F.T., Chance, P.F., and Ochs, H.D. (2001). The immune dysregulation, polyendocrinopathy, enteropathy, X-linked syndrome (IPEX) is caused by mutations of FOXP3. Nat Genet *27*, 20-21.

Bettelli, E., Pagany, M., Weiner, H.L., Linington, C., Sobel, R.A., and Kuchroo, V.K. (2003). Myelin oligodendrocyte glycoprotein-specific T cell receptor transgenic mice develop spontaneous autoimmune optic neuritis. J Exp Med *197*, 1073-1081.

Bluml, S., Bonelli, M., Niederreiter, B., Puchner, A., Mayr, G., Hayer, S., Koenders, M.I., van den Berg, W.B., Smolen, J., and Redlich, K. (2011). Essential role of microRNA-155 in the pathogenesis of autoimmune arthritis in mice. Arthritis Rheum *63*, 1281-1288.

Bolisetty, M.T., Dy, G., Tam, W., and Beemon, K.L. (2009). Reticuloendotheliosis virus strain T induces miR-155, which targets JARID2 and promotes cell survival. J Virol *83*, 12009-12017.

Boniface, K., Bernard, F.X., Garcia, M., Gurney, A.L., Lecron, J.C., and Morel, F. (2005). IL-22 inhibits epidermal differentiation and induces proinflammatory gene expression and migration of human keratinocytes. J Immunol *174*, 3695-3702.

Brohee, S., and Bontempi, G. (2012). D-peaks: a visual tool to display ChIP-seq peaks along the genome. Transcription *3*, 255-259.

Brunkow, M.E., Jeffery, E.W., Hjerrild, K.A., Paeper, B., Clark, L.B., Yasayko, S.A., Wilkinson, J.E., Galas, D., Ziegler, S.F., and Ramsdell, F. (2001). Disruption of a new forkhead/winged-helix protein, scurfin, results in the fatal lymphoproliferative disorder of the scurfy mouse. Nat Genet *27*, 68-73.

Burchill, M.A., Yang, J., Vogtenhuber, C., Blazar, B.R., and Farrar, M.A. (2007). IL-2 receptor beta-dependent STAT5 activation is required for the development of Foxp3+ regulatory T cells. J Immunol *178*, 280-290.

Chong, M.M., Rasmussen, J.P., Rudensky, A.Y., and Littman, D.R. (2008). The RNAseIII enzyme Drosha is critical in T cells for preventing lethal inflammatory disease. J Exp Med *205*, 2005-2017.

Chung, Y., Chang, S.H., Martinez, G.J., Yang, X.O., Nurieva, R., Kang, H.S., Ma, L., Watowich, S.S., Jetten, A.M., Tian, Q., and Dong, C. (2009). Critical regulation of early Th17 cell differentiation by interleukin-1 signaling. Immunity *30*, 576-587.

Ciofani, M., Madar, A., Galan, C., Sellars, M., Mace, K., Pauli, F., Agarwal, A., Huang, W., Parkurst, C.N., Muratet, M., *et al.* (2012). A validated regulatory network for Th17 cell specification. Cell *151*, 289-303.

Douek, D.C., Picker, L.J., and Koup, R.A. (2003). T cell dynamics in HIV-1 infection. Annu Rev Immunol *21*, 265-304.

Duerr, R.H., Taylor, K.D., Brant, S.R., Rioux, J.D., Silverberg, M.S., Daly, M.J., Steinhart, A.H., Abraham, C., Regueiro, M., Griffiths, A., *et al.* (2006). A genome-wide association

study identifies IL23R as an inflammatory bowel disease gene. Science *314*, 1461-1463.

Durant, L., Watford, W.T., Ramos, H.L., Laurence, A., Vahedi, G., Wei, L., Takahashi, H., Sun, H.W., Kanno, Y., Powrie, F., and O'Shea, J.J. (2010). Diverse targets of the transcription factor STAT3 contribute to T cell pathogenicity and homeostasis. Immunity *32*, 605-615.

Egwuagu, C.E. (2009). STAT3 in CD4+ T helper cell differentiation and inflammatory diseases. Cytokine *47*, 149-156.

Escobar, T., Yu, C.R., Muljo, S.A., and Egwuagu, C.E. (2013). STAT3 activates miR-155 in Th17 cells and acts in concert to promote experimental autoimmune uveitis. Invest Ophthalmol Vis Sci *54*, 4017-4025.

Friedman, R.C., Farh, K.K., Burge, C.B., and Bartel, D.P. (2009). Most mammalian mRNAs are conserved targets of microRNAs. Genome Res *19*, 92-105.

Fujita-Sato, S., Ito, S., Isobe, T., Ohyama, T., Wakabayashi, K., Morishita, K., Ando, O., and Isono, F. (2011). Structural basis of digoxin that antagonizes RORgamma t receptor activity and suppresses Th17 cell differentiation and interleukin (IL)-17 production. J Biol Chem *286*, 31409-31417.

Ghoreschi, K., Laurence, A., Yang, X.P., Tato, C.M., McGeachy, M.J., Konkel, J.E., Ramos, H.L., Wei, L., Davidson, T.S., Bouladoux, N.*, et al.* (2010). Generation of pathogenic T(H)17 cells in the absence of TGF-beta signalling. Nature *467*, 967-971.

Gomez, J.A., Wapinski, O.L., Yang, Y.W., Bureau, J.F., Gopinath, S., Monack, D.M., Chang, H.Y., Brahic, M., and Kirkegaard, K. (2013). The NeST long ncRNA controls microbial susceptibility and epigenetic activation of the interferon-gamma locus. Cell *152*, 743-754.

Goswami, R., and Kaplan, M.H. (2011). A brief history of IL-9. J Immunol *186*, 3283-3288.

Guttman, M., Amit, I., Garber, M., French, C., Lin, M.F., Feldser, D., Huarte, M., Zuk, O., Carey, B.W., Cassady, J.P*., et al.* (2009). Chromatin signature reveals over a thousand highly conserved large non-coding RNAs in mammals. Nature *458*, 223-227.

Guttman, M., Donaghey, J., Carey, B.W., Garber, M., Grenier, J.K., Munson, G., Young, G., Lucas, A.B., Ach, R., Bruhn, L*., et al.* (2011). lincRNAs act in the circuitry controlling pluripotency and differentiation. Nature *477*, 295-300.

Herz, H.M., and Shilatifard, A. (2010). The JARID2-PRC2 duality. Genes Dev *24*, 857-861.

Hirota, K., Duarte, J.H., Veldhoen, M., Hornsby, E., Li, Y., Cua, D.J., Ahlfors, H., Wilhelm, C., Tolaini, M., Menzel, U*., et al.* (2011). Fate mapping of IL-17-producing T cells in inflammatory responses. Nat Immunol *12*, 255-263.

Hu, G., Tang, Q., Sharma, S., Yu, F., Escobar, T.M., Muljo, S.A., Zhu, J., and Zhao, K. (2013). Expression and regulation of intergenic long noncoding RNAs during T cell development and differentiation. Nat Immunol *14*, 1190-1198.

Huang, W., Na, L., Fidel, P.L., and Schwarzenberger, P. (2004). Requirement of interleukin-17A for systemic anti-Candida albicans host defense in mice. J Infect Dis *190*, 624-631.

Huber, S., Gagliani, N., Zenewicz, L.A., Huber, F.J., Bosurgi, L., Hu, B., Hedl, M., Zhang, W., O'Connor, W., Jr., Murphy, A.J.*, et al.* (2012). IL-22BP is regulated by the inflammasome and modulates tumorigenesis in the intestine. Nature *491*, 259-263.

Huh, J.R., Leung, M.W., Huang, P., Ryan, D.A., Krout, M.R., Malapaka, R.R., Chow, J., Manel, N., Ciofani, M., Kim, S.V.*, et al.* (2011). Digoxin and its derivatives suppress TH17 cell differentiation by antagonizing RORgammat activity. Nature *472*, 486-490.

Inglese, J., Auld, D.S., Jadhav, A., Johnson, R.L., Simeonov, A., Yasgar, A., Zheng, W., and Austin, C.P. (2006). Quantitative high-throughput screening: a titration-based approach that efficiently identifies biological activities in large chemical libraries. Proc Natl Acad Sci U S A *103*, 11473-11478.

Jeker, L.T., and Bluestone, J.A. (2013). MicroRNA regulation of T-cell differentiation and function. Immunol Rev *253*, 65-81.

Jetten, A.M. (2011). Immunology: A helping hand against autoimmunity. Nature *472*, 421-422.

Kanno, Y., Vahedi, G., Hirahara, K., Singleton, K., and O'Shea, J.J. (2011). Transcriptional and Epigenetic Control of T Helper Cell Specification: Molecular Mechanisms Underlying Commitment and Plasticity. Annu Rev Immunol.

Kaplan, M.H., Schindler, U., Smiley, S.T., and Grusby, M.J. (1996a). Stat6 is required for mediating responses to IL-4 and for development of Th2 cells. Immunity *4*, 313-319.

Kaplan, M.H., Sun, Y.L., Hoey, T., and Grusby, M.J. (1996b). Impaired IL-12 responses and enhanced development of Th2 cells in Stat4-deficient mice. Nature *382*, 174-177.

Kebir, H., Kreymborg, K., Ifergan, I., Dodelet-Devillers, A., Cayrol, R., Bernard, M., Giuliani, F., Arbour, N., Becher, B., and Prat, A. (2007). Human TH17 lymphocytes promote blood-brain barrier disruption and central nervous system inflammation. Nat Med *13*, 1173-1175.

Kent, W.J., Sugnet, C.W., Furey, T.S., Roskin, K.M., Pringle, T.H., Zahler, A.M., and Haussler, D. (2002). The human genome browser at UCSC. Genome Res *12*, 996-1006.

Korn, T., Bettelli, E., Gao, W., Awasthi, A., Jager, A., Strom, T.B., Oukka, M., and Kuchroo, V.K. (2007). IL-21 initiates an alternative pathway to induce proinflammatory T(H)17 cells. Nature *448*, 484-487.

Krek, A., Grun, D., Poy, M.N., Wolf, R., Rosenberg, L., Epstein, E.J., MacMenamin, P., da Piedade, I., Gunsalus, K.C., Stoffel, M., and Rajewsky, N. (2005). Combinatorial microRNA target predictions. Nat Genet *37*, 495-500.

Langmead, B., Trapnell, C., Pop, M., and Salzberg, S.L. (2009). Ultrafast and memory-efficient alignment of short DNA sequences to the human genome. Genome Biol *10*, R25.

Lee, P.P., Fitzpatrick, D.R., Beard, C., Jessup, H.K., Lehar, S., Makar, K.W., Perez-Melgosa, M., Sweetser, M.T., Schlissel, M.S., Nguyen, S*., et al.* (2001). A critical role for Dnmt1 and DNA methylation in T cell development, function, and survival. Immunity *15*, 763-774.

Lewis, B.P., Shih, I.H., Jones-Rhoades, M.W., Bartel, D.P., and Burge, C.B. (2003). Prediction of mammalian microRNA targets. Cell *115*, 787-798.

Li, G., Margueron, R., Ku, M., Chambon, P., Bernstein, B.E., and Reinberg, D. (2010). Jarid2 and PRC2, partners in regulating gene expression. Genes Dev *24*, 368-380.

Li, P., Spolski, R., Liao, W., Wang, L., Murphy, T.L., Murphy, K.M., and Leonard, W.J. (2012). BATF-JUN is critical for IRF4-mediated transcription in T cells. Nature *490*, 543-546.

Liesenfeld, O. (2002). Oral infection of C57BL/6 mice with Toxoplasma gondii: a new model of inflammatory bowel disease? J Infect Dis *185 Suppl 1*, S96-101.

Loeb, G.B., Khan, A.A., Canner, D., Hiatt, J.B., Shendure, J., Darnell, R.B., Leslie, C.S., and Rudensky, A.Y. (2012). Transcriptome-wide miR-155 binding map reveals widespread noncanonical microRNA targeting. Mol Cell *48*, 760-770.

Lu, L.F., Thai, T.H., Calado, D.P., Chaudhry, A., Kubo, M., Tanaka, K., Loeb, G.B., Lee, H., Yoshimura, A., Rajewsky, K., and Rudensky, A.Y. (2009). Foxp3-dependent microRNA155 confers competitive fitness to regulatory T cells by targeting SOCS1 protein. Immunity *30*, 80-91.

Ma, F., Xu, S., Liu, X., Zhang, Q., Xu, X., Liu, M., Hua, M., Li, N., Yao, H., and Cao, X. (2011). The microRNA miR-29 controls innate and adaptive immune responses to intracellular bacterial infection by targeting interferon-gamma. Nat Immunol *12*, 861-869.

Muljo, S.A., Ansel, K.M., Kanellopoulou, C., Livingston, D.M., Rao, A., and Rajewsky, K. (2005). Aberrant T cell differentiation in the absence of Dicer. J Exp Med *202*, 261-269.

Muljo, S.A., Kanellopoulou, C., and Aravind, L. (2010). MicroRNA targeting in mammalian genomes: genes and mechanisms. Wiley Interdiscip Rev Syst Biol Med *2*, 148-161.

Mullen, A.C., High, F.A., Hutchins, A.S., Lee, H.W., Villarino, A.V., Livingston, D.M., Kung, A.L., Cereb, N., Yao, T.P., Yang, S.Y., and Reiner, S.L. (2001). Role of T-bet in commitment of TH1 cells before IL-12-dependent selection. Science *292*, 1907-1910.

Murphy, K., Travers, P., Walport, M., and Janeway, C. (2008). Janeway's immunobiology, 7th edn (New York: Garland Science).

Murugaiyan, G., Beynon, V., Mittal, A., Joller, N., and Weiner, H.L. (2011). Silencing microRNA-155 ameliorates experimental autoimmune encephalomyelitis. J Immunol *187*, 2213-2221.

Mysliwiec, M.R., Chen, J., Powers, P.A., Bartley, C.R., Schneider, M.D., and Lee, Y. (2006). Generation of a conditional null allele of jumonji. Genesis *44*, 407-411.

Nurieva, R., Yang, X.O., Martinez, G., Zhang, Y., Panopoulos, A.D., Ma, L., Schluns, K., Tian, Q., Watowich, S.S., Jetten, A.M., and Dong, C. (2007). Essential autocrine regulation by IL-21 in the generation of inflammatory T cells. Nature *448*, 480-483.

O'Connell, R.M., Chaudhuri, A.A., Rao, D.S., and Baltimore, D. (2009). Inositol phosphatase SHIP1 is a primary target of miR-155. Proc Natl Acad Sci U S A *106*, 7113-7118.

O'Connell, R.M., Kahn, D., Gibson, W.S., Round, J.L., Scholz, R.L., Chaudhuri, A.A., Kahn, M.E., Rao, D.S., and Baltimore, D. (2010). MicroRNA-155 promotes autoimmune inflammation by enhancing inflammatory T cell development. Immunity *33*, 607-619.

O'Connor, W., Jr., Zenewicz, L.A., and Flavell, R.A. (2010). The dual nature of T(H)17 cells: shifting the focus to function. Nat Immunol *11*, 471-476.

O'Shea, J.J., and Paul, W.E. (2010). Mechanisms underlying lineage commitment and plasticity of helper CD4+ T cells. Science *327*, 1098-1102.

Oertli, M., Engler, D.B., Kohler, E., Koch, M., Meyer, T.F., and Muller, A. (2011). MicroRNA-155 is essential for the T cell-mediated control of Helicobacter pylori infection and for the induction of chronic Gastritis and Colitis. J Immunol *187*, 3578-3586.

Oh, H.M., Yu, C.R., Lee, Y., Chan, C.C., Maminishkis, A., and Egwuagu, C.E. (2011). Autoreactive memory CD4+ T lymphocytes that mediate chronic uveitis reside in the bone marrow through STAT3-dependent mechanisms. J Immunol *187*, 3338-3346.

Ouyang, W., Rutz, S., Crellin, N.K., Valdez, P.A., and Hymowitz, S.G. (2011). Regulation and functions of the IL-10 family of cytokines in inflammation and disease. Annu Rev Immunol *29*, 71-109.

Pasini, D., Cloos, P.A., Walfridsson, J., Olsson, L., Bukowski, J.P., Johansen, J.V., Bak, M., Tommerup, N., Rappsilber, J., and Helin, K. (2010). JARID2 regulates binding of the Polycomb repressive complex 2 to target genes in ES cells. Nature *464*, 306-310.

Peng, J.C., Valouev, A., Swigut, T., Zhang, J., Zhao, Y., Sidow, A., and Wysocka, J. (2009). Jarid2/Jumonji coordinates control of PRC2 enzymatic activity and target gene occupancy in pluripotent cells. Cell *139*, 1290-1302.

Rhee, H.S., and Pugh, B.F. (2012). ChIP-exo method for identifying genomic location of DNA-binding proteins with near-single-nucleotide accuracy. Curr Protoc Mol Biol *Chapter 21*, Unit 21 24.

Rodriguez, A., Vigorito, E., Clare, S., Warren, M.V., Couttet, P., Soond, D.R., van Dongen, S., Grocock, R.J., Das, P.P., Miska, E.A.*, et al.* (2007). Requirement of bic/microRNA-155 for normal immune function. Science *316*, 608-611.

Rodriguez, C.I., Buchholz, F., Galloway, J., Sequerra, R., Kasper, J., Ayala, R., Stewart, A.F., and Dymecki, S.M. (2000). High-efficiency deleter mice show that FLPe is an alternative to Cre-loxP. Nat Genet *25*, 139-140.

Rutz, S., Noubade, R., Eidenschenk, C., Ota, N., Zeng, W., Zheng, Y., Hackney, J., Ding, J., Singh, H., and Ouyang, W. (2011). Transcription factor c-Maf mediates the TGF-beta-dependent suppression of IL-22 production in T(H)17 cells. Nat Immunol *12*, 1238-1245.

Sato, K., Suematsu, A., Okamoto, K., Yamaguchi, A., Morishita, Y., Kadono, Y., Tanaka, S., Kodama, T., Akira, S., Iwakura, Y.*, et al.* (2006). Th17 functions as an osteoclastogenic helper T cell subset that links T cell activation and bone destruction. J Exp Med *203*, 2673-2682.

Schulz, S.M., Kohler, G., Schutze, N., Knauer, J., Straubinger, R.K., Chackerian, A.A., Witte, E., Wolk, K., Sabat, R., Iwakura, Y.*, et al.* (2008). Protective immunity to systemic infection with attenuated Salmonella enterica serovar enteritidis in the absence of IL-12 is associated with IL-23-dependent IL-22, but not IL-17. J Immunol *181*, 7891-7901.

Shaw, M.H., Kamada, N., Kim, Y.G., and Nunez, G. (2012). Microbiota-induced IL-1beta, but not IL-6, is critical for the development of steady-state TH17 cells in the intestine. J Exp Med *209*, 251-258.

Shen, X., Kim, W., Fujiwara, Y., Simon, M.D., Liu, Y., Mysliwiec, M.R., Yuan, G.C., Lee, Y., and Orkin, S.H. (2009). Jumonji modulates polycomb activity and self-renewal versus differentiation of stem cells. Cell *139*, 1303-1314.

Shibata, K., Yamada, H., Hara, H., Kishihara, K., and Yoshikai, Y. (2007). Resident Vdelta1+ gammadelta T cells control early infiltration of neutrophils after Escherichia coli infection via IL-17 production. J Immunol *178*, 4466-4472.

Smoot, M.E., Ono, K., Ruscheinski, J., Wang, P.L., and Ideker, T. (2011). Cytoscape 2.8: new features for data integration and network visualization. Bioinformatics *27*, 431-432.

Solt, L.A., Kumar, N., Nuhant, P., Wang, Y., Lauer, J.L., Liu, J., Istrate, M.A., Kamenecka, T.M., Roush, W.R., Vidovic, D., *et al.* (2011). Suppression of TH17 differentiation and autoimmunity by a synthetic ROR ligand. Nature *472*, 491-494.

Stark, G.R., and Darnell, J.E., Jr. (2012). The JAK-STAT pathway at twenty. Immunity *36*, 503-514.

Steiner, D.F., Thomas, M.F., Hu, J.K., Yang, Z., Babiarz, J.E., Allen, C.D., Matloubian, M., Blelloch, R., and Ansel, K.M. (2011). MicroRNA-29 regulates T-box transcription factors and interferon-gamma production in helper T cells. Immunity *35*, 169-181.

Sundrud, M.S., Koralov, S.B., Feuerer, M., Calado, D.P., Kozhaya, A.E., Rhule-Smith, A., Lefebvre, R.E., Unutmaz, D., Mazitschek, R., Waldner, H._, et al._ (2009). Halofuginone inhibits TH17 cell differentiation by activating the amino acid starvation response. Science _324_, 1334-1338.

Takeda, K., Tanaka, T., Shi, W., Matsumoto, M., Minami, M., Kashiwamura, S., Nakanishi, K., Yoshida, N., Kishimoto, T., and Akira, S. (1996). Essential role of Stat6 in IL-4 signalling. Nature _380_, 627-630.

Thai, T.H., Calado, D.P., Casola, S., Ansel, K.M., Xiao, C., Xue, Y., Murphy, A., Frendewey, D., Valenzuela, D., Kutok, J.L._, et al._ (2007). Regulation of the germinal center response by microRNA-155. Science _316_, 604-608.

Tili, E., Croce, C.M., and Michaille, J.J. (2009). miR-155: on the crosstalk between inflammation and cancer. Int Rev Immunol _28_, 264-284.

Trapnell, C., Pachter, L., and Salzberg, S.L. (2009). TopHat: discovering splice junctions with RNA-Seq. Bioinformatics _25_, 1105-1111.

Vahedi, G., Takahashi, H., Nakayamada, S., Sun, H.W., Sartorelli, V., Kanno, Y., and O'Shea, J.J. (2012). STATs shape the active enhancer landscape of T cell populations. Cell _151_, 981-993.

van den Berg, W.B., and Miossec, P. (2009). IL-17 as a future therapeutic target for rheumatoid arthritis. Nat Rev Rheumatol _5_, 549-553.

van Dongen, S., Abreu-Goodger, C., and Enright, A.J. (2008). Detecting microRNA binding and siRNA off-target effects from expression data. Nat Methods *5*, 1023-1025.

Veldhoen, M., Hirota, K., Westendorf, A.M., Buer, J., Dumoutier, L., Renauld, J.C., and Stockinger, B. (2008). The aryl hydrocarbon receptor links TH17-cell-mediated autoimmunity to environmental toxins. Nature *453*, 106-109.

Veldhoen, M., Hocking, R.J., Atkins, C.J., Locksley, R.M., and Stockinger, B. (2006). TGFbeta in the context of an inflammatory cytokine milieu supports de novo differentiation of IL-17-producing T cells. Immunity *24*, 179-189.

Wang, L., Feng, Z., Wang, X., and Zhang, X. (2010). DEGseq: an R package for identifying differentially expressed genes from RNA-seq data. Bioinformatics *26*, 136-138.

Wei, G., Wei, L., Zhu, J., Zang, C., Hu-Li, J., Yao, Z., Cui, K., Kanno, Y., Roh, T.Y., Watford, W.T.*, et al.* (2009). Global mapping of H3K4me3 and H3K27me3 reveals specificity and plasticity in lineage fate determination of differentiating CD4+ T cells. Immunity *30*, 155-167.

Wildin, R.S., Ramsdell, F., Peake, J., Faravelli, F., Casanova, J.L., Buist, N., Levy-Lahad, E., Mazzella, M., Goulet, O., Perroni, L.*, et al.* (2001). X-linked neonatal diabetes mellitus, enteropathy and endocrinopathy syndrome is the human equivalent of mouse scurfy. Nat Genet *27*, 18-20.

Wilson, M.S., Feng, C.G., Barber, D.L., Yarovinsky, F., Cheever, A.W., Sher, A., Grigg, M., Collins, M., Fouser, L., and Wynn, T.A. (2010). Redundant and pathogenic roles for IL-22 in mycobacterial, protozoan, and helminth infections. J Immunol *184*, 4378-4390.

Witte, E., Witte, K., Warszawska, K., Sabat, R., and Wolk, K. (2010). Interleukin-22: a cytokine produced by T, NK and NKT cell subsets, with importance in the innate immune defense and tissue protection. Cytokine Growth Factor Rev *21*, 365-379.

Xiao, C., Srinivasan, L., Calado, D.P., Patterson, H.C., Zhang, B., Wang, J., Henderson, J.M., Kutok, J.L., and Rajewsky, K. (2008). Lymphoproliferative disease and autoimmunity in mice with increased miR-17-92 expression in lymphocytes. Nat Immunol *9*, 405-414.

Xu, H., Koch, P., Chen, M., Lau, A., Reid, D.M., and Forrester, J.V. (2008). A clinical grading system for retinal inflammation in the chronic model of experimental autoimmune uveoretinitis using digital fundus images. Exp Eye Res *87*, 319-326.

Yang, X.P., Ghoreschi, K., Steward-Tharp, S.M., Rodriguez-Canales, J., Zhu, J., Grainger, J.R., Hirahara, K., Sun, H.W., Wei, L., Vahedi, G., *et al.* (2011). Opposing regulation of the locus encoding IL-17 through direct, reciprocal actions of STAT3 and STAT5. Nat Immunol *12*, 247-254.

Yosef, N., Shalek, A.K., Gaublomme, J.T., Jin, H., Lee, Y., Awasthi, A., Wu, C., Karwacz, K., Xiao, S., Jorgolli, M., *et al.* (2013a). Dynamic regulatory network controlling T17 cell differentiation. Nature.

Yosef, N., Shalek, A.K., Gaublomme, J.T., Jin, H., Lee, Y., Awasthi, A., Wu, C., Karwacz, K., Xiao, S., Jorgolli, M., *et al.* (2013b). Dynamic regulatory network controlling TH17 cell differentiation. Nature *496*, 461-468.

Yu, C.R., Mahdi, R.R., Oh, H.M., Amadi-Obi, A., Levy-Clarke, G., Burton, J., Eseonu, A., Lee, Y., Chan, C.C., and Egwuagu, C.E. (2011). Suppressor of cytokine signaling-1 (SOCS1) inhibits lymphocyte recruitment into the retina and protects SOCS1 transgenic rats and mice from ocular inflammation. Invest Ophthalmol Vis Sci *52*, 6978-6986.

Zang, C., Schones, D.E., Zeng, C., Cui, K., Zhao, K., and Peng, W. (2009). A clustering approach for identification of enriched domains from histone modification ChIP-Seq data. Bioinformatics *25*, 1952-1958.

Zenewicz, L.A., and Flavell, R.A. (2011). Recent advances in IL-22 biology. Int Immunol *23*, 159-163.

Zheng, Y., Danilenko, D.M., Valdez, P., Kasman, I., Eastham-Anderson, J., Wu, J., and Ouyang, W. (2007). Interleukin-22, a T(H)17 cytokine, mediates IL-23-induced dermal inflammation and acanthosis. Nature *445*, 648-651.

Zhu, J., Yamane, H., and Paul, W.E. (2010). Differentiation of effector CD4 T cell populations (*). Annu Rev Immunol *28*, 445-489.

8. Curriculum Vitae

Thelma M. Escobar

1620 East Jefferson Street, Apt 211

Rockville, MD 20852

Phone: (714) 614-3988 (cell)

Email: tescoba1@jhu.edu

Education:

Johns Hopkins University, Baltimore, MD

Ph.D. in Cell, Molecular, Developmental & Biophysics (Expected April 2014)

University of California Los Angeles, Los Angeles, CA

B.S. in Molecular, Cell & Developmental Biology, Los Angeles, CA (June 2007)

Research Experience

9/2008 – Present – Ph.D. Candidate –

NIH-Johns Hopkins Graduate Partnership Program: Joint program, course work and degree from Johns Hopkins and thesis research at the NIH.

Advisor: Dr. Stefan Muljo – National Institute of Allergy and Infectious Diseases

☐ microRNA-mediated regulation of $CD4^+$ T helper cell differentiation.

9/2007 – 7/2008 – <u>NIH Academy Postbaccalaureate Program</u>

Advisor: Dr. Ira Pastan – National Cancer Institute

☐ Determining ANKRD26 interacting partners in adipogenesis.

10/2004 – 06/2007 – <u>Undergraduate Research</u>

Advisor: Dr. Alexander van der Bliek – UCLA Deparment of Biological Chemistry.

☐ Studying the functional role of mitochondrial fission protein Fis-1 and Fis-2 in *Caenorhabditis elegans*.

Awards and Funding

☐ National Science Foundation Graduate Research Fellowship Program (GRFP) Honorable Mentions Recipient, 2010.

☐ NIH Academy Post-baccalaureate Program in the Laboratory of Molecular Biology, National Cancer Institute, 2007-2008.

☐ UCLA Women for Change 2007 Student Leadership Award Recipient, May 2007.

☐ UCLA 2007 Chancellor's Service Award Recipient, May 2007

☐ UCLA Science Poster Day Dean's Prize Award Recipient, April 2006

☐ Minority Access to Research Careers (MARC) Program, 2005-2007

Teaching Experience

☐ Laboratory mentor for medical student, January 2012-June 2012.

☐ Laboratory mentor for summer intern, June 2012 – August 2012.

☐ Volunteer for Latino Student Fund in District of Columbia, 2010-present. Two

hours per week tutoring for middle and high school students.

☐ Teaching assistant for Cell Biology Laboratory at Johns Hopkins University,

Spring Semester 2009, a 20-student section.

☐ Teaching assistant for Biochemistry Laboratory at Johns Hopkins University,

Fall Semester 2008, a 20-student section

☐ Pre-calculus tutor for high school students in Upward Bound Los Angeles

Summer Program, June-August 2007.

Poster Presentations

1.   **Escobar T**, Kanellopoulou C, Kugler DG, Nguyen CK, Gokhul K, Nagarajan V,

Bhairavabhotla RK, Northrup D, Zahr R, Burr P, Zhao K, Sher A, Jankovic D,

Zhu J, and Muljo SA. Jarid2, a Polycomb member and target of miR-155, regulates the fates of Th17 and Treg cells. NIH Immunology Interest Group Workshop, September 3-4, 2013.

2.   **Escobar T**, Nguyen CK, Kugler DG, Bhairavabhotla RK, Northrup D, Zahr R, Kanellopoulou C, Zhao K, Sher A, Jankovic D, Zhu J, and Muljo SA. miR-155 promotes Th17 cytokine expression by targeting Jarid2. Cold Spring Harbor RNA Meeting, September 2012.

3.   **Escobar T**, Nguyen C, Zahr R, Zhu J, and Muljo SA. Interleukin 22 production is regulated by miR-155 in CD4$^+$ T helper 17 cells. NIH Immunology Interest Group Annual Retreat, September 2011.

4.   **Escobar T**, Head B, and van der Bliek A. Determing Fis-1 and Fis-2 Function in Mitochondrial Dynamics. Annual Biomedical Research Conferences for Minority Students (ABRCMS), Anaheim, CA. November 2006.

5.   **Escobar T**, Head B, and van der Bliek A. Determining Fis-1 and Fis-2 Function in Mitochondrial Dynamics. UCLA Science Poster Day. May 2006.

6.   **Escobar T**, Head B, and van der Bliek A. Determining Fis-1 and Fis-2 function. Society for Advancement of Chicanos and Native Americans in Sciences (SACNAS) Annual Meeting in Denver, CO. September 2005.

Oral Presentations

1. Thelma Escobar. miR-155 modulates Th17 cell fates through Jarid2. NIH Immunology Interest Group Workshop, September 3, 2013.

2. Thelma Escobar. Interleukin 22 production is regulated by miR-155 in CD4$^+$ T helper 17 cells. NIH Immunology Interest Group Annual Retreat, September 12, 2011.

Publications

1. **Escobar T**, Kanellopoulou C, Kugler DG, Nguyen CK, Gokhul K, Nagarajan V, Bhairavabhotla RK, Northrup D, Zahr R, Burr P, Zhao K, Sher A, Jankovic D, Zhu J, and Muljo SA. Jarid2, a Polycomb member and target of miR-155, regulates the fates of Th17 and Treg cells. Immunity, accepted.

2. Hu G, Tang Q, Sharma S, Yu F, **Escobar TM**, Muljo SA, Zhu J, Zhao K. Expression and regulation of long noncoding RNAs during T cell development and differentiation. Nature Immunology, September 2013.

3. **Escobar T**, Yu CR, Muljo SA, Egwuagu CE. STAT3 Activates miR-155 in Th17 Cells and Acts in Concert to Promote Experimental Autoimmune Uveitis. Investigative Ophthalmology & Visual Science. 2013 June; 54(6):4017-25.

4. Dudda JC, Salaun B, Ji Y, Palmer DC, Monnot GC, Merck E, Boudousquie C, Utzscheider DT, **Escobar TM**, Perret R, Muljo SA, Hebeisen M, Rufer N, Zehn D, Donda A, Restifo NP, Held W, Gattinoni L, Romero P. MicroRNA-155 is

required for effector CD8^{+} T cell responses to virus infection and cancer. Immunity. 2013 April; 38(4):742-53.

5. Liu XF, Bera TK, Kahue C, **Escobar T**, Fei Z, Raciti GA, Pastan I. ANKRD26 and its interacting partners TRIO, GPS2, HMMR and DIPA regulate adipogenesis in 3T3-L1 cells. PLoS One. 2012 May;7(5)e38130.

6. McKnight JN, Jenkins KR, Nodelman IM, **Escobar T**, Bowman GD. Extranucleosomal DNA binding directs nucleosome sliding by Chd1. Mol Cell Biology. 2011 December; 31(23):4746-59.

7. Wiench M, John S, Baek S, Johnson TA, Sung MH, **Escobar T**, Simmons CA, Pearce KH, Biddie SC, Sabo PJ, Thurman RE, Stamatoyannopoulos JA, Hager GL. DNA methylation status predicts cell type-specific enhancer activity. EMBO J. 2011 June;30(15):3028-39.